

TECHNICAL REPORT 1868  
December 2001

# **Site Characterization and Analysis Penetrometer System (SCAPS) Heavy Metal Sensors Demonstration/Validation**

## **Technology Demonstration Report**

S. H. Lieberman  
P. A. Boss  
**SSC San Diego**

J. Cortes  
**U. S. Army Engineer Research and  
Development Center**

W. T. Elam  
**Naval Research Laboratory**

Approved for public release;  
distribution is unlimited



**SSC San Diego**  
**San Diego, CA 92152-5001**

**SSC SAN DIEGO**  
**San Diego, California 92152-5001**

---

---

**P. A. Miller, CAPT, USN**  
**Commanding Officer**

**R. C. Kolb**  
**Executive Director**

**ACKNOWLEDGMENT**

This project was supported by the Environmental Security Technology Certification Program.

This technology is related to the subject matter of one or more U.S. Patents assigned to the U.S. Government, including Patent No. 6,147,754, serial number 09/162,418 and N.C. 79859. Licensing inquiries may be directed to:

Harvey Fendelman, Patent Counsel  
Space and Naval Warfare Systems Center (D0012)  
San Diego, CA 92152-5765

## EXECUTIVE SUMMARY

To clean up a hazardous waste site, the contamination at the site must first be delineated. Site characterization can be very costly, accounting for a third or more of the total cleanup cost. Until recently, the most common method to determine the extent of subsurface cleanup was to collect samples from soil borings or monitoring wells and send them to a laboratory for analysis. This approach is inefficient and expensive.

The Site Characterization and Analysis Penetrometer System (SCAPS) was developed to address the requirement for improved subsurface measurement of contaminants. SCAPS combines traditional cone penetrometer technology with real-time direct push chemical sensors to rapidly delineate the subsurface distribution of contaminants and hydrogeological conditions. To broaden the applicability of SCAPS, the Strategic Environmental Research and Development Program (SERDP) funded the development of several real-time *in situ* sensor technologies for screening of heavy metal contamination in soils.

This technology demonstration report documents the performance and cost evaluation of three direct push metal sensor technologies conducted as part of a series of comprehensive side-by-side, field, and laboratory evaluations supported by the Environmental Security Technology Certification Program (ESTCP). The technologies include two sensor systems based on Laser-Induced Breakdown Spectroscopy (LIBS) and one system based on X-Ray fluorescence. Field evaluations were conducted at four different sites selected to reflect different hydrogeological conditions, metal contaminants, and modes of introduction of the metal contaminant into the environment (e.g., dissolved vs. particulate). Test sites included the Lake City Army Ammunition Plant in Independence, MO; Naval Air Station North Island at North Island, CA; Hunters Point Shipyard in San Francisco, CA; and Camp Keller, an off-base site at Keesler AFB in Biloxi, MS. Performance assessments in which results from the three sensors were compared against inductively-coupled-plasma (ICP) laboratory analysis of discrete samples showed mean accuracy of 91.7%, 97% and 97% respectively for XRF, Fiber-Optic LIBS (FO-LIBS) and Downhole Laser LIBS (DL-LIBS) for the four site demonstrations. Cost comparison of the SCAPS Metal Sensors with conventional Sampling and Discrete Push Sampling and offsite chemical analyses showed a cost advantage for the direct push sensors, on a cost per sample basis, of 98% compared with conventional soil borings and 96% compared to direct push sampling methods.



# TABLE OF CONTENTS

	<u>Page</u>
<b>LIST OF FIGURES .....</b>	<b>vii</b>
<b>LIST OF TABLES .....</b>	<b>viii</b>
<b>LIST OF ABBREVIATIONS AND ACRONYMS .....</b>	<b>ix</b>
<b>1. INTRODUCTION.....</b>	<b>1</b>
1.1 Background Information .....	2
1.2 Official Department of Defense (DoD) Requirement Statement .....	3
1.2.1 How Requirement(s) Were Addressed.....	3
1.3 Demonstration Purpose and Objectives .....	4
1.4 Regulatory Acceptance of SCAPS Innovative Technology.....	5
1.5 Previous Testing of the Technology.....	5
<b>2. TECHNOLOGY DESCRIPTION.....</b>	<b>7</b>
2.1 Background and Applications .....	7
2.1.1 Laser-Induced Breakdown Spectroscopy (LIBS) .....	8
2.1.1.1 FO-LIBS Sensor.....	9
2.1.1.2 DL-LIBS Sensor.....	12
2.1.2 X-Ray Fluorescence (XRF) Sensor.....	15
2.2 Advantages and Limitations of the Technology .....	18
2.2.1 Comparison to Current Technology.....	18
2.2.2 Comparison to Competing New Technologies .....	18
2.2.3 Limits of the Technology .....	18
2.2.3.1 Limitations of the LIBS Technique for <i>in situ</i> Measurement .....	19
2.2.3.1.1 FO-LIBS Sensor Specific Limitations .....	19
2.2.3.1.2 DL-LIBS Sensor Specific Limitations .....	20
2.2.3.2 XRF Sensor Limitations.....	20
2.2.3.3 Matrix and Moisture Effects .....	20
2.3 Factors Influencing Cost and Performance .....	21
<b>3. SITE/FACILITY DESCRIPTION .....</b>	<b>23</b>
3.1 Background .....	23
3.2 Site/Facility Description.....	23
3.2.1 LCAAP, Independence, MO .....	23
3.2.2 IWTP at Naval Air Station, North Island, CA .....	25
3.2.3 Former Ship Repair Area (Parcel D), Hunters Point Shipyard, San Francisco, CA ...	28
3.2.4 Camp Keller Small-Arms Range, Keesler Air Force Base, Biloxi, MS .....	32
<b>4. DEMONSTRATION APPROACH.....</b>	<b>35</b>
4.1 Performance Objectives .....	35
4.2 Physical Setup and Operation .....	36
4.3 Sampling Procedures.....	37
4.4 Analytical Procedures .....	38

<b>5. PERFORMANCE ASSESSMENT .....</b>	<b>41</b>
5.1 Performance Data .....	41
5.1.1 LCAAP, Independence, MO .....	42
5.1.2 IWTP at Naval Air Station, North Island, CA .....	44
5.1.3 Former Ship Repair Area (Parcel D), Hunters Point Shipyard, San Francisco, CA .....	48
5.1.4 Camp Keller Small-Arms Range, Keesler Air Force Base, Biloxi, MS .....	50
5.2 Data Assessment .....	53
5.3 Technology Comparison .....	54
<b>6. COST ASSESSMENT .....</b>	<b>55</b>
6.1 Cost Performance .....	55
6.2 Cost Comparisons to Conventional and Other Technologies .....	55
<b>7. REGULATORY ISSUES .....</b>	<b>59</b>
7.1 Approach to Regulatory Compliance and Acceptance .....	59
<b>8. TECHNOLOGY IMPLEMENTATION .....</b>	<b>65</b>
8.1 DoD Need .....	65
8.2 Transition .....	65
<b>9. LESSONS LEARNED .....</b>	<b>67</b>
9.1 Technical Lessons .....	67
9.1.1 SCAPS FO-LIBS Metals Sensor .....	67
9.1.2 SCAPS XRF Metals Sensor .....	68
9.1.3 SCAPS DL-LIBS Metals Sensor .....	68
<b>10. REFERENCES .....</b>	<b>71</b>
<b>APPENDIX A: POINTS OF CONTACT .....</b>	<b>A-1</b>
<b>APPENDIX B: DATA ARCHIVING .....</b>	<b>B-1</b>
B1. Introduction .....	B-1
B2. FO-LIBS .....	B-1
B2.1 Preparation of Calibration Standards .....	B-2
B2.2 Generation and Manipulation of Spectral Data for the Calibration Curve and <i>ex situ</i> Laboratory Data .....	B-3
B2.3 Generation and Manipulation of Spectral Data for the <i>in situ</i> Push Data .....	B-5
B3. XRF .....	B-11
B3.1 Spectral Data .....	B-11
B3.2 Calibration .....	B-12
B3.3 XRF References .....	B-17
B4. DL-LIBS .....	B-17
B4.1 Preparation of Calibration Standard .....	B-17
B4.2 Data Manipulation .....	B-18
B4.2.1 LCAAP .....	B-18
B4.2.2 NASNI .....	B-20
B4.2.3 HPS .....	B-22
B4.2.4 Camp Keller .....	B-24

## LIST OF FIGURES

	Page
Figure 1. Schematic of FO-LIBS System .....	9
Figure 2. Dependence of Sample Power on Lens-to-Sample Distance.....	10
Figure 3. FO-LIBS Fixed Sample-to-Lens Distance Design .....	11
Figure 4. Modified FO-LIBS Design with Stepping Motor.....	11
Figure 5. FO-LIBS Sapphire Windows.....	12
Figure 6. Schematic of DL-LIBS Sensor .....	13
Figure 7. Schematic of NRL XRF Sensor.....	16
Figure 8. LCAAP Independence, MO, Location Map .....	24
Figure 9. LCAAP Site Map.....	25
Figure 10. NASNI San Diego, CA, Location Map .....	26
Figure 11. IWTP (Site 11) Site Map .....	27
Figure 12. Detailed Map of IWTP Site .....	28
Figure 13. Site Map of Hunters Point Shipyard, San Francisco, CA.....	29
Figure 14. Location of Parcel D at Hunters Point Shipyard.....	30
Figure 15. Site map of Keesler Air Force Base and Camp Keller .....	33
Figure 16. Contingency Plot Analysis Where DLT is the Detection Limit Threshold.....	42
Figure 17. LCAAP Demonstration Site .....	43
Figure 18. <i>In situ</i> Lead Data for Push 3 Obtained for all Three Metal Sensor Technologies Demonstrated at LCAAP .....	44
Figure 19. NASNI Demonstration Site .....	46
Figure 20. <i>In situ</i> Chromium Data for Push 2 Obtained for all Three Metal Sensor Technologies Demonstrated at NASNI.....	47
Figure 21. Hunters Point Shipyard (HPS) Demonstration Site.....	48
Figure 22. <i>In situ</i> Chromium Data for Push 3 Obtained for all Three Metal Sensor Technologies Demonstrated HPS.....	50
Figure 23. Camp Keller Demonstration Site.....	51
Figure 24. <i>In situ</i> Lead Data for Push 9 Obtained for all Three Metal Sensor Technologies Demonstrated Camp Keller .....	52
Figure 25. FO-LIBS Spectrum of NASNI Soil Obtained Using a Zr-Coated Sapphire Window .....	68
Figure B-1. FO-LIBS Spectra Obtained for a LCAAP Laboratory Sample Obtained from Hole 1 at a Depth of 0 to 6 bgs .....	B-4
Figure B-2. Un-Normalized and Normalized LIBS Spectra of a NASNI Laboratory Sample Obtained from Hole 1 at a Depth of 36 to 48 bgs .....	B-5
Figure B-3. Effect of Moisture Content on LIBS Signal .....	B-7
Figure B-4. XRF Spectrum Generated Using Data Summarized in File Lc1s41a.asp .....	B-13

## LIST OF TABLES

	Page
1. LCAAP Lead Contingency Analysis Result Summary of Laboratory Data for Three Sensors .....	45
2. NASNI Chromium Contingency Analysis Results Summary of <i>ex situ</i> Laboratory Data for Three SCAPS Metal Sensor Technologies.....	48
3. HPS Chromium Contingency Analysis Results Summary of Laboratory Data for Three Sensors .....	50
4. Camp Keller Lead Contingency Analysis Results Summary of Laboratory Data for Three Sensors .....	53
5. Contingency Analysis Results Summary of Benchtop Laboratory Data Obtained by Three Sensors for Four Site Demonstrations .....	54
6. Cost Comparison of SCAPS Metal Sensors with Conventional Sampling and Direct Push Sampling.....	57
7. Summary of Publications for ERDC DL-LIBS Metals Sensor.....	61
8. Summary of Publications for NRL XRF Metals Sensor.....	62
9. Summary of Publications for SSC San Diego FO-LIBS Metals Sensor.....	63
B-1. Summary of Archived FO-LIS LCAAP Raw and Processed Data (folder ‘LCAAP’ in Folder ‘FO-LIBS Data’).....	B-9
B-2. Summary of Archived FO-LIS NASNI Raw and Processed Data (Folder ‘NASNI’ in Folder ‘FO-LIBS Data’).....	B-9
B-3. Summary of Archived FO-LIS HPS Raw and Processed Data (Folder ‘HPS’ in Folder ‘FO-LIBS Data’).....	B-10
B-4. Summary of Archived FO-LIS Camp Keller Raw and Processed Data (Folder ‘Camp Keller’ in Folder ‘FO-LIBS Data’) .....	B-10
B-5. Summary of Files Archived in Folder ‘xrf’ data’ on the CD-ROM.....	B-16
B-6. Summary of Archived DL-LIB LCAAP Data (Folder ‘LCAAP’ in Folder ‘DL-LIBS Data’).....	B-19
B-7. Summary of Archived DL-LIB NASNI Data (Folder ‘NASNI’ in Folder ‘DL-LIBS Data’).....	B-21
B-8. Summary of Archived DL-LIB HPS Data (Folder ‘HPS’ in Folder ‘DL-LIBS Data’).....	B-23
B-9. Summary of Archived DL-LIB Camp Keller Data (Folder ‘Camp Keller’ in Folder ‘DL-LIBS Data’) .....	B-25
B-10. Summary of Archived in Folder ‘Summary of Data’ .....	B-26

## LIST OF ABBREVIATIONS AND ACRONYMS

AEC	Army Environmental Center
As	Arsenic
ASTM	American Society for Testing and Materials
bbbl	Barrel (Equivalent to 42 U.S. Gallons)
bgs	Below Ground Surface
cm	centimeter
CAS	Chemical Abstract Service
CLP	Contract Laboratory Program
CPT	Cone Penetrometer Testing
CSC	Computer Sciences Corporation
CSCT	Consortium for Site Characterization Technology
CW	Continuous Wave
DL	Downhole Laser
DoD	Department of Defense
DOE	Department of Energy
DOT	Department of Transportation
DQO	Data Quality Objective
EDM	Engineering Development Model
EMMC	Environmental Monitoring Management Council
EMSL	Environmental Monitoring Systems Laboratory
EnTICE	Environmental Technology Innovation, Commercialization, and Enhancement (Program)
EPA	Environmental Protection Agency
ERDC	U.S. Army Engineer Research and Development Center
ESTCP	Environmental Security Technology Certification Program
ETI	Environmental Technology Initiative
Fe	Iron
ft	feet
FO	Fiber Optic
FY	Fiscal Year
GC/FID	Gas Chromatograph/Flame Ionization Detector
GFAA	Graphite-Furnace Atomic Absorption Spectrometry
GW/cm <sup>2</sup>	giga watts per square centimeter
HASP	Health and Safety Plan
HeNe	Helium Neon
Hg	Mercury
HSA	Hollow Stem Auger
Hz	hertz
ICP	Inductively Coupled Plasma Emission Spectroscopy
IDW	Investigation Derived Waste
IR	Installation Restoration

IRP	Installation Restoration Program
ITER	Innovative Technology Evaluation Report
kV	kilovolt
LCAAP	Lake City Army Ammunition Plant
LIBS	Laser-Induced Breakdown Spectroscopy
LIF	Laser-Induced Fluorescence
m	meter
µm	micrometer
µsec	microsecond
mg/kg	milligrams per kilogram
mg/L	milligrams per liter
mJ	milliJoules
ml	milliliter
mm	millimeter
m/min	meters per minute
ms	millisecond
msl	Mean Sea Level
mW	milliwatt
Nd	Neodymium
ND:YAG	Neodymium Yttrium Aluminum Garnet
NEX	Naval Exchange
NFESC	Naval Facilities Engineering Service Center
NIST	National Institute of Standards and Technology
nm	nanometer
NRaD	NCCOSC RDT&E Division (now SSC San Diego)
NRL	Naval Research Laboratory
ns	nanosecond
OMA	Optical Multichannel Analyzer
Pb	Lead
PDA	Photodiode Array
PE	Performance Evaluation
PIN	P-type/Intrinsic/N-type diode
PM	Program Manager
POL	Petroleum, Oil and Lubricant
PPE	Personal Protective Equipment
ppm	parts per million
PRC	PRC Environmental Management, Inc.
psec	picosecond
PWC	Public Works Center
QA	Quality Assurance
QAP	Quality Assurance Plan
QC	Quality Control
R <sup>2</sup>	Correlation Coefficient
RAB	Restoration Advisory Board
RRAD	Red River Army Depot
RI/FS	Remedial Investigation/Feasibility Studies

ROST	Rapid Optical Screening Tool
SCAPS	Site Characterization and Analysis Penetrometer System
SERDP	Strategic Environmental Research and Development Program
Si	Silicon
SOP	Standard Operating Procedure
SPT	Standard Penetrometer Testing
SRM	Standard Reference Material
SSC San Diego	Space and Naval Warfare Systems Center, San Diego
TER	Technology Evaluation Report
TPM	Technical Project Manager
TSF	Tons per Square Foot
U.S.	United States
USCS	Unified Soil Classification System
UV	Ultraviolet
WTM	Wavelength Time Matrix
XRF	X-ray Fluorescence
YAG	Yttrium Aluminum Garnet



# **Site Characterization and Analysis Penetrometer System (SCAPS) Heavy Metal Sensors Demonstration/Validation Technology Demonstration Report**

**Space and Naval Warfare Systems Center  
(SSC San Diego)  
Code D36  
San Diego, CA**

**March 2001**

## **1. Introduction**

This technology demonstration report documents the field and laboratory methods used to verify three direct push metal sensor technologies, two based on Laser-Induced Breakdown Spectroscopy (LIBS) and one based on X-Ray Fluorescence (XRF), and presents demonstration results. SPAWAR Systems Center, San Diego (SSC San Diego) has prepared this report following the guidelines in the Environmental Security Technology Certification Program (ESTCP) Offices' document: "Final Report Guidelines for Funded Projects" dated 15 April 1996. The technology demonstration report is divided into 10 sections. Section 1 provides the purpose and background of the demonstration and a description of the demonstration process used for the technologies. Section 2 describes the Fiber-Optic (FO)-LIBS, Downhole Laser (DL)-LIBS, and XRF technology sensors. Section 3 describes the demonstration sites. Section 4 presents the demonstration approach with sampling and analytical procedures. Section 5 assesses the technical performance of each system. Section 6 provides cost-related information. Section 7 discusses regulatory issues. Section 8 outlines metal sensor technology implementation. Section 9 reviews lessons learned as a result of the four ESTCP technology demonstrations. Section 10 provides references to cited documents. Two appendices supplement this report: (1) Points of Contact (Appendix A) and (2) Data Archiving (Appendix B).

## 1.1 Background Information

To clean up a hazardous waste site, the contamination at the site must first be delineated. Site characterization can be very costly, accounting for a third or more of the total cleanup cost. Until recently, the most common way to determine the extent of subsurface contamination was to collect samples from soil borings or monitoring wells and send them to a laboratory for analysis. This approach is inefficient and expensive. Furthermore, the trend towards risk-based clean-up strategies may actually dictate that the clean-up process will not require removal and/or treatment, but only long-term monitoring to ensure that there is no unexpected migration of the contaminant. Consequently, improved methods of monitoring contaminants in the subsurface are important for the characterization and the remediation of a site.

The Site Characterization and Analysis Penetrometer System (SCAPS) was developed to address this requirement for improved subsurface measurement of contaminants. SCAPS combines traditional cone penetrometer technology with real-time chemical sensors to rapidly delineate the subsurface distribution of contaminants and hydrogeological conditions. The first chemical sensor fielded with SCAPS, the laser-induced fluorescence (LIF) sensor for petroleum, oils, and lubricants (POLs), has been successfully commercialized (LIEBERMAN, 1998) and has achieved acceptance by the regulatory community, as evidenced by its recent certification by the California Environmental Protection Agency (EPA) (CALIFORNIA ENVIRONMENTAL PROTECTION AGENCY DEPARTMENT OF TOXIC SUBSTANCES CONTROL, 1996) and verification by the US EPA (BUJEWSKI and RUTHERFORD, 1997) as well as numerous states via the Interstate Technology Regulatory Cooperation (ITRC) workgroup (CONE PENETROMETER TASK GROUP REPORT, 1996).

To broaden the applicability of SCAPS, the Strategic Environmental Research and Development Program (SERDP) funded the development of sensor technologies for other contaminants. In particular, sensor systems have been developed for real-time *in situ* field screening of heavy metal contamination in soils. These three heavy metal sensor technologies include two sensor systems that are based on LIBS and the one system based on XRF. All three technologies emerged from the SERDP-sponsored Accelerated Tri-Service SCAPS Sensor Development Program. The major factor limiting full utilization of these heavy metal sensors is the lack of familiarity and, as a result, lack of acceptance of these new, innovative technologies by the environmental community (i.e., users and regulators).

ESTCP has an established program to accelerate acceptance and application of innovative monitoring and site characterization technologies that improve the way the nation manages its environmental problems. The ESTCP helped support demonstration/validation of the LIF

petroleum sensor, the first direct push chemical sensor technology, to build regulatory acceptance for the SCAPS LIF sensor technology. As part of this effort, the SCAPS LIF sensor system and the Rapid Optical Screening Tool (ROST) LIF were evaluated and/or demonstrated in conjunction with several technology certification programs including the following: U.S. EPA–Consortium for Site Characterization Technology; California Environmental Protection Agency (Cal-EPA)–Technology Certification Program; Western Governor’s Association–Committee to Develop Onsite Innovative Technologies (DOIT); and the ITRC program. Experience from these past efforts has shown that obtaining regulatory acceptance does not ensure that users will accept a new technology. Users may invoke lack of regulatory acceptance as a reason for not using a new technology, but regulatory acceptance does not ensure that users will embrace the new technology. Ultimately, for a new technology to become established in the marketplace it must be embraced by the commercial sector. Therefore, it is important to demonstrate and validate the utility and cost-effectiveness of a new technology to viable commercial entities.

For the LIBS and XRF heavy metals sensors, our objective was to promote the commercialization of direct push metal sensor technologies by generating a field performance database that provides side-by-side comparison of the three technologies. Information provided in this database will assist potential commercial developers in selecting which of the three technologies (or features from the individual technologies) are commercially viable for field screening of heavy metal contamination. Note that the current commercial LIF sensor combines the best features of the two original LIF sensor configurations (SCAPS LIF and ROST LIF) tested as part of the original demonstration/validation effort. This combination might not have happened if both sensors had not been tested side-by-side. Consequently, SSC San Diego, formerly NCCOSC RDTE Division, in collaboration with the Naval Research Laboratory (NRL) and the U.S. Army Engineer Research and Development Center (ERDC), under the coordination of the U.S. Army Environmental Center (AEC), has demonstrated three metal sensor systems using the SCAPS platform to facilitate its acceptance and use for field screening of metal contaminants in the subsurface.

## **1.2 Official Department of Defense (DoD) Requirement Statement**

The demonstration of the three SCAPS metal sensing technologies falls under the ESTCP focus area 1. Cleanup, subarea b. Site Characterization.

**1.2.1 How Requirement(s) Were Addressed.** The Site Characterization and Analysis Penetrometer System uses a truck-mounted hydraulic cone penetrometer system to push an

instrumented probe into the ground to depths of up to 100 feet or more. The FO-LIBS, DL-LIBS, and XRF heavy metal sensor probes were configured for deployment on a standard cone penetrometer system. LIBS technology involves the analysis of the spectral emission from a plasma spark formed by focusing a high-energy pulsed laser on a small amount of sample material. FO-LIBS uses a fiber-optic line to deliver the laser light and generate the plasma. The DL-LIBS system uses a laser located in the probe head to generate the spark. Both systems use a fiber-optic cable to collect the emission signal from the sample and transmit the signal to a detector located in the SCAPS truck data acquisition room. The XRF sensor system uses an x-ray source located in the probe to excite the soil sample with x-radiation energy. The x-rays excite metal atoms into a higher energy level and induce the metals atoms to emit fluorescent x-rays at discrete spectral energy levels; these fluorescing x-rays are quantified using a detector located in the probe, and the metals in the soil are identified using spectral analysis techniques.

Site characterization often accounts for approximately one-third of the total cost of remediation at U.S. Department of Defense sites. Demonstrating that penetrometer-deployed metal sensor technologies are effective for real-time delineation of heavy metal contamination at hazardous waste sites will provide a time- and cost-effective alternative to conventional sampling and analysis methods.

### **1.3 Demonstration Purpose and Objectives**

The purpose of the metal sensor technology's demonstration was to generate field data appropriate for verifying the performance of the technology and to facilitate acceptance of SCAPS metals sensor for field screening of heavy metal contamination in the subsurface by the user and regulator communities. To obtain the data required to verify the performance of the three SCAPS metal sensing technologies for field screening of heavy metal contamination in the subsurface, primary and secondary demonstration objectives were identified.

The primary objectives of this demonstration were to evaluate the *in situ* SCAPS metal sensing technologies in the following areas: (1) their performance compared to conventional sampling and analytical methods, (2) the logistical and economic resources necessary to operate the technologies, (3) data quality, and (4) the range of environments in which the technologies can be operated. Secondary objectives for this demonstration were to evaluate the SCAPS metal sensing technologies for reliability, ruggedness, and ease of operation. Performance of the FO-LIBS, the DL-LIBS, and the XRF-based sensor systems were evaluated to determine agreement between data collected *in situ* and verification analytical sample analyses by EPA Method 6010 (inductively coupled plasma emission spectroscopy [ICP]). Additionally, sample

splits from homogenized laboratory samples were re-analyzed with each sensor system to account for any variability due to sampling heterogeneity.

The demonstration evaluated the three SCAPS heavy metal sensing technologies as field-screening methods by comparing the FO-LIBS sensor, the DL-LIBS sensor, and the XRF sensor response to data produced by a conventional sampling and analytical method. For the demonstration, conventional sampling and analysis consisted of pushing a penetrometer soil sampler (e.g., Mostap sampler) in very close proximity (within 8 inches) of the three SCAPS metal sensor push holes, collecting soil samples as close as possible to the push cavities, and analyzing discrete samples for heavy metal contamination by EPA Method 6010. The demonstration objectives were achieved by collecting data during four separate demonstrations. The performance of the three SCAPS metal sensing technologies during each field demonstration were compared to conventional sampling and analytical methods used in site characterization.

#### **1.4 Regulatory Acceptance of SCAPS Innovative Technology**

The major factor limiting full utilization and expedient commercialization of the heavy metals sensor technologies has been lack of acceptance by users and regulators. Users and regulators are often slow to accept new methods and technologies due to limited exposure, inadequate technical understanding, and lack of high-quality validation data. Acceptance requires exposure leading to understanding and comprehensive data validation. Acceptance by the regulatory community will help eliminate a major hurdle that often limits the use of a new technology by the user community. Expedited regulatory and user acceptance will lead to more widespread use of these innovative approaches to mapping underground contaminant plumes at DoD, and other Federal, State, and private sites. These technologies will characterize and monitor activities quickly and effectively, with potential savings of millions of dollars.

#### **1.5 Previous Testing of the Technology**

The sensitivities of all three technical approaches have been documented at or below the regulatory limits for metal-contaminated soils under laboratory conditions. The FO-LIBS probe was successfully field-tested in January 1996. The probe that was tested used a “fixed focal point” design (i.e., laser ablation occurred at the same place on the window). The initial test consisted of six pushes at uncontaminated sites with soils that ranged from medium-grain to coarse-grain silty sand. The emission of naturally occurring Fe in the soil was profiled at depths up to 20 ft. The spectra obtained from a pure Fe powder was shown to overlay with the emission lines observed from the *in situ* soil measurements in the region from 390 nm to 440 nm. In these initial tests, the same probe and window were used for the duration of the experiment and

withstood several thousand laser pulses with no measurable loss in transmission. Subsequent tests encountered difficulties with severe transmission losses due to pitting of the sapphire window. The probe was redesigned to provide a capability to reposition the focusing optics onto an undamaged portion of the window. This “scanning” FO-LIBS probe was field-tested at a lead battery dumpsite at Mare Island Naval Shipyard in April 1997. The distribution of the battery waste at the site was variable. Several contaminated locations were identified that coincided with plastic battery casings and metal at the surface.

After fabrication of the DL-LIBS probe in 1996, it was installed in the SCAPS truck. System checks were conducted at the ERDC to ensure system operability. Then, the DL-LIBS probe was tested at the Louisiana Army Ammunition Plant. Nine pushes were done in a landfill used primarily to dump chromium-bearing sludge. Chromium was readily detected in all holes pushed at the landfill. Field investigations also showed that no meaningful data could be obtained when the probe was pushed below the water table. In August 1997, the DL-LIBS probe conducted field investigations at the Joliet Army Ammunition Plant in Joliet, IL. The DL-LIBS sensor detected lead contamination from lead azide, which was used during fuse manufacturing. Depth profiles indicated a high degree of lead contamination at 2 feet below ground surface (bgs). These field tests demonstrated the probe’s capabilities in soil media ranging from sandy soil to expansive clay soil and its ability to detect two target metals of DoD concern: chromium and lead.

The XRF probe was also tested at the Joliet Army Ammunition Plant in 1997. Eleven pushes were done. Acceptable data were obtained for all the holes pushed.

In the previous testing of the three sensors, confirmational laboratory data were not obtained. The purpose of these initial field investigations was to (1) demonstrate that the LIBS and XRF sensor systems had the capability to obtain field-screening data, and (2) show that the probe configurations were robust.

## 2. Technology Description

This section describes the three SCAPS metal sensor technologies developed by SSC San Diego, NRL, and ERDC, and includes background information and a description of the equipment. General operating procedures, training, and maintenance requirements are also discussed.

### 2.1 Background and Applications

The SCAPS cone penetrometer truck is the platform for a family of new, rapid cone penetrometer test (CPT) field-screening technologies for surficial and subsurface media interrogation for contaminant identification and quantification. The three SCAPS metal sensing technologies that were demonstrated are (1) the fiber optic laser-induced breakdown spectroscopy (FO-LIBS) system (developed and provided by SSC San Diego), (2) the downhole laser-induced breakdown spectroscopy (DL-LIBS) system (developed and provided by ERDC), and (3) the XRF-based sensor system (developed and provided by NRL).

SCAPS metal sensors are *in situ* field-screening tools for characterizing and delineating the subsurface distribution of heavy metal contamination before installing groundwater monitoring wells or soil borings. These methods are not intended to be a complete replacement for traditional soil borings and monitoring wells, but a means of optimizing the placement and reduction of the number of borings and monitoring wells required to achieve site characterization and monitoring of restoration activities.

The three SCAPS metal sensor systems were developed in response to the need for real-time *in situ* measurements of subsurface heavy metal contamination at hazardous waste sites. The SCAPS metal sensor systems perform rapid field screening to determine either the presence or absence of heavy metal contamination within the subsurface media of the site. The site can be further characterized with limited numbers of carefully placed soil samplings, borings, or wells. In addition, remediation efforts can be directed on an expedited basis as a result of the immediate availability of this *in situ* sensor and soil matrix data.

Standard CPT equipment has been widely used in the geotechnical industry for determining soil strength and soil type from measurements of tip resistance and sleeve friction on an instrumented probe. The SCAPS uses a truck-mounted CPT platform to advance chemical and geotechnical-sensing probes. The CPT platform provides a 20-ton static reaction force associated with the weight of the truck. The forward portion of the truck-mounted laboratory is the push room. It contains the penetrometer rods, hydraulic rams, and associated system controllers. The rear

portion of the truck-mounted laboratory is the isolatable data collection room in which components of the instrumentation systems, data acquisition/processing system and onboard computers are located. The combination of reaction mass and hydraulics can advance a 1-m long by 3.57-cm-diameter, threaded-end rod into the ground at a rate of 1 m/min in accordance with ASTM Method D3441, the standard for CPT. The rods, various sensing probes, or sampling tools can be advanced to depths in excess of 50 meters in naturally occurring soils. The platform is fitted with a self-contained decontamination system that allows the rods and probe to be steam cleaned as they are withdrawn from the push hole, through a steam-cleaning manifold, and back into the SCAPS truck rod-handling room. During demonstrations of the heavy metal sensors, soil samples for validation purposes were obtained either by using the soil sampling tool, Mostap 35PS stab sampler, or a hand auger.

**2.1.1 Laser-Induced Breakdown Spectroscopy (LIBS).** LIBS involves the analysis of the spectral emission from a laser-induced spark. The spark is generated by focusing the high-power emission from a pulsed laser onto a small spot on a sample material, resulting in a power density on the sample in excess of several giga watts per square centimeter ( $\text{GW}/\text{cm}^2$ ). Within the small volume about the focal point, rapid heating, vaporization, and ionization of a small amount of sample material occurs. The subsequent laser-induced plasma emission is spectroscopically analyzed to yield qualitative and quantitative information about the elemental species present in the target media.

The LIBS technique has been used successfully in the laboratory to identify and quantify elemental species in solids, liquids, and gases. The method is well-suited to *in situ* detection of heavy metal contamination in soil because it is highly sensitive while requiring no sample preparation. Because the emission of different elements occurs at unique wavelengths, the method can be used for simultaneous analysis of multiple elemental components.

The two LIBS probes developed under SERDP sponsorship differ in the method of delivery of the laser excitation energy that is used to generate the laser-induced spark. In the first configuration, the FO-LIBS uses an optical fiber to deliver the excitation energy from a laser located in the truck to the subsurface media. In the second configuration, DL-LIBS has the laser physically located in the CPT probe.

LIBS can generally be used to excite emission spectra from any atomic species with species-dependent efficiency. To perform LIBS measurements remotely and in real time, as required of CPT-based sensor systems, several operational and design trade-offs must be made between analytical precision and accuracy and timeliness of data collection. Because LIBS techniques

under study use fiber-optic coupling to deliver the emitted spectra to an up-hole spectral data acquisition/processing system, the choice of spectral lines used to characterize the species under study must fall in a spectral range that is consistent with the transmission capability of the optical fiber. Since the LIBS measurements are done *in situ*, there may be soil matrix effects that are due to changes in grain size or moisture content that can affect the intensity of the response of the LIBS systems.

**2.1.1.1 FO-LIBS Sensor.** The FO-LIBS sensor (Figure 1) uses the Q-switched output of a Nd: YAG laser operating at 30 Hz at 1064 nm, which is delivered through a low-OH, fused-silica fiber to the probe. A low *f/#* optical system (with *f/#* ~1) is used in the probe to focus the laser output. This system minimizes the size of the focused image of the optical fiber face on the sample and provides a power density at the sample that is sufficient to generate a laser-induced plasma. The low *f/#* of the focusing system introduces a high dependence of the sample power density on the lens-to-sample distance (Figure 2).

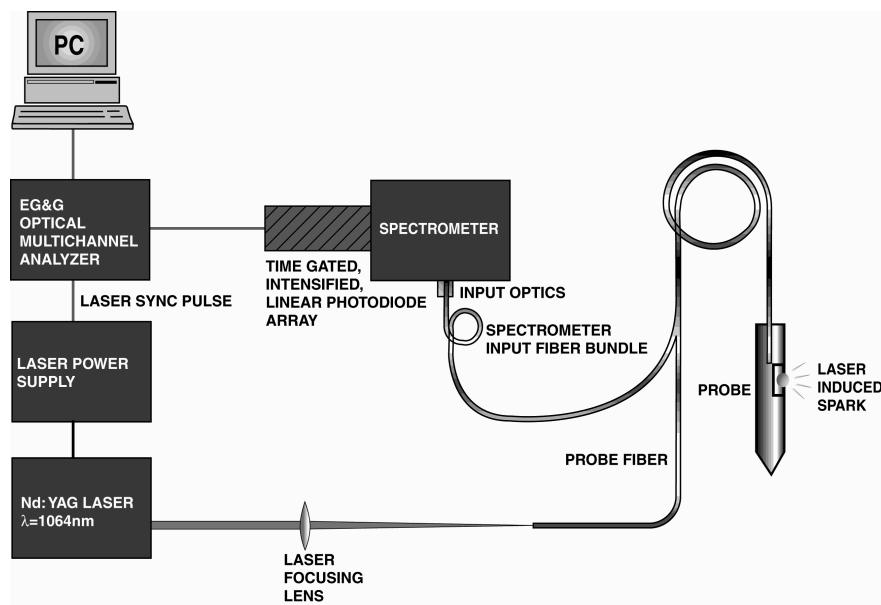


**Figure 1.** Schematic of FO-LIBS System

The design used to keep the sample-to-lens distance fixed to within a small tolerance incorporates a disposable optical window at the sample/probe interface (Figure 3). In this design, the laser energy emitted from the fiber in the probe is collimated, turned by a quartz prism, and focused by a short-focal-length quartz lens through a sapphire window in the side-wall of the probe. Since the soil is pressed against the window, the lens-to-sample distance is fixed. Contamination is not an

issue because the FO-LIBS probe is entirely sealed, allowing for operation in the vadose zone and saturated zones of the subsurface.

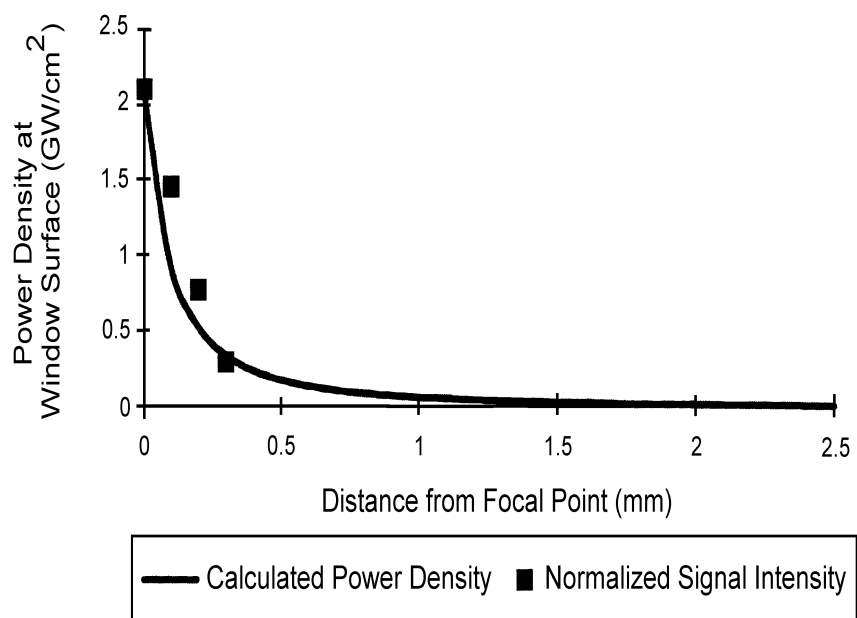


**Figure 2.** Dependence of Sample Power on Lens-to-Sample Distance

The symmetry of the probe optical design for excitation delivery and emission collection is advantageous because the fiber bundle is self-aligned. The choice of a 90° prism rather than a mirror to turn both of the collimated beams (IR excitation and the UV/visible emission) is robust in terms of damage threshold. A prism can also be used in widely separated spectral regions without component substitution. This prism is an attractive feature because LIBS can be used for simultaneous analysis of multiple elemental components.

In an early prototype FO-LIBS system, the sapphire window became pitted by the spark after several thousand laser pulses and reduced laser energy transmission through the window material. To minimize the effect of window pitting on the integrity of the *in situ* data, a system was developed for repositioning the spark on the window surface by scanning the fiber and focusing optics using the modified probe design in Figure 4. This design incorporates two stepping motors to drive a block that houses the optics and provides two-axis control of the position of the spark on the window surface. Because of the relatively small size of the focused spot compared to the size of the sapphire window, the number of discrete positions available is in excess of 1000 (Figure 5). After the window surface has been completely used (typically 1 week of operation), a new window is inserted in the probe window housing at a replacement cost of approximately \$17.00.

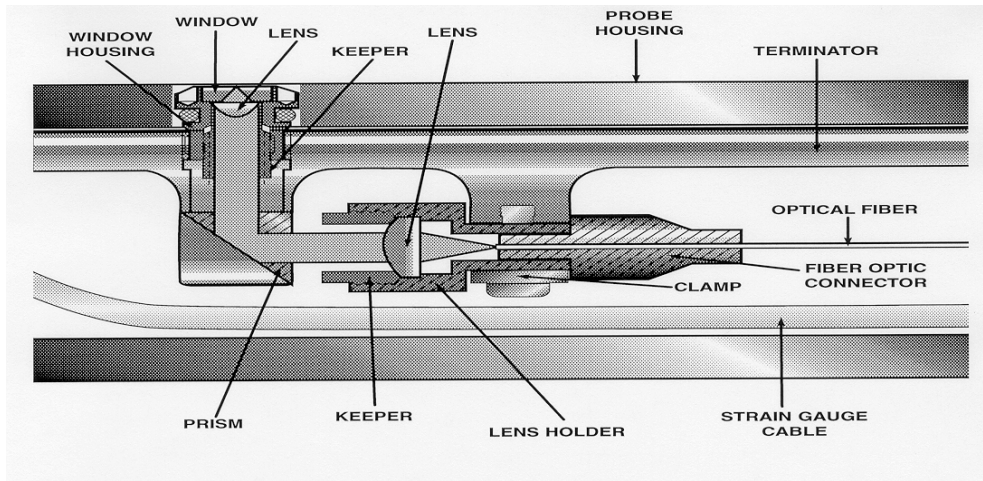


**Figure 3.** FO-LIBS Fixed Sample-to-Lens Distance Design

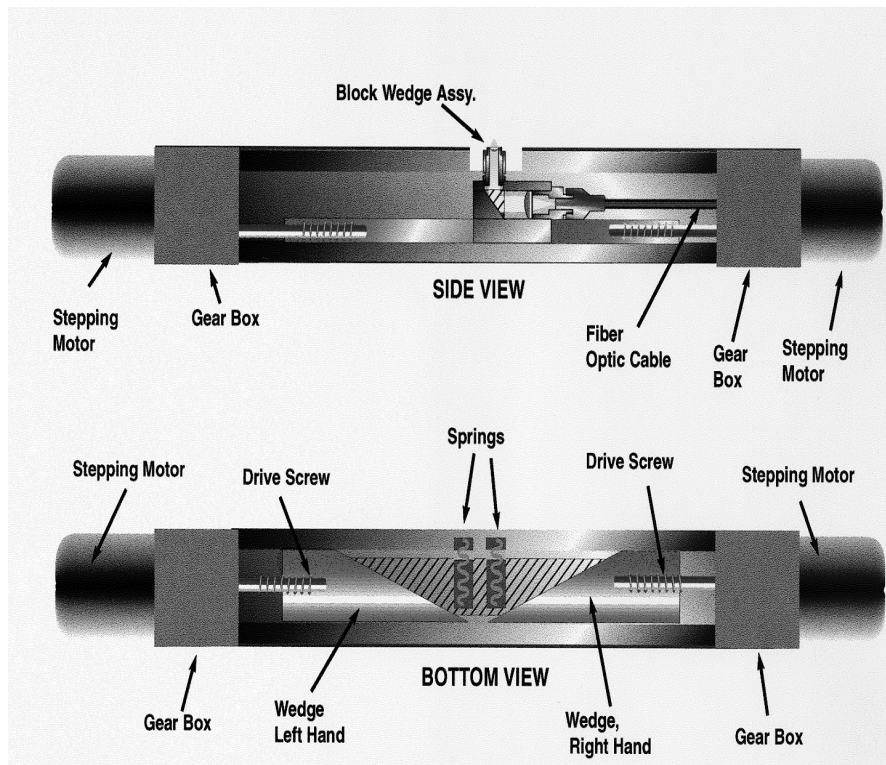


**Figure 4.** Modified FO-LIBS Design with Stepping Motor



**Figure 5.** FO-LIBS Sapphire Windows (Larger Window Shows Concentric Ablation Pattern Generated by Moving the Laser Pulse Across the Window)

The 600- $\mu\text{m}$ -diameter excitation fiber is surrounded by 12 200- $\mu\text{m}$ -diameter, high OH fused-silica collection fibers used to collect the emission light (Figure 1). The spark emission enters the fiber bundle and is transmitted to the surface where it is coupled to a spectrograph that disperses the emitted light onto a time-gated, intensified, linear detector array. The time gating of the detector during data collection is crucial due to the initial broadband background continuum during the evolution of the plasma. Signal resolution is enhanced from the elemental metal emission by delaying the application of the gate pulse to the detector until after the short-lived broadband background has decayed. The duration of the gate pulse is chosen to correspond with the duration of the metal emission to optimize the signal-to-noise ratio. Like the probe design, this configuration is robust and can be operated over a large spectral range, allowing the analysis of different spectral regions with no system adjustment or component substitution.

To reduce the standard deviation of the data, signal averaging is required. Each measurement is the result of, typically, 300 single-shot spectra accumulated in the memory of the detector controller. Because the repetition rate of the laser is 30 Hz, acquisition of 300 spectra requires 10 seconds. Depth resolution can be controlled by the operator and is typically 2 inches.

**2.1.1.2 DL-LIBS Sensor.** There are two significant design differences between the FO-LIBS approach described above and the DL-LIBS sensor systems (Figure 6). First, the DL-LIBS sensor has a miniaturized Nd:YAG excitation laser located in the probe itself. This laser provides much higher irradiances ( $1000 \text{ GW}/\text{cm}^2$ ) than a fiber-illuminated system for two

reasons: (1) the fiber has a limit to the amount of energy that can be successfully transmitted through it without damage (fiber-based LIBS system's pulse energies are often limited by this fact), and (2) a multimode fiber system as used in FO-LIBS can never achieve diffraction limited focused spot sizes and must spread the laser energy over a larger area. Hence, the FO-LIBS system delivers less laser energy to the sample media than the DL-LIBS that is configured with the laser in the probe. Additionally, the DL-LIBS system uses a relatively slow f/3.2 optical transmit section that provides a large depth of focus that minimizes the effect soil position has on irradiance.

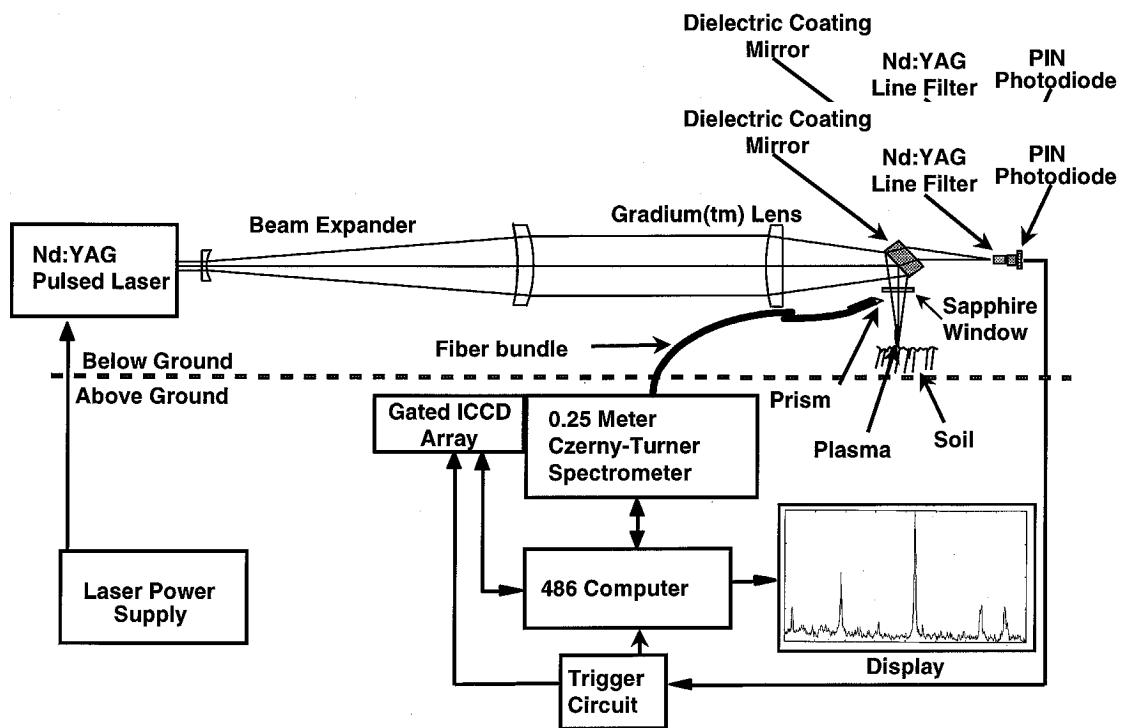


**Figure 6.** Schematic of DL-LIBS Sensor

A second significant difference is that the sapphire output window is recessed from the soil wall (Figure 6). Unlike a window in contact with the soil, a recessed window is not subject to pitting when the laser is fired. Laser energy is focused directly onto the soil (without passing through a fiber) as the probe is withdrawn from the push hole. This approach uses a special probe design with a drop-off sacrificial sleeve that covers and protects the recessed window during penetration. The sleeve slides off the probe during retraction and is left at the bottom of the hole. Together, these offer the potential of high-peak power densities and plasma temperature, thereby maximizing the ionization of the soil/contaminant sample.

The DL-LIBS sensor uses a non-imaging optical receiver design. There are no intervening focusing optics between the spark and fiber. Although non-imaging optical receivers may be less efficient than imaging optical receivers that use focusing optics, non-imaging systems do not suffer from spectral bias. All species radiating from the plasma are collected equally.

DL-LIBS collects different data in the penetration and retraction modes. All downhole data is recorded on the computer's hard disk as it is acquired. During penetration, the DL-LIBS system collects cone force, sleeve resistance, hydraulic ram force, and inferred soil classification as a function of depth. During retraction, DL-LIBS data are collected as a function of depth in the form of integer counts per unit time per wavelength interval for all wavelengths in the spectral region of interrogation. Typically, the DL-LIBS probe integrates for 100 microseconds ( $\mu\text{sec}$ ) to achieve the sensor detection limits for average concentrations. Subsurface media interrogation is conducted every 5 seconds and provides spatial resolution of approximately 1.3 cm per sample interrogation.

In LIBS, the sensor response is determined by plasma conditions and optical detection parameters. In general, the hotter the plasma, the stronger the LIBS signal; in practice, the plasma becomes reflective as the plasma temperature increases so there is a limit to the plasma temperature that can be achieved. This is simply a direct result of Planck's blackbody law. In theory, the actual LIBS transition spectra could be calculated with the right inputs. For instance, the actual energy produced by a single transition is a complex combination of assumptions of the plasma condition (e.g., the plasma is in local thermodynamic equilibrium, the plasma is optically thin, etc.) and parameters such as the single particle partition function, the transition probability, level degeneracy, plasma size, species number, and plasma temperature. In general, predictions of plasma conditions based on plasma physics have much uncertainty, even with simple scenarios such as plasma formation in a gas. This uncertainty is partially due to the uncertainty in the tabulated transition probabilities that are often quoted as having accuracies of  $\pm 15\%$  or worse. Thus, accurately calculating plasma signatures in a plasma of unknown size that is formed on the interface of a constantly changing granular matrix (soil) and air is almost impossible.

The efficiency of the detection system, i.e., how much light it collects, increases system response in a linear fashion. Likewise, the detector response factor, often specified in amps/watts of incident radiation, governs the optical-to-electrical efficiency of the detector itself. Lastly, DL-LIBS, like most other LIBS systems, is a gated system and, as such, has an integration window. The onset of integration and the integration duration affect the total recorded signal.

Detection limits for DL-LIBS are dependent on the standard deviation of the background or low concentration sample measurements. The three-sigma detection limit is defined as the concentration (determined via the instrument calibration curve) corresponding to three times the standard deviation of the normalized intensity of the metal peak of interest divided by the slope of the concentration curve. In DL-LIBS, the peak intensity of the metal of interest is divided by the integral of all intensities in the spectrum. This normalization aids in reducing the effects of shot to shot pulse energy variation. In a typical soil matrix, the detection limit for the SCAPS DL-LIBS Metals Sensor is 100 ppm for lead contamination.

**2.1.2 X-Ray Fluorescence (XRF) Sensor.** X-ray fluorescence operates by detecting characteristic x-radiation energy emitted by excited atoms in a sample. When an x-ray source bombards a sample with incident x-radiation energy, the atoms undergoing interrogation are excited and emit fluorescent x-ray energy that is detected as a function of the energy of the x-rays. At the atomic level, an incident x-ray excites an electron into a higher energy level, which then decays and produces a fluorescing x-ray. Since the electron energy states producing a fluorescent x-ray are entirely within the atom, the x-ray is produced with a constant and discrete energy level that is different for each elemental atom.

X-ray fluorescence is a well-established, non-destructive method of determining elemental concentrations at parts per million (ppm) levels in complex samples. It operates with no sample preparation. It is currently used as a laboratory analysis method for samples obtained from hazardous waste sites and its characteristics are ideally suited to field analysis applications.

Recent advances in instrumentation have allowed the construction of a spectrometer that will meet the size restrictions imposed by the diameter of the cone penetrometer probe. Figure 7 shows this configuration. High sensitivities can be achieved while the head is stationary for several minutes. Continuous monitoring at lower sensitivities is possible depending on descent rates, contaminant concentration, and soil type.

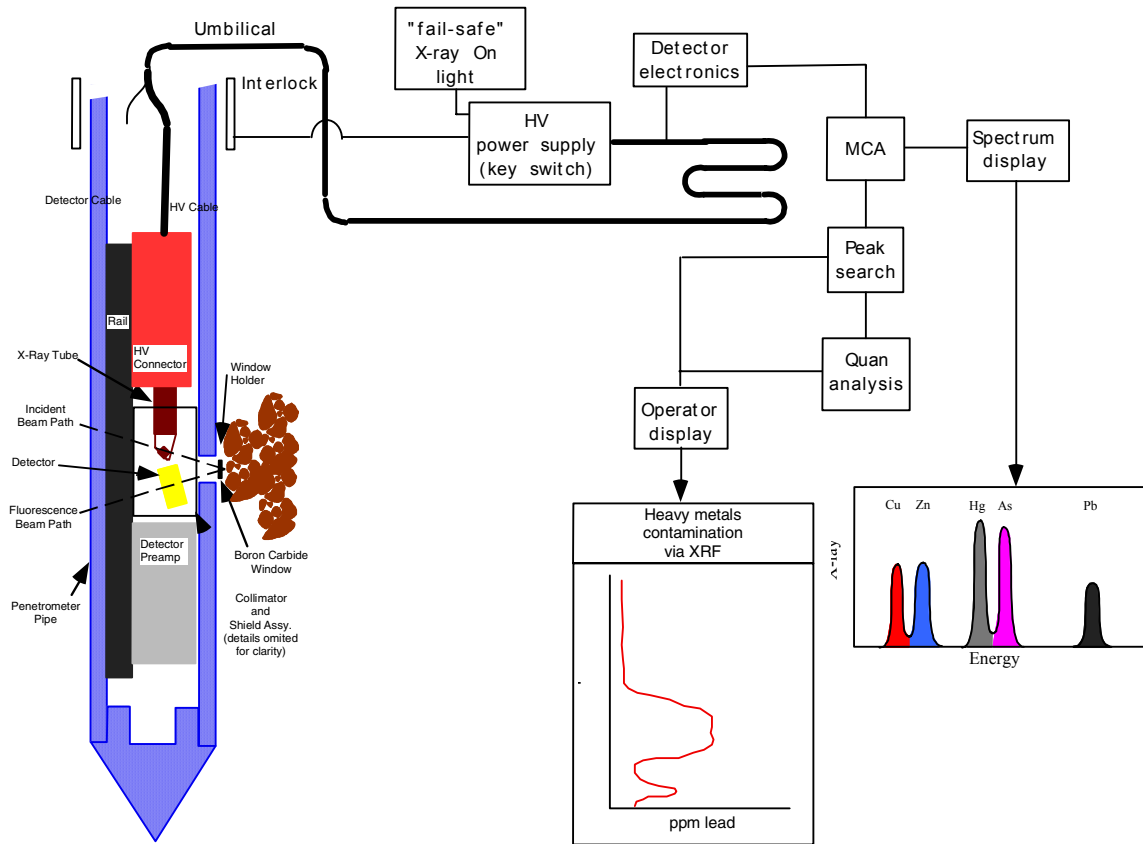


**Figure 7.** Schematic of NRL XRF Sensor

The XRF metals sensor consists of three subsystems (Figure 7): the below-ground probe, the umbilical cable, and the above-ground electronics package and data processing system. The probe contains the x-ray source, detector and preamplifier, appropriate x-ray optics, the mounting system, and a rugged x-ray transparent window. The SCAPS XRF metals sensor uses a sealed x-ray tube as the excitation source to achieve adequate detection limits in the allotted time and to avoid the licensing and safety issues of a radioactive source. The detector is a silicon P-type/Intrinsic/N-type (Si-PIN) diode in a small case with self-contained cooling that is connected to a low-noise preamp. The preamplifier provides sufficient signal to drive the umbilical cable. The x-ray window is usually a 1-mm thick boron carbide, a low atomic number material that is relatively transparent to x-rays in the relevant energy range. A thinner window is used for less sensitive metals such as chromium.

The umbilical cable conducts the high voltage required to operate the x-ray tube, the electronics and cooling power for the detector and preamplifier, and transmits the signal pulses from the detector to the surface for processing. The umbilical cable is fully shielded for noise immunity and high-voltage safety and may be configured for stratigraphy sensors.

The above-ground electronics package contains the x-ray tube power supply with safety interlocks and the driver electronics for the detector. The x-ray power supply for the x-ray tube provides adjustable high voltage (to 30 kV) and filament voltage, which is regulated to provide constant emission current and, thus, constant x-ray output. The detector electronics provides the necessary power supplies and contains pulse-shaping circuitry. The detector cable connects to a standard multichannel analyzer for data collection and analysis. The electronics package connects to an interlock shield that ensures that the probe is inserted into the ground before the x-ray tube is energized. This shield also allows test samples to be measured above ground through a sample introduction port. This port allows calibration samples, blanks, and test samples to be run during field operations without danger of x-ray exposure to operational personnel. The remainder of the above-ground system consists of a multichannel analyzer and portable computers to collect, process, and display the data.

Once the sensor window is brought into contact with the subsurface soils, the x-ray tube is energized and an XRF spectrum is collected for 100 seconds. This spectrum is then stored and analyzed in accordance with the methods outlined below. This data acquisition process takes a few seconds while the sensor is moved to a new depth and the process repeated. This method of operation provides the best detection limits, but requires collecting data at each depth. The sensor can also be used in a continuous mode where data are collected during descent. Any hot spots will be visible as rapid changes in the spectrum and can be investigated as desired. The entire 100-second spectrum indicates the average analyte concentration throughout the depth covered during spectrum collection. The continuous operation made provides a compromise between detection limits, quantitation, and rapid survey coverage. Experiments have determined that a push rate of 0.5 cm/sec is ideal for this purpose. Hot spots above 2000 ppm can be detected on the fly (UNSELL, 1998) while the ability to achieve the sensor detection limits for average concentrations is retained.

Detection limits for x-ray fluorescence spectra depend almost entirely on counting statistics in the spectrum. The three-sigma detection limit is defined as the concentration (determined via the instrument calibration curve) corresponding to three times the standard deviation of the background intensity under the peak (measured on a low-concentration sample or on the same region of the spectrum from a blank). The standard deviation is the square root of the number of x-ray counts. This method provides a reliable limit for detection by automated peak calculation algorithms. The limit of quantitation is 10 times this standard deviation. A typical detection limit for the SCAPS XRF Metals Sensor is 100 ppm for lead.

XRF is a well-developed and widely accepted method for measuring metal content. Its capabilities are well-known and its comparability to laboratory analysis results has been documented (MCDONALD et al., 1996). Matrix and interference effects are thoroughly understood and it is the subject of a draft EPA method entitled "Field Portable X-ray Fluorescence Spectrometry for the Determination of Elemental Concentrations in Soil and Sediment" (FORDHAM, 1997). Its only weakness is that detection limits for most metals are in the 10-ppm range with current instruments.

## **2.2 Advantages and Limitations of the Technology**

**2.2.1 Comparison to Current Technology.** Because there are no other methods currently available for the real-time *in situ* delineation of metal contamination in soils, the primary advantage of the three metal sensor technologies is that they provide a completely new capability for the *in situ* field-screening of metals. The CPT configuration quickly and cost-effectively distinguishes heavy metal-contaminated areas from uncontaminated areas. The CPT platform allows further investigation and remediation decisions to be made more efficiently and greatly reduces the number of samples that must be submitted to laboratories for analysis. In addition, the SCAPS truck characterizes contaminated sites with minimal exposure of site personnel and the community to toxic contaminants, and minimizes the volume of investigation-derived waste (IDW) generated during typical drill and sample characterization activities. By achieving rapid cost-effective site characterization, resources can be directed to studying the actual risks posed by the hazardous waste site and for remediation activities.

**2.2.2 Comparison to Competing New Technologies.** No other new technologies for real-time *in situ* delineation of metal contamination in soil are known. The results of this ESTCP effort will allow an informed evaluation to be made of each method.

**2.2.3 Limits of the Technology.** The three technologies under study were designed for cone penetrometer truck deployment. In the demonstrations of the technologies, the three sensor systems were deployed using standard 20-ton cone penetrometer push vehicles. Two demonstrations were conducted using the Army (ERDC) SCAPS research and development cone penetrometer system and two demonstrations were conducted using the Navy (SSC San Diego) system. Consequently, these demonstrations were subject to the push limits of this particular type of CPT platform. The dimensions of the truck require a minimum access width of 10 feet and a height clearance of 15 feet. It is conceivable that some sites, or certain areas of sites, might not be accessible to a vehicle the size of the 20-ton CPT truck. Note that the access limits for a

20-ton CPT vehicle are similar to those for conventional drill rigs and heavy excavation equipment. Although standard 20-ton CPT trucks were used for all demonstrations conducted as part of this study, experience has shown that at many sites, heavy metal contamination is frequently confined to the upper 20 feet. The three SCAPS metal sensors may also be deployed using a lighter weight vehicle with fewer access limitations. Regardless of the support platform used in the deployment of these sensors, the CPT sensors and sampling tools may be difficult to advance in subsurface lithologies containing cemented sands and clays, buried debris, gravel, cobbles, boulders, and shallow bedrock. As with all intrusive site characterization methods, it is extremely important that all underground utilities and structures be located before undertaking site characterization activities.

**2.2.3.1 Limitations of the LIBS Technique for *in situ* Measurement.** Because of the high specificity of the line spectra obtainable from LIBS measurements, the method is, in general, qualitatively very good for identification of most metal contaminants. The primary limitation on the qualitative *in situ* identification of a particular species is the presence of other species that may have interfering spectra. For example, a naturally occurring species that contains a high density of lines throughout the visible spectrum is iron. Resolution of the spectrum of a given contaminant above the background (primarily iron) is a matter of using a spectrometer with adequate dispersion in the spectral region of interest, and is not generally a problem. Because of the manner in which the two LIBS methods ablate a small sample (typically  $\sim 10^{-9}$  g) of soil per measurement, they are essentially point measurement methods that are subject to sampling errors that can be reduced by spatial signal averaging. This averaging can be achieved by sampling with high spatial resolution. Due to the relatively high standard deviation associated with a single LIBS measurement, temporal signal averaging is used to reduce the detection limit. Variation in soil matrix is another factor that potentially limits the analytical precision and accuracy associated with LIBS measurements. As discussed in Section 5 of this report, site-specific calibration curves are used to minimize the effect of variations in the soil matrix. Another potential limitation of using optical fibers for transmitting the emission signal to the detector system is the relatively high attenuation of the optical fibers in the deep ultra-violet spectral range, which may limit the use of some emission lines for some elements. However, most elements have multiple emission lines and provide usable lines within the working range of the fiber.

**2.2.3.1.1 FO-LIBS Sensor Specific Limitations.** The major limitation of the FO-LIBS sensor was degradation of the window, which was overcome by the scanning optical

system. There are no specific limitations other than those typical of LIBS in general, as listed in the previous section.

**2.2.3.1.2 DL-LIBS Sensor Specific Limitations.** There are no known limitations to the type of atomic element that DL-LIBS can detect. Due to the very high irradiances (1000 GW/cm<sup>2</sup>) that can be achieved with DL-LIBS, even elements with difficult to excite transitions can be detected.

Because DL-LIBS uses a compact laser in the probe, it has certain restrictions because of its ultra-small size. The primary limitation is pulse rate; the laser is currently limited to 1/3 Hz with ambient laser cooling. If the laser is cooled by liquid, the pulse rate can reach 1 to 2 Hz. For the current DL-LIBS configuration, the lifetime of the laser will be dramatically reduced if pulse rates exceed 1/3 Hz.

The optical window, which protects the interior of the DL-LIBS probe from water leakage, is recessed. The laser energy used to create the micro-plasma is focused in front of this window. Consequently, there is a gap between the focal point and the optical window. If the probe is pushed into the saturated zone, this slot may fill with soil and the sensor will not obtain data. Hence, the current DL-LIBS probe is limited to the vadose zone.

**2.2.3.2 XRF Sensor Limitations.** Certain x-ray lines from different elements occur at energies very close in energy and, thus, overlap in the spectrum. The cooled Si-PIN detector in the SCAPS XRF Metals Sensor has an energy resolution of 250 eV, which resolves all but the most severe overlaps. A typical example is the overlap of the K-beta line of an element with the K-alpha line of an element with one lower atomic number. Since the interfering K-beta line is 5 to 10 times weaker than the K-alpha line, the interfering metal must be present at large concentrations to cause a problem. Another example is the lead (Pb) L-alpha line interference with the Arsenic (As) K-alpha line. Lead can be measured using the L-beta line to avoid the interference with little or no loss of sensitivity. In the presence of large amounts of lead, arsenic must be measured with the As K-beta line, whose lower intensity causes a corresponding loss of sensitivity.

**2.2.3.3 Matrix and Moisture Effects.** XRF sensor response is affected to some extent by the composition and particle size of the soil matrix, but the effect is not serious for field-screening usage. For the XRF sensor, soil moisture effects for zero to about 20% moisture are negligible. For saturated soils, the effect is about 20%. The most significant effects are from

other heavy metals present and from the size of the metal particles. Since lead oxide is 98% lead by weight, lead present in the form of lead oxide particles will absorb x-rays depending on their size, and will affect the signal accordingly. For example, lead sulfide with a particle size of 12 microns reduces the signal by about 20% (CRISS, 1976). If the lead is dispersed on the soil, then the signal is not affected. Since the soil consists mostly of low atomic number materials, the particle size of the soil has little effect.

Matrix and moisture also affect the LIBS technology sensors. The primary variables that affect quantification of the LIBS measurement are soil moisture and soil grain size (MILES, CORTEZ, and CESPEDES, 1992), (THERIAULT, BOSS, and LIEBERMAN, 1999). Specifically, given two soils with the same contamination level, a clay soil will exhibit a weaker LIBS signal than a sandy soil. Likewise, a wet soil will exhibit a weaker signal than a dry soil of the same contamination. For these reasons, LIBS sensor responses are more accurate in dry soil and when the effects of soil moisture and soil grain size are monitored and used in the calibration algorithms. Other research has indicated that soil pH may also have an effect on LIBS signals (CORTEZ, CESPEDES, and MILES, 1996).

The presence of complex mixtures of contaminants (e.g., a site where organic contaminants are present along with heavy metals) is not expected to significantly affect the performance of either LIBS or XRF metal sensors. Both sensor technologies are highly specific for the target analytes. Because extremely high temperatures are generated during plasma in LIBS analysis, it is expected that organic compounds will be broken down to elemental species during the analysis. LIBS has been used successfully to quantify metals directly in oil (FICHET et al., 2001). For XRF, the presence of organic contaminants and heavy metals would not affect the detection abilities of the XRF sensor significantly. High levels of organics may cause as much as 10 to 15% in quantitation errors due to the difference in matrix absorption versus typical (aluminosilicate) soils.

### **2.3 Factors Influencing Cost and Performance**

As with any measurement, the cost for a site investigation is dependent upon the number of samples analyzed. For the CPT-deployed metal sensors, this represents the number of data points collected. The number of data points collected is a function of the number of pushes and the depth per push. Thus, the major factor influencing cost at a site is the aerial extent to be investigated, i.e., the size of the site. For the SCAPS system, cost is normally quoted on a per day basis assuming a specified production rate, and includes all facets of operation (field crew

labor, permits, plans and data reporting, transit time to and from the site, and the SCAPS CPT truck).

Many site and system factors affect performance. Penetrometer limitations prevent use in hilly terrain and in some soils such as conglomerate with cobbles and boulders or cemented material. The contaminant metal as well as soil matrix effects and soil moisture content affect LIBS system sensitivity. For the FO-LIBS system, performance can be affected by system alignment and fiber length. Coupling efficiency due to alignment and attenuation over the fiber length influence the amount of excitation energy out of the probe window and emission energy delivered to the detector. These same factors can impact the DL-LIBS system. Because the optical window, which protects the interior of the DL-LIBS probe from water leakage, is recessed, the DL-LIBS probe can only be used reliably in the vadose zone. In the saturated zone, the slot of the DL-LIBS system may fill with silt and the sensor can no longer obtain data. For the XRF system, alignment is not as critical an issue. The mechanical mounting keeps the sensor components in alignment with an approximate tolerance of 0.020 inches. The biggest factors that affect the performance of the XRF sensor are the window thickness and window purity.

### 3. Site/Facility Description

#### 3.1 Background

Early on, it was decided that two demonstrations would take place at east coast sites and two at west coast sites. The sites that were selected for technology demonstrations had to meet the following criteria:

- The US Department of Defense (DoD) (as site owner) agreed to allow access to the site for the demonstration.
- The site is accessible to two-wheel drive vehicles.
- The soils at the site have been contaminated by heavy metals that are detectable by the three SCAPS metal sensor technologies.
- The soil types at the site consist of unconsolidated sediments of sands, silts, clays, and gravel. These soil types are suitable for CPT pushing and present acceptable subsurface matrices for the three SCAPS metal sensor technologies.
- The soil contaminant levels identified during previous investigations ranged from below analytical laboratory detection limits to heavily impacted. These data indicate contamination in the subsurface in concentration ranges comparable with the SCAPS metal sensing technologies to be demonstrated.

The first demonstration was conducted at the Lake City Army Ammunition Plant (LCAAP), Independence, MO. The second demonstration site was conducted at the Industrial Waste Treatment Plant (IWTP) at Naval Air Station, North Island, CA. The third demonstration was at the former ship repair area, which is part of Parcel D at Hunters Point Shipyard, San Francisco, CA. The fourth demonstration site was at Camp Keller Small Arms Range that is part of Keesler Air Force Base in Mississippi.

#### 3.2 Site/Facility Description

**3.2.1 LCAAP, Independence, MO.** LCAAP is located in Jackson County, MO, mostly within the eastern corporate boundary of Independence, Missouri, and 23 miles east of Kansas City, MO. Figure 8 shows the general location of LCAAP. Lake City is situated at the intersection of Highway 78 (23<sup>rd</sup> Street, Independence, MO) and Highway 7, 5 miles north of Blue Springs, MO. The SCAPS metal sensors evaluated LCAAP Site 30, a Demolition Dump. Figure 9 shows the map for this site.

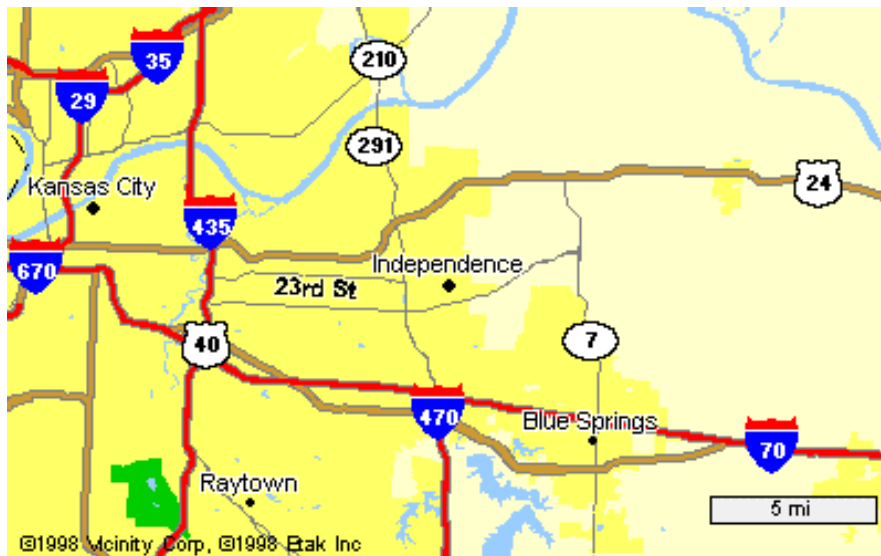


**Figure 8.** LCAAP Independence, MO, Location Map

LCAAP was the first new government-owned facility in the early 1940s to expand small-arms ammunition production. Operations at LCAAP (i.e., the manufacture, storage, and testing of ammunition) led to the use of various process waste treatment systems and onsite disposal. Chemicals used onsite in the production process include soaps, detergents, bleaches, hydrochloric acid, sulfuric acid, nitric acid, explosive compounds (e.g., lead azide and lead styphnate), phosphate cleaners, petroleum and lubricating oils, trichloroethane, trichloroethene, and other cleaning solvents. The waste for the production areas includes mixtures and reaction products of these chemicals. Previous investigations have indicated that heavy metals, including arsenic (As), barium (Ba), beryllium (Be), cadmium (Cd), chromium (Cr), copper (Cu), lead (Pb), mercury (Hg), nickel (Ni), silver (Ag) and zinc (Zn), are present on the surface and/or at depths up to 10 feet. These previous investigations were summarized in a report entitled, “Investigation Report of Operable Unit LCAAP Independence, Missouri” (EA ENGINEERING SCIENCE AND TECHNOLOGY, 1994).

The Area 30 Demolition Dump is located in the northwest portion of LCAAP. This site is near the LCAAP boundary and adjacent to the community of Lake City. It was used by the LCAAP fire department from 1951 to 1967 to burn wooden boxes. Antimony, barium, cadmium, copper, lead, mercury, silver and zinc have been detected above background. Antimony, lead, and copper have been found in high levels on the surface and 5 to 7.5 feet bgs. Detection of lead ranged from 200,000 ppm at depth to 25,000 ppm on the surface. Lead contamination was evaluated at this site by the three SCAPS heavy metal sensors.





**Figure 10.** NASNI San Diego, CA, Location Map

NASNI was commissioned in 1917 and used to train pilots and aircraft mechanics. Operations at NASNI, including the repair and service of fleet squadrons, have resulted in the use of various waste processing systems and onsite disposal. The IWT/OWTP was built in 1972 and used to process nine waste streams containing hazardous materials.

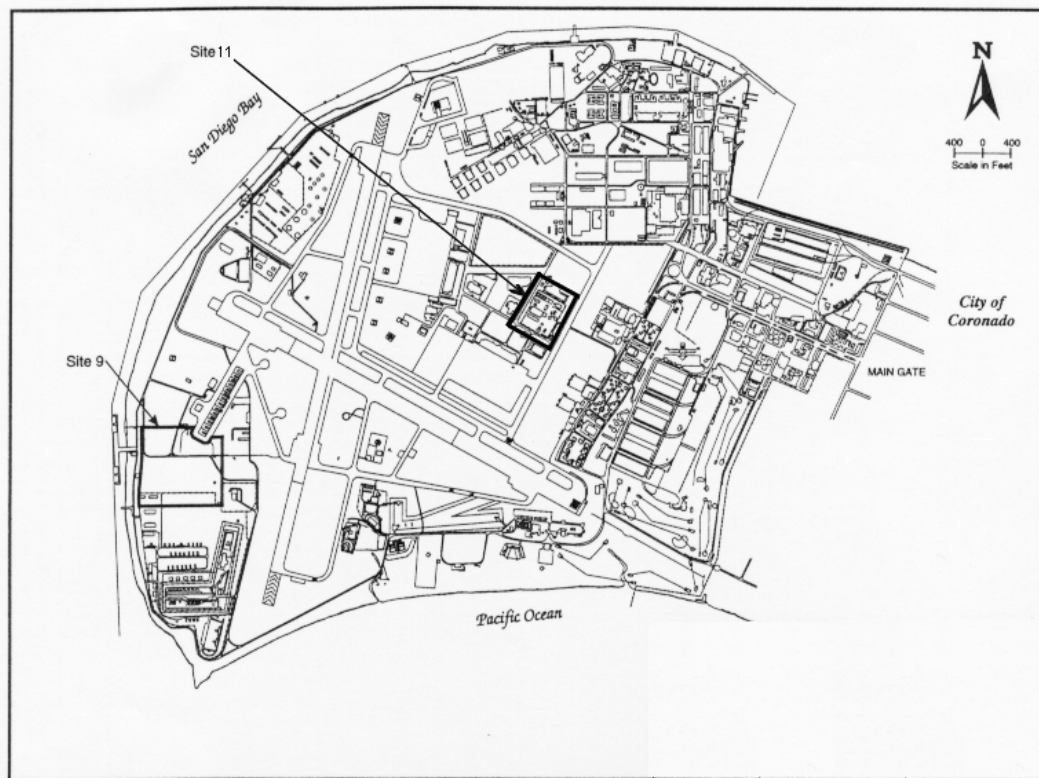


**Figure 11.** IWTP (Site 11) Site Map

Initially, most of the wastes were disposed of in unlined impoundments. In 1976, the unlined surface impoundments were lined with either concrete or PVC. Before liner installation, approximately 12 inches of contaminated soils were removed from the surface of each impoundment. The Paint Basin (Figure 12) is one of four waste sludge basins built in 1973 on the east side of the IWTP. It was used for evaporation of paint chip sludge from water curtain spray booths and consisted of one concrete-lined basin that measured 25 feet by 25 feet by 3 feet deep. The concrete liners were reinforced with steel rods, with each liner being approximately 4 inches thick. However, several cracks were found along the joints where the basin floors intersected the sidewalls. These cracks provided the most probable conduits for contaminant leakage and migration into the underlying sediments. Previous investigations have indicated that heavy metals, including primarily chromium (Cr) with much smaller amounts of barium (Ba), cadmium (Cd), copper (Cu), lead (Pb), nickel (Ni), and zinc (Zn), are present beneath the Paint Basin. These previous investigations were completed by the Hazardous Waste Remedial Actions Program (HAZWRAP) of Martin Marietta Energy Systems, Inc. This effort was documented in the NASNI, Site 11, Final Site Characterization Report dated January 20, 1995. The three SCAPS heavy metal sensors were deployed to evaluate chromium contamination at this site.

The NASNI Industrial Waste Treatment Paint Basin is above sand and silt sediments of the Late Pleistocene Bay Point Formation, which is composed primarily of marine, fossiliferous, loosely consolidated fine to medium grained brown sand, underlain by undifferentiated granitic rocks of the Southern California Batholith and prebatholithic metavolcanic rocks. Groundwater is present at approximately 20 feet bgs, but is subject to minor fluctuations as a result of tidal forces. The terrain is topographically flat. The concrete liner of the paint basin is in place and contains holes drilled from previous investigations.

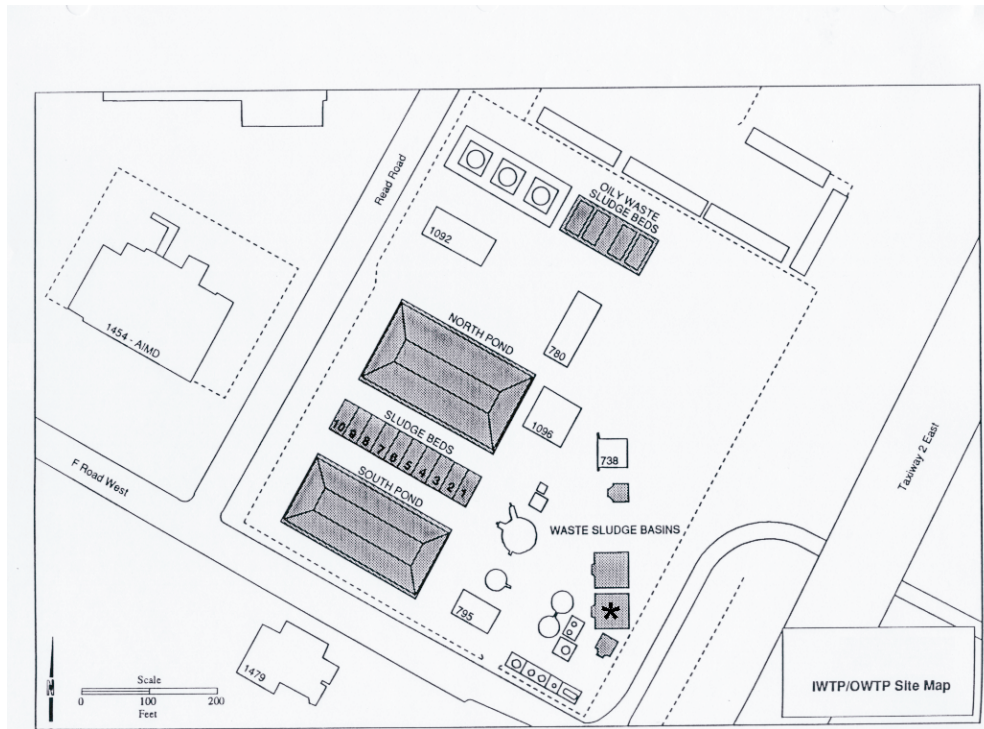


**Figure 12.** Detailed Map of IWTP Site (\* Indicates the Paint Waste Sludge Basin).

### 3.2.3 Former Ship Repair Area (Parcel D), Hunters Point Shipyard, San Francisco, CA.

The main portion of Hunters Point Shipyard (HPS) is situated on a long promontory located in the southeastern part of San Francisco extending eastward into San Francisco Bay (Figure 13). The promontory is bounded on the north and east by San Francisco Bay and on the south and west by the Bayview Hunters Point district of San Francisco. The HPS property consists of about 936 acres, 493 of which are on land and 443 of which are below bay waters. Parcel D is a 128-acre tract of land located in the southeast central portion of HPS (Figure 14). Parcel D is bounded by Parcels A, C, E, and San Francisco Bay.

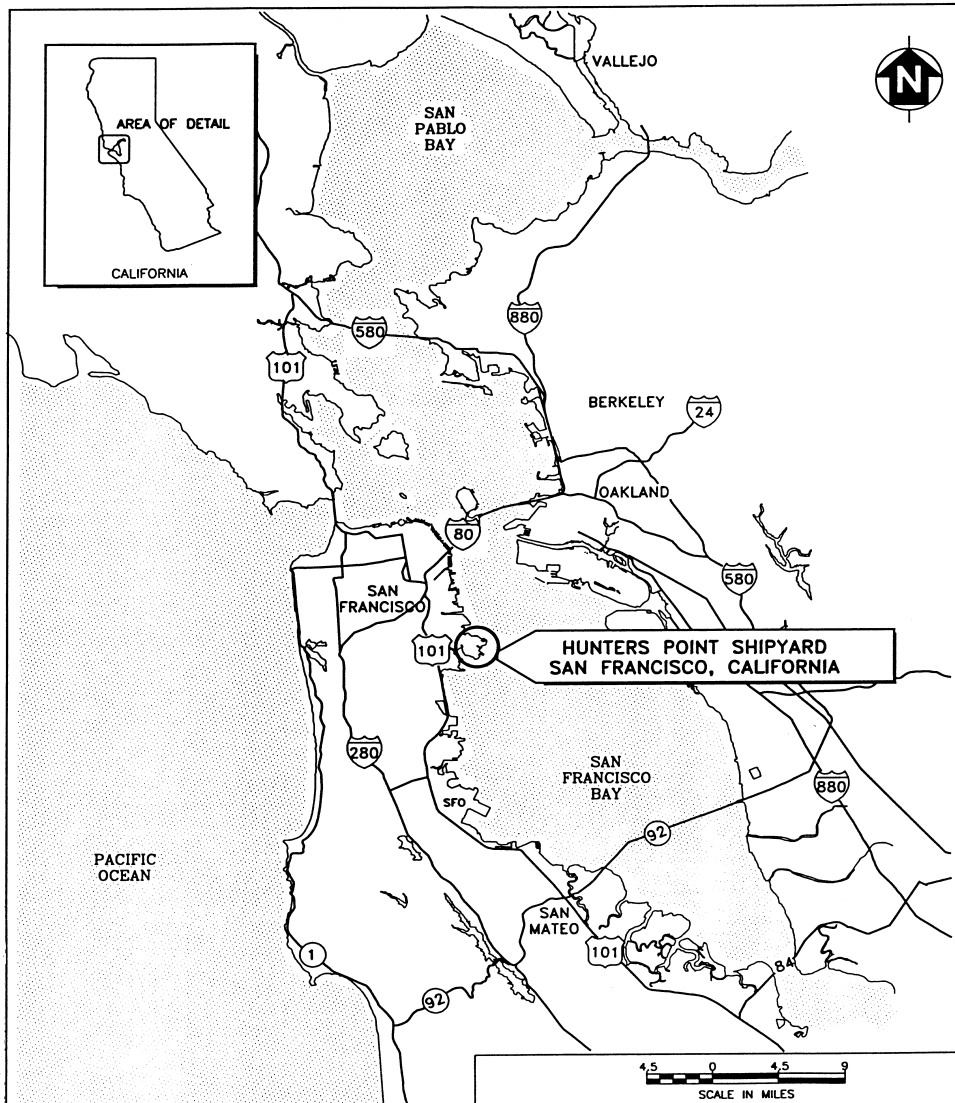


**Figure 13.** Site Map of Hunters Point Shipyard, San Francisco, CA

The land at HPS can be divided into three functional areas: (1) the industrial production area, which consists of the waterfront and shop facilities for the structural machinery, electrical, and HPS service groups; (2) the industrial support area, which consists of supply and public works facility; and (3) the non-industrial area, which consists of former Navy personnel residential facilities and recreation areas. The former ship repair area in the south and southwest portions of HPS (Parcel D) was investigated. Figure 14 shows the location of Parcel D at HPS as well as the installation restoration (IR) areas within Parcel D.

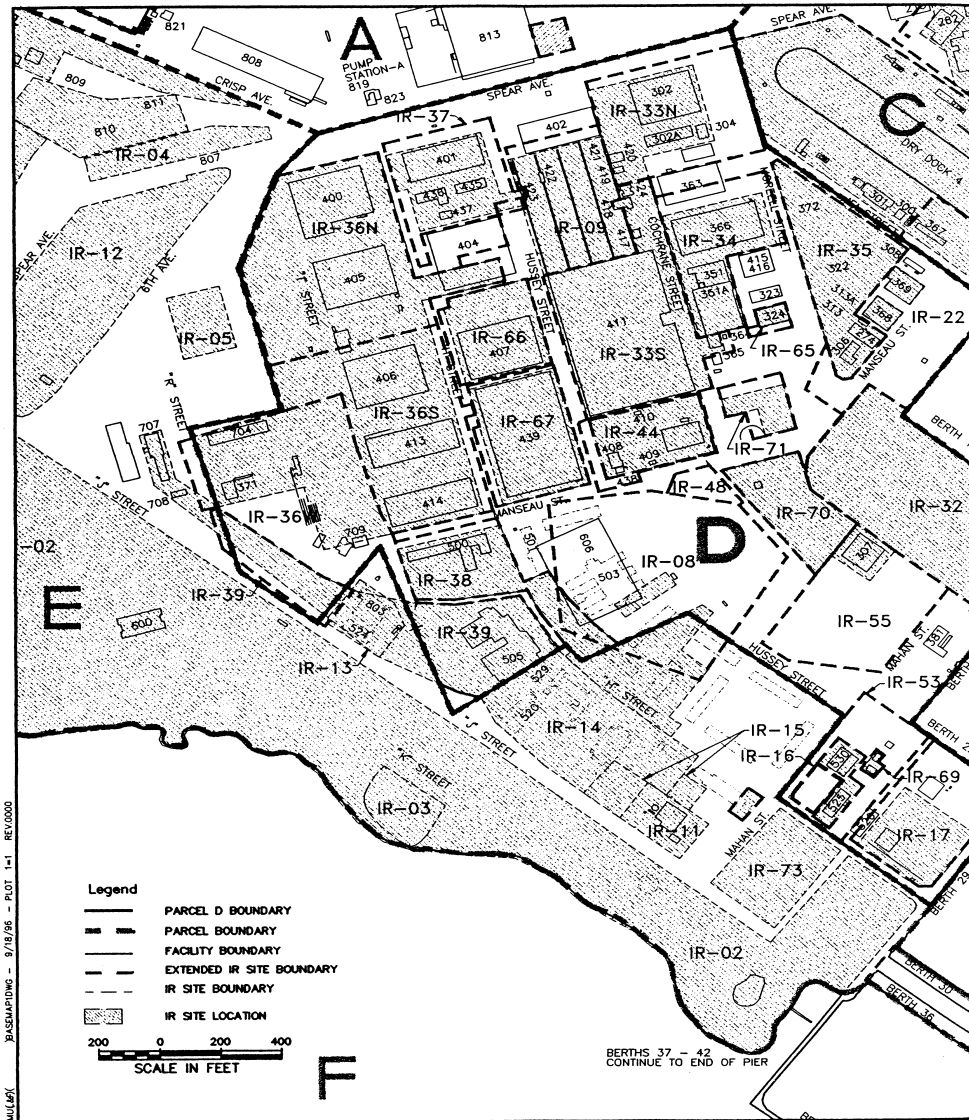


**Figure 14.** Location of Parcel D at Hunters Point Shipyard, San Francisco, CA

The promontory on which HPS is located has been recorded in maritime history since 1776, first as Spanish mission lands used for cattle grazing and later, in the 1840s, for its dry dock facilities. The Treasure Island Naval Station-Hunters Point Annex, also known as the Hunters Point Naval Shipyard, was established in 1869 as the first dry dock on the Pacific Coast. In 1940, the Navy obtained ownership of the shipyard for ship building, repair, and maintenance activities. After World War II, activities shifted from ship repair to submarine servicing and testing. The Navy operated Hunters Point Annex as a shipbuilding and repair facility from 1941 until 1976. Between 1976 and 1986, the Navy leased most of the shipyard to Triple A, a private ship-repair company. The shipyard was an annex of Naval Station Treasure Island until 1974 when the

Navy's Engineering Field Activity West assumed the management of it. In 1987, PCBs, trichloroethylene and other solvents, pesticides, petroleum hydrocarbons, and metals including lead were confirmed at a number of shipyard locations. These findings and the shipyard's proximity to an offsite drinking water source (the aquifer used by a water bottling company) resulted in the EPA placing HPS on the National Priority List in 1989. However, subsequent Navy investigations indicate that the aquifers beneath HPS and that used by the bottling company do not appear to be connected. In 1991, the Department of Defense listed the shipyard for closure.

During the 1960s, zinc chromate had been used extensively as a primer for aluminum. Consequently, there are elevated concentrations of chromium present. For example, in IR-09 of Parcel D where zinc chromate spraying operations took place, chromium concentrations as high as 2700 ppm have been reported. The three SCAPS heavy metal sensors were deployed to evaluate chromium concentration at this site.

Parcel D at HPS consists of about 128 acres of southeast central shoreline and lowland coast (Figure 14). The land surface at Parcel D is mostly covered by asphalt, buildings, or other structures. Between 70 and 80 percent of HPS land consists of relatively level lowlands constructed by excavating portions of surrounding hills and placing non-engineered fill materials along the margin of San Francisco Bay. Parcel D is located in the lowlands, with surface elevations ranging from 10 to 40 feet above mean sea level (msl).

The peninsula forming HPS is within a northwest-trending belt of Franciscan Complex bedrock known as the Hunters Point Shear Zone. The depth to Franciscan complex bedrock from the ground surface in Parcel D varies from less than 1 foot in the northern area to greater than 200 feet in the southeastern area. Directly south of the Parcel D boundary is an outcrop of bedrock, called Shag Rock. Undifferentiated sedimentary deposits overlie bedrock over much of Parcel D, occurring beneath Bay Mud Deposits or, rarely, directly beneath Artificial Fill; these deposits range up to 110 feet in thickness. Bay Mud Deposits underlie most (about 80 percent) of Parcel D except for a strip along the northern margin of the site and over the bedrock high point directly south of Parcel D. Where present, Bay Mud Deposits range up to 100 feet thick. Undifferentiated Upper Sand Deposits are rather scattered in occurrence beneath Parcel D; where existent, these sands generally overlie Bay Mud Deposits but may be interfingered with Bay Mud Deposits and, in a few localities, directly overlie Undifferentiated sedimentary deposits. These sands range in thickness up to 20 feet. Artificial fill overlies all of the naturally occurring units and ranges in thickness up to 80 feet. The thickness of the artificial fill and all naturally

occurring surficial deposits generally increases toward the bay, with the exception of the bedrock high point in the southern part of Parcel D.

**3.2.4 Camp Keller Small-Arms Range, Keesler Air Force Base, Biloxi, MS.** Keesler Air Force Base is located in Biloxi, MS. Camp Keller, which is part of Keesler Air Force Base, is located 15 miles north of Keesler on state route 67 (Figure 15). Several small arms firing ranges are located within Camp Keller. These firing ranges are currently in use by the Air Force, Navy, and reserve units. Each firing range consists of a firing area, a clear standoff area providing distance to the target, and an impact berm. Due to firing range activities, the primary contaminant of concern is lead. In October 1996, the ERDC SCAPS truck was used in field investigations using the DL-LIBS metal sensor at Camp Keller in front of the Air Force impact berm. Measurements showed that the highest lead concentrations (up to 6000 ppm) were found near the surface. However, leached lead contamination was detected from the surface to depths of 4 feet. No difficulties were encountered during pushing. The water table was encountered at 10 ft bgs.

The landmass of Camp Keller consists of the Gulf Coastal Plain, which is a continuation of the Atlantic Plain and borders the Gulf of Mexico from Florida to Mexico, stretching also northward to include the lowlands of the Mississippi Valley as far as St. Louis, Missouri. Geologically, the coastal plain is an extension of the submerged continental shelf. The Atlantic and Gulf coastal plains have subsided and emerged several times since the end of the Mesozoic era, as shown by the types of sedimentary deposits, of Cretaceous age and younger, that underlie and comprise them. During the last Ice Age, when sea level was hundreds of feet lower, the coastal plains were much broader and shorelines far offshore of their present positions. The coastal lowlands consist of a heterogeneous, unconsolidated to poorly consolidated wedge of discontinuous beds of sand, silt, and clay that thickens towards the Gulf of Mexico.

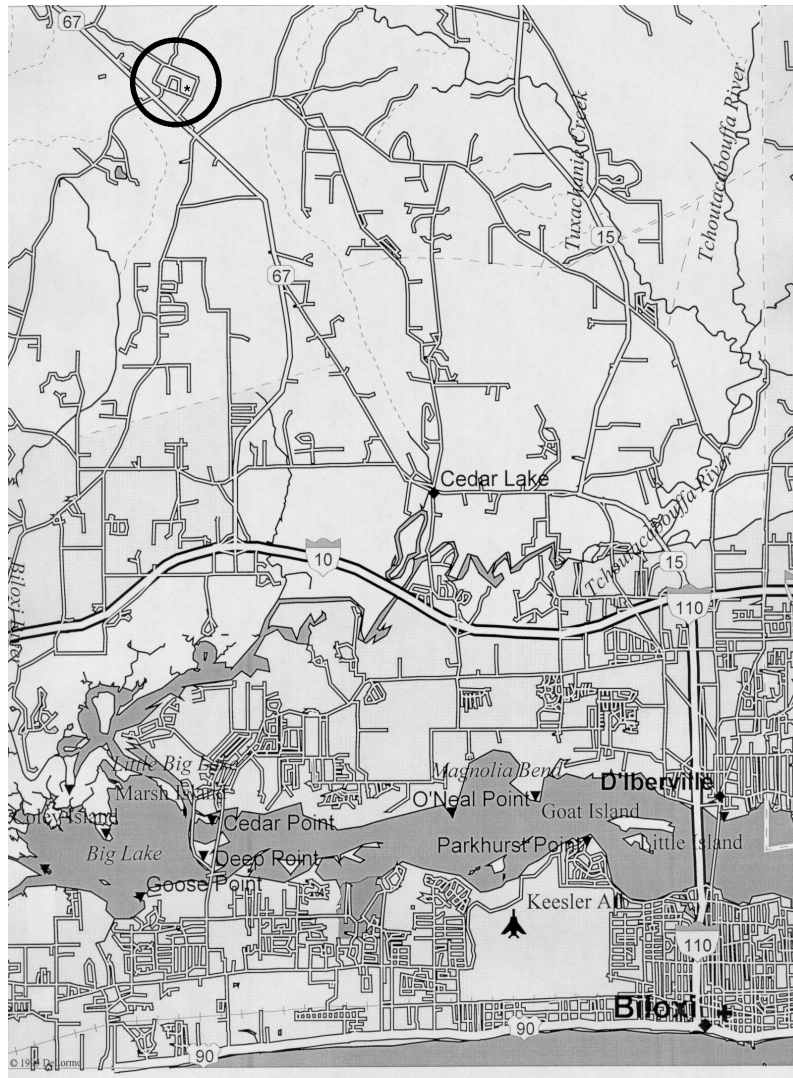


**Figure 15.** Site Map of Keesler Air Force Base and Camp Keller



## 4. Demonstration Approach

This section discusses the performance objectives established for the demonstration, provides an overview of operational issues, and summarizes sampling procedures and analytical methods.

### 4.1 Performance Objectives

These methods provide semi-quantitative data on the presence of heavy metal contamination *in situ*. Specific claims for the three SCAPS metal sensors are as follows:

1. Near continuous measurements generated by the sensor provide detailed mapping of the distribution of subsurface heavy metal contamination. These three metal sensors typically collect data at 0.2-ft intervals.
2. Good qualitative agreement with the pattern of contamination derived from analytical measurements (EPA Method 6010) of semi-continuous soil samples.
3. Direct comparison of sensor data with samples collected using conventional CPT soil sampler tools by pushing in close proximity to the metal sensors' pushes show good agreement with conventional laboratory methods (EPA Method 6010).
4. Collection and storage of multichannel atomic emission spectra throughout each push.
5. Data from the three SCAPS metal sensors is available in real time as the sensor is advanced into the ground or retracted from the subsurface. Real-time decisions can be made on how deep to collect verification samples on the site.
6. The location of future pushes can also be decided in real time at the site using the information available from previous pushes. This information can greatly speed the delineation of the contamination plumes.
7. The three SCAPS metal sensors can detect the presence of heavy metals, which includes, but may not be limited to lead, cadmium, chromium, mercury, arsenic, zinc and copper in the bulk soil matrix.

8. Measurements can be made to depths up to 150 feet in normally compacted soil, when the three SCAPS metal sensors are used in conjunction with an industry-standard 20-ton penetrometer push vehicle.
9. Geotechnical sensors (cone pressure, sleeve friction) may be integrated with the three SCAPS metal sensors to provide simultaneous continuous geotechnical and stratigraphic information to aid in interpreting contaminant distributions.
10. The *in situ* nature of the three SCAPS metal sensors minimizes possibilities for contaminating or altering soil samples that are inherent with traditional collection, transport, and analysis procedures.
11. The three SCAPS metal sensors provide more accurate measurement of the depth of the contaminant because the three SCAPS metal sensors do not suffer from the sampling difficulties encountered by other common methods such as soil boring/split spoon sampling and stab sampling.
12. The SCAPS sensor probes produce minimal IDW. A typical 6-meter push with the SCAPS probes produces approximately 40 liters of water IDW (used to clean the push rods). A typical 6-meter boring produces 210 to 285 liters of soil IDW and 40 liters of water used to clean the augers. Furthermore, the penetrometer rods are steam cleaned directly upon removal from the ground, protecting site personnel from potential contamination hazards.

#### **4.2 Physical Setup and Operation**

The SCAPS truck-mounted CPT platform is a standalone unit that requires no outside sources of electricity during operation. No special structures, either temporary or permanent, are required for operation. All power is supplied from a generator operated by the “power take off” (PTO) of the truck diesel motor and is regulated through an uninterruptible power supply with a bank of batteries. An external electrical power connection is also available. A hydraulic system, integrated into the truck, provides the force to push the probe into the ground and also powers a grout pump. Water, from onboard tanks, is consumed in the steam-cleaning system and during grouting. Retraction grouting is currently not configured in the three metals sensor probes but may be included in operational configurations. A local source of water is required for refilling the onboard tanks. Another consumable is grout. These items may be acquired locally or carried along in the SCAPS support vehicles. Waste water from the steam-cleaning system is collected

in Department of Transportation (DOT)-rated 208-liter (55-gallon) drums and handled as potentially hazardous waste. Operations yield approximately half a drum of rinsate waste a day. Wastewater disposal is coordinated with site personnel and handled locally after results of rinsate sampling are completed.

### **4.3 Sampling Procedures**

To assess the comparability of the data acquired by the three SCAPS metal sensing technologies to data generated by established, conventional analytical methods, the SCAPS metal sensors data were compared to analysis results of sampled soil. A series of pushes and comparison borings were advanced. Sets of collocated pushes (i.e., one SCAPS XRF metal sensor push, one SCAPS FO-LIBS metal sensor push, one SCAPS DL-LIBS metal sensor push, and one CPT soil sampler push) were performed inside and outside of the heavy metal contaminated plume area. Six sets of pushes along a transect from impacted to non-impacted were made to delineate the plume at each demonstration site. Soil samples were obtained either by hand-augering or by using the CPT soil-sampling probe, and are included as a push in each set of pushes. The three SCAPS sensor pushes were triangulated around each CPT soil sample location in a manner to co-locate within approximately 8 inches of the verification sample.

During the demonstration sampling, the SCAPS CPT pushed the three SCAPS metal probes as they acquired data (the DL-LIBS probe acquired data as the probe was retracted from the hole). Each probe push was above groundwater. After each push, the SCAPS metal probe was retracted and the CPT push hole was backfilled with a dilute Portland cement, bentonite, and Sikament mixture using the “trimmy grout” method.

After the real-time metal sensor data were collected from each set of sensor interrogation holes, verification samples for that push hole were obtained either by pushing a CPT soil-sampling probe or by hand-augering. Typically, three 6.6-inch long, 1.5-inch-diameter stainless steel tubes of sample soils were collected from every 1 to 1.5 feet of boring using a Mostap 35PS sampler with a fishtool. The soil samples were collected at depths determined from review of the metal sensors’ profile data. Only tubes containing sample soils that appear relatively undisturbed were used. The sampler was pushed using the SCAPS truck, in accordance with the ASTM D3441, the standard for CPT soil sampling. The Mostap 35PS sampler is an approximately 34-inch long, 2-inch diameter steel penetrometer tip, which includes a 21-inch long sample barrel containing three 6.6-inch long stainless steel soil sampling tubes. Samples for confirmatory analysis were collected from the lower and middle (deeper) 6.6-inch soil tubes in the 21-inch sampler. Each soil-sampling hole was backfilled with a dilute Portland cement,

bentonite, and Sikament mixture. Each soil sample was handled as described in the following paragraphs. The hand auger was used in those instances where the groundwater was shallow (less than or equal to about 6 feet).

After each soil sample was retrieved, the individual soil sample collection tubes were visually inspected. Each soil sample was handled as follows:

- The soil samples were homogenized onsite and divided into four EPA-approved clean containers for further study. The containers with the soil samples were labeled with sample identification information. Following each demonstration, each of the three metals sensors evaluated one of the homogenized soil aliquots. The fourth sample was sent offsite to the analytical laboratory.
- The soil containers with the soil samples were sealed with Teflon<sup>®</sup> swatches. The end-caps of the sealed, labeled soil sample container was then placed into an insulated cooler, entered onto the chain-of-custody form, and held for shipment to the offsite analytical laboratory.
- The soil samplers were analyzed by EPA Method 6010. The remaining portions of the soil samples were returned to SSC San Diego for archiving.

#### **4.4 Analytical Procedures**

The inductively coupled plasma (ICP) method for determining metal contaminants, EPA Method 6010, was used as the standard analytical laboratory method for all confirmation samples. This method was selected as the confirmatory analytical method for the three SCAPS metal technologies due to its widespread and generally accepted use in delineating heavy metal contamination. This method requires that the solid soil sample be solubilized or digested before evaluation. Although this analytical method does measure the same metal constituents that are targeted by the three SCAPS metal sensors, some variability will occur because the analytical technique is carried out on an “average” digested sample, while the SCAPS metal sensors will evaluate only a spot location of the sample. However, this analytical method was chosen because it represents the technology that is currently used daily to make decisions about the distribution of subsurface heavy metal contamination.

The ICP method measures element-emitted light by optical spectroscopy. Samples are nebulized and the resulting aerosol is transported to the plasma torch. Element-specific atomic-line emission spectra are produced by a radio frequency inductively coupled plasma. The spectra are dispersed by a grating spectrometer, and the intensities of the lines are monitored by photomultiplier tubes. ICP can determine the presence of several metals simultaneously.

Standard solutions of each metal of interest are prepared and evaluated. Then, mixed calibration standard solutions are prepared from those individual metal standard solutions and evaluated. For quality control, a calibration blank and at least three standards must be run to generate a calibration curve. At least one matrix spike and one matrix spike duplicate are run to determine digestion recoveries.

One of the main difficulties in comparing the methods is caused by differences in small-scale spatial heterogeneity. Each metal sensing probe was pushed in close proximity to each other and to the soil verification sample location. However, there was some uncertainty in establishing the depth from which the soil sample was obtained. Because of sharp vertical boundaries of the contamination plume, an error of 6 inches or less in the sample depth can change from strongly impacted (greater than 10,000 ppm) to clean (less than 100 ppm for most metals). Additionally, it is important to reiterate that the analytical method tests a digested sample that represents an “average” result for that sample, whereas the SCAPS metal sensors interrogate a small and discrete sample spot. For this reason, before shipping the soil samples to the analytical laboratory, each soil sample was homogenized onsite and split into four aliquots. Then, one of the homogenized aliquots was re-evaluated by each of the three SCAPS metal sensors as quickly as possible after completion of the field demonstration. At the same time, the samples were properly packaged and sent to the laboratory for analysis.



## 5. Performance Assessment

### 5.1 Performance Data

The validation process for the two LIBS and XRF sensors consisted of deploying each probe at four predetermined sites. For each site, two sets of measurements were conducted. In the first set, *in situ* measurements were conducted at many locations (usually a transect of six separate push locations). These measurements provided a general picture of the contaminant distribution at the site. In the second set of measurements, discrete samples, gathered at each site, were homogenized. Splits of each homogenized sample were sent to the respective sensor laboratory and to an analytical laboratory for analysis.

At each site, a sample of uncontaminated soil was collected. The sample was homogenized and splits were sent to each sensor laboratory. The sample of uncontaminated soil was assumed to represent the grain-size distribution of the site and was used by each of the respective sensor laboratories to prepare calibration standards. The soil was allowed to air dry and standards were prepared by spiking aliquots of soil with known quantities of a solution containing 10,000 ppm of the metal contaminant of interest undergoing investigation. Using these standards, a site-specific calibration curve was generated to minimize soil matrix effects.

These SCAPS metal sensors are intended as semi-quantitative field-screening tools, not as quantitative analytical methods. Therefore, the performances of the sensor systems were evaluated using a standard contingency analysis. In a contingency analysis, the results from each of the three technologies were plotted versus the concentration reported by the analytical laboratory. The resultant scatter plot has a format similar to that shown in Figure 16. The final results for each technology at each site were stated in the site report in terms of percent (%) agreement with the laboratory results by summing the number of true positive and true negative points from the scatter plot and dividing by the total number of samples. The final report includes the overall percent agreement for each technology summed over all site verification data.

Data reports have been completed for LCAAP, NASNI, HPS, and Camp Keller. The reports summarize the *in situ* sensor data, laboratory *ex situ* data sensor data obtained for the three sensor systems, offsite laboratory results, and notes and observations from field operations. Copies of these reports may be obtained from Dr. S. Lieberman (address listed in Appendix A).

The raw and processed data for the pushes and laboratory data for each sensor at each site has been archived on CDs, which comprise Appendix B.

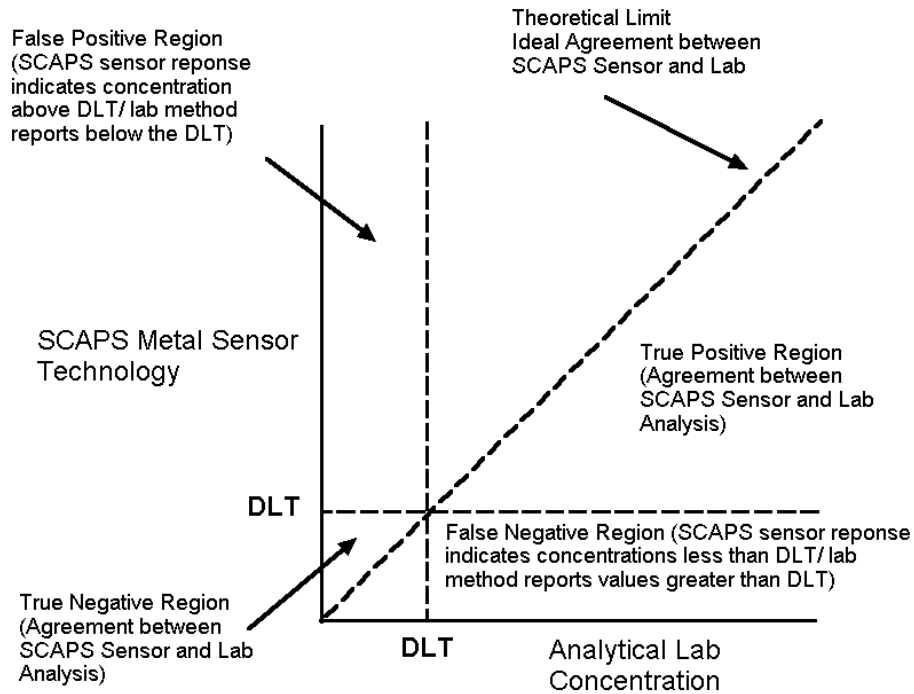


**Figure 16.** Contingency Plot Analysis Where DLT is the Detection Limit Threshold

**5.1.1 LCAAP, Independence, MO.** Four sets of collocated investigations (i.e., SSC San Diego FO-LIBS push, ERDC DL-LIBS push, NRL XRF push, and hand-auger boring) were conducted during demonstration operations at LCAAP (Figure 17) from 15–23 June 1998. Pushing at the site was uneventful. Fifty-eight discrete soil samples were collected and analyzed by traditional methods as part of the demonstration effort. The lead contamination at LCAAP was in the form of discrete particulate and was dispersed somewhat randomly throughout the soil vertically and horizontally. Even within eight horizontal inches, as the probes were placed and soil-sampled, lead content varied. Homogeneity at the site was tested by running replicate ICP laboratory analyses of five discrete 1-g aliquots for six different samples. The relative standard deviations for the samples ranged from 24 to 147%. The analytical laboratory considers a site homogeneous if the relative standard deviation is within 25%. The LCAAP is outside this criterion and is therefore considered a heterogeneous site.



**Figure 17.** LCAAP Demonstration Site

Figure 18 shows the *in situ* depth logs for push 3 obtained for all three sensors at LCAAP. The analytical laboratory data results are also shown. These results were typical for all six *in situ* pushes done by each of the sensors at LCAAP. In general, each sensor successfully detected the presence of subsurface lead. The heterogeneity of the site limited the ability of all three sensors and the analytical laboratory to quantify the data with high precision. Despite the high degree of heterogeneity in the distribution of the lead contamination at the site, there is reasonably good agreement between the *in situ* data and the laboratory analysis data (Figure 18).

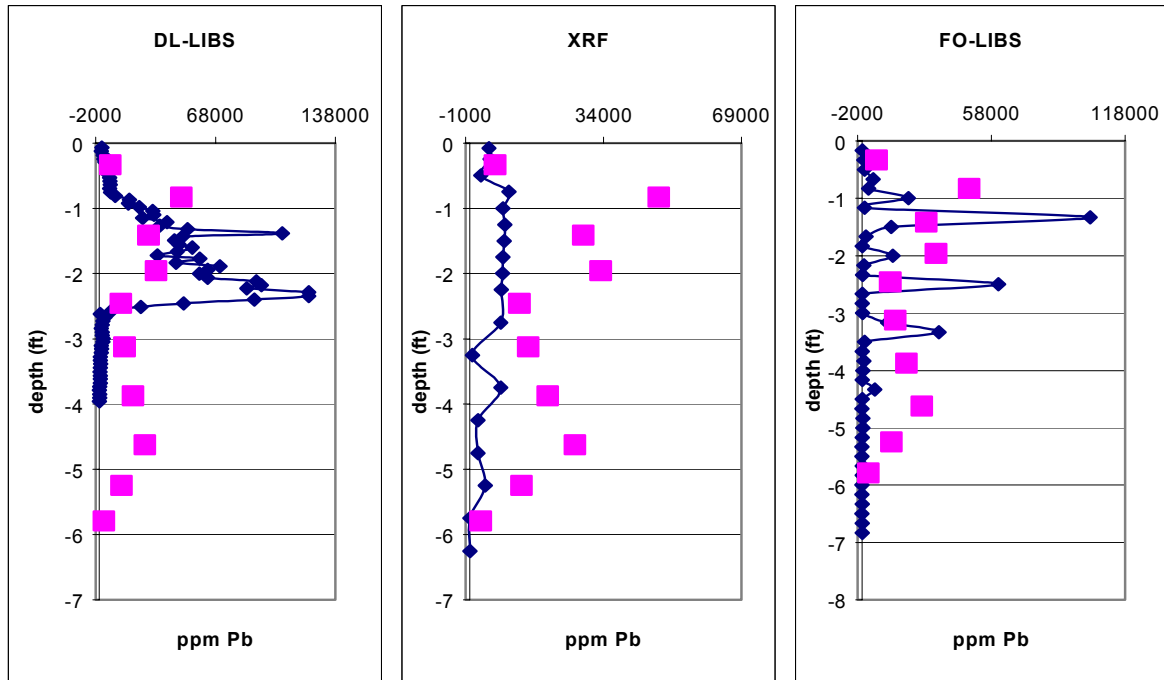


**Figure 18.** *In situ* Lead Data for Push 3 Obtained for all Three Metal Sensor Technologies Demonstrated at LCAAP (The Squares Indicate the Results of the Laboratory Analysis. Push 3 Corresponded to Soil Sample 4)

Bench *ex situ* analysis of the homogenous splits of the soil samples were conducted by the three sensors. These results were compared to the ICP laboratory results and documented in the contingency analysis summarized in Table 1. The limit of detection for the three sensors was determined to be 100 ppm (the California EPA screening level for lead is 130 ppm). All three sensors could identify high concentrations of lead in the laboratory *ex situ* samples and during field demonstrations *in situ*. Unfortunately, the levels of contamination at LCAAP were so high that there were very few “clean” samples to use for evaluation of the sensors at low concentrations.

**5.1.2 IWTP at Naval Air Station, North Island, CA.** Four sets of collocated investigations (i.e., SSC San Diego FO-LIBS push, ERDC DL-LIBS push, NRL XRF push, and hand-auger boring) were conducted during demonstration operations at NASNI from 2 March through 28 April 1999. Thirty-eight discrete soil samples were collected and analyzed by traditional methods as part of the demonstration effort.

Table 1. LCAAP Lead Contingency Analysis Results Summary of Laboratory Data for Three Sensors.

	<b>XRF</b>	<b>FO-LIBS</b>	<b>DL-LIBS</b>
True Positive	56/56	56/56	56/56
True Negative	1/2	0/2	0/2
False Positive	1	2	2
False Negative	0	0	0
<b>Accuracy</b>	<b>98.3%</b>	<b>96.6%</b>	<b>96.6%</b>

The chromium contamination at NASNI was localized in an industrial waste pit in which plating waste had leached into the ground (Figure 19). Five pushes were conducted inside the waste pit and one was conducted outside. Because the concrete liner of the paint basin was still in place, holes were cored through the concrete liner before the SCAPS metal sensor deployment. The upper 2 feet of soil consisted of very compacted sand that was difficult to penetrate. A gas-powered auger was used to punch through the upper 2 feet of very compacted soil. As a result, very little *in situ* data were obtained for the first 2 feet of push for each sensor deployment. Because chromium was released into the environment at the NASNI in an aqueous rather than particulate form, a more homogeneous contaminant distribution was expected at the NASNI than was observed for lead at the LCAAP. Reduced variability in soil metal contaminant distribution was verified by homogeneity testing. Homogeneity at the site was determined by analytical laboratory ICP analysis of five discrete 1-g aliquots for six different samples. The relative standard deviations for the samples ranged from 2 to 24%. Since the relative standard deviations fell below 25%, the site met the criterion for homogeneous contaminant distribution.



**Figure 19.** NASNI Demonstration Site

Figure 20 shows the *in situ* depth logs for push 2 obtained for all three sensors at NASNI. The analytical laboratory results are also shown. These results were typical for all six *in situ* pushes conducted by each of the sensors at NASNI. In general, each sensor successfully detected the presence of subsurface chromium. The *in situ* push data for the three metal sensors demonstrated remarkable agreement with analytical laboratory results and with each sensor result.

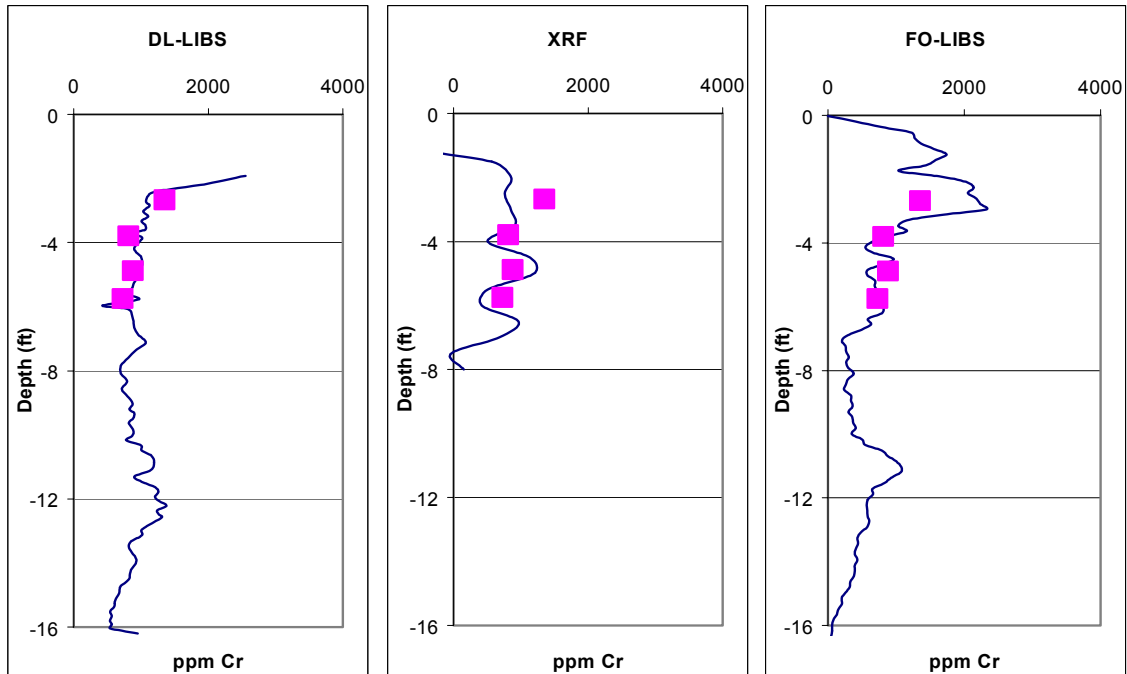


**Figure 20.** *In situ* Chromium Data for Push 2 Obtained for all Three Metal Sensor Technologies Demonstrated at NASNI (The Squares Indicate the Results of the Laboratory Analysis. Push 2 Corresponded to Soil Sample 2)

Bench *ex situ* analyses of the homogenous splits of the soil samples were conducted by the three sensors. These results were compared to the ICP laboratory results, resulting in the contingency analysis summarized in Table 2. The limit of detection for all three sensors was 100 ppm. For the EPS Region 9, soil preliminary remediation goals for total chromium (1:6 ratio  $\text{Cr}^{\text{VI}}$  :  $\text{Cr}^{\text{III}}$ ) was 210 ppm in residential areas and 450 ppm in industrial areas. ICP analysis indicated high chromium concentrations inside the waste pit. Outside the waste pit, ICP results indicated chromium concentrations below 50 ppm. All three sensors could identify high concentrations of chromium in the waste pit, both in laboratory *ex situ* samples and during field demonstrations *in situ*. Outside the waste pit, all three sensors reported no detection of chromium in the *ex situ* samples and during field demonstrations *in situ*.

Table 2. NASNI Chromium Contingency Analysis Results Summary of *ex situ* Laboratory Data for Three SCAPS Metal Sensor Technologies

	XRF	FO-LIBS	DL-LIBS
True Positive	28/28	28/28	28/28
True Negative	10/10	10/10	10/10
False Positive	0	0	0
False Negative	0	0	0
<b>Accuracy</b>	<b>100%</b>	<b>100%</b>	<b>100%</b>

### 5.1.3 Former Ship Repair Area (Parcel D), Hunters Point Shipyard, San Francisco, CA.

Four sets of collocated investigations (i.e., SSC San Diego FO-LIBS, ERDC DL-LIBS, NRL XRF, and MOSTAP 35 sampler boring) were conducted during demonstration operations at HPS from 5–21 April 2000 (Figure 21). Thirty-six discrete soil samples were collected and analyzed by traditional methods as part of the demonstration effort.



**Figure 21.** Hunters Point Shipyard (HPS) Demonstration Site

The chromium contamination at HPS was the result of zinc chromate spraying operations. The artificial fill used during site development consisted of chipped bedrock mixed with bay silt and clay. Consequently, pushing and sampling at the site was very difficult. The FO-LIBS probe experienced several refusals, but did not incur any damages. However, there are gaps in the FO-LIBS *in situ* push data. These gaps are attributed to either voids present below the ground

surface or to ablating gravel instead of the contaminated soil. The XRF sensor probe could only complete two of the six *in situ* pushes. Near the end of the second XRF push, the window holder of the probe was gouged out by a rock, and the thin boron carbide window was compromised. Since the probe was below the water table, water entered the probe and shorted the electronic components of the sensor (x-ray tube, amplifier, detector, etc.). A backup XRF probe configured with an older prototype x-ray tube failed to function correctly. Although attempts were made to repair the probes onsite, the XRF sensor group could not get either probe to operate sufficiently to complete the XRF *in situ* pushes. The DL-LIBS sensor group also experienced difficulties. During their second push, the probe was pushed below the water table and the recessed area of the probe (where the sapphire window was placed) became filled with silt. Water leaked inside and clouded the prism area and caused a reduction in signal. The backup DL-LIBS probe was used to successfully complete all six *in situ* pushes.

The chromium contamination at HPS was released into the environment in a dissolved phase rather than particulate form and provided a uniform contaminant distribution. Homogeneity at the site was determined from ICP laboratory analysis of five discrete 1-g aliquots for six different samples. The relative standard deviations for the samples ranged from 10.8 to 30.1%. A site is considered homogeneous if the relative standard deviation is within 25%. Except for the one sample that had a 30.1% relative standard deviation, this criterion was met.

Figure 22 shows the *in situ* depth logs for Push 3 obtained for all three sensors at HPS. The analytical laboratory results are also shown. These results were typical for the six *in situ* pushes done by LIBS sensors and the two *in situ* pushes done by the XRF sensor at HPS. In general, each sensor successfully detected the presence of subsurface chromium. The *in situ* push data for all three sensors showed good agreement with the analytical laboratory results and with the other sensor technologies.

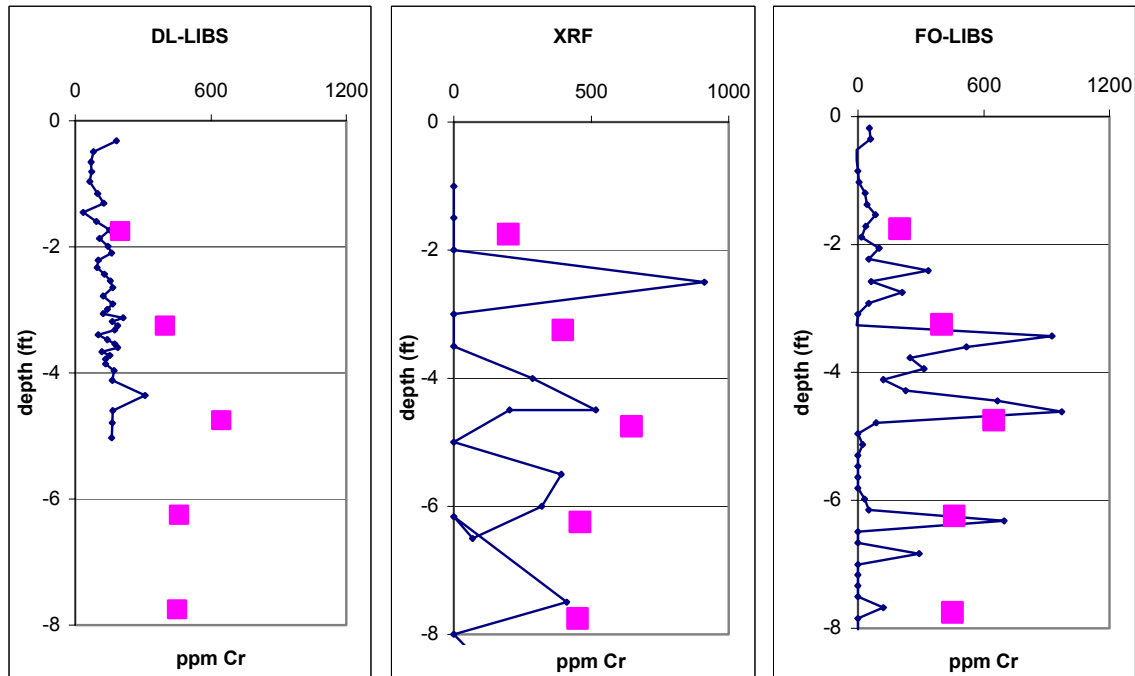


**Figure 22.** *In Situ* Chromium Data for Push 3 Obtained for all Three Metal Sensor Technologies Demonstrated at HPS (The Squares Indicate the Results of the Laboratory Analysis. Push 3 Corresponded to Soil Sample 3)

Bench *ex situ* analyses of the homogenous splits of the soil samples were conducted by the three sensors. The results were compared to the ICP laboratory results; Table 3 summarizes the contingency analysis. The limit of detection for all three sensors was 120 ppm. For the EPS Region 9, soil preliminary remediation goals for total chromium (1:6 ratio Cr<sup>VI</sup> : Cr<sup>III</sup>) were 210 ppm in residential areas and 450 ppm in industrial areas.

Table 3. HPS Chromium Contingency Analysis Results Summary of Laboratory Data for Three Sensors.

	<b>XRF</b>	<b>FO-LIBS</b>	<b>DL-LIBS</b>
True Positive	21/31	29/31	30/31
True Negative	5/5	5/5	5/5
False Positive	0	0	0
False Negative	10	2	1
<b>Accuracy</b>	<b>72.2%</b>	<b>94.4%</b>	<b>97.2%</b>

**5.1.4 Camp Keller Small-Arms Range, Keesler Air Force Base, Biloxi, MS.** Four sets of collocated investigations (i.e., SSC San Diego FO-LIBS, ERDC DL-LIBS, NRL XRF, and

MOSTAP 35 sampler boring) were conducted during demonstration operations at Camp Keller, MS, from 26 –31 October 2000. Thirty-six discrete soil samples were collected and analyzed by traditional methods as part of the demonstration effort. Pushing and sampling at the site were uneventful.

The CPT *in situ* pushes and sampling were conducted at an old, but active, small-arms firing range. Numerous small arms projectiles were visible on and below the impact berm. The lead contamination at Camp Keller is caused by the effects of weathering on the lead projectiles. The lead contamination is in particulate form and leached lead compounds. Five pushes were done along the impact berm of the firing range where high lead contamination was expected (Figure 23). The sixth push was conducted approximately 50 feet south of the impact berm where no surface projectiles were observed.



**Figure 23.** Camp Keller Demonstration Site

Because most of the lead contamination was released into the environment in particulate form the contaminant distribution was expected to be heterogeneous. Site homogeneity was determined by laboratory ICP analysis of five discrete 1-g aliquots for six different samples. The relative standard deviations for six samples ranged from 7.8 to 113%. A site is considered to be homogeneous if the relative standard deviation is within 25%. This homogeneity criterion was met for three of the six interrogation locations.

Figure 24 shows the *in situ* response versus depth for push 9 for the three SCAPS metal sensors at Camp Keller and the analytical laboratory results of verification samples. These results were typical for the six *in situ* pushes conducted by the LIBS and XRF sensors. The *in situ* push data for all three sensors showed good agreement with analytical laboratory results. In general, each sensor successfully detected the presence of subsurface lead. The *in situ* push data indicated that heaviest lead contamination was along the impact berm. The highest concentration of lead contamination was located near the surface and decreased with depth. No lead contamination was detected below 2.5 feet. No lead contamination was detected as a function of depth for a push conducted approximately 50 feet in front of the impact berm.

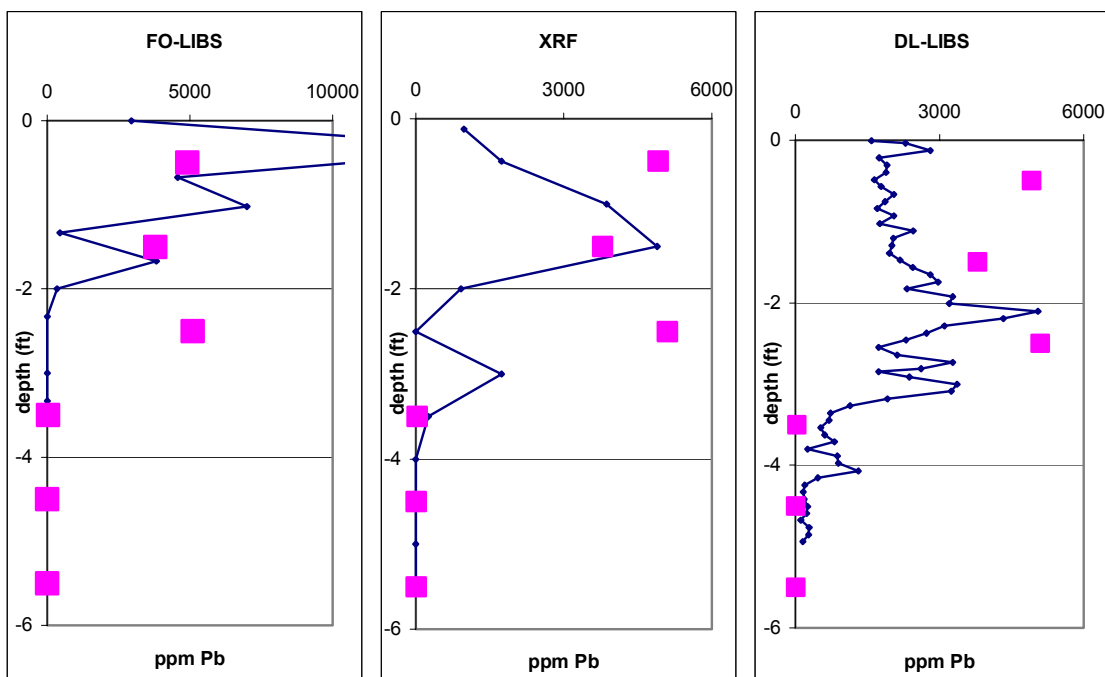


**Figure 24** *In situ* Lead Data for Push 9 Obtained for all Three Metal Sensor Technologies Demonstrated at Camp Keller (The Squares Indicate the Results of the Laboratory Analysis. Push 9 Corresponded to Soil Sample 4)

Bench *ex situ* analysis of the homogenous splits of the soil samples were conducted by the three sensors. These results were compared to ICP laboratory results and a contingency analysis is summarized in Table 4. The limit of detection for all the three sensors was 200 ppm, which was a higher screening level than the California screening level for lead of 130 ppm.

Table 4. Camp Keller Lead Contingency Analysis Results Summary of Laboratory Data for Three Sensors.

	<b>XRF</b>	<b>FO-LIBS</b>	<b>DL-LIBS</b>
True Positive	11/12	11/12	11/12
True Negative	22/24	24/24	23/24
False Positive	2	0	1
False Negative	1	1	1
<b>Accuracy</b>	<b>91.7%</b>	<b>97.2%</b>	<b>94.4%</b>

## 5.2 Data Assessment

The data presented above provides realistic comparisons to assess the demonstration's objectives. The primary objective of this demonstration was to evaluate the performance of three *in situ* SCAPS metal sensing technologies compared to conventional sampling and analytical methods. The *in situ* measurements of the three sensor systems compare favorably with laboratory measurements of validation soil samples. Additionally, the above data show that each of the systems (i.e., the ERDC DL-LIBS, the SSC FO-LIBS, and the NRL XRF) successfully detected and differentiated heavy metal contamination in the varying soil matrices. In all cases, data quality exceeded acceptable standards to meet the objectives. Design of the sampling scheme for verification of an *in situ* measurement by *ex situ* analysis remains the biggest problem. Varying contaminant distribution and small-scale soil heterogeneity can lead to samples that are not representative of the soil measured *in situ*.

Secondary objectives for this demonstration were to evaluate the SCAPS metal sensing technologies for their reliability, ruggedness, and ease of operation. For the most part, all three sensors displayed good reliability and ruggedness. The greatest difficulty was encountered at HPS, where pushing was very difficult. The XRF and DL-LIBS sensors were compromised by water entering the probes. For CPT deployed sensors, it is common practice to have backup probes on hand in case a probe breaks below the ground surface and cannot be retrieved. ERDC successfully deployed a backup DL-LIBS probe and completed the scheduled six *in situ* pushes. The backup XRF probe was not functional; the XRF sensor completed two of the six *in situ* pushes. After the HPS demonstration, the NRL sensor group repaired both XRF probes and successfully conducted the Camp Keller demonstration. With regards to ease of operation, typically, a four-person crew completes all aspects of field operations: a field site manager, two push room personnel, and a metal sensor system operator. All three SCAPS metal sensors

should be operated by a trained technician. Important personnel in the DL-LIBS and FO-LIBS sensor groups (i.e., the investigators who had designed the systems and acted as the metal sensor operator) had left before completion of the demonstrations. Qualified personnel took over the projects and completed the remaining field demonstrations, *ex situ* laboratory analyses, and data processing.

### 5.3 Technology Comparison

The SCAPS metal sensors provide real-time data as the probe is either pushed or retracted from the soil, enabling field modifications to the sampling plan. This capability provides a more timely and thorough investigation and avoids the drawn-out iterative process typical of conventional site characterization methods (e.g., traditional sampling and offsite laboratory analysis).

The validation effort produced comparison data to support the effectiveness of the three SCAPS-deployed metal sensor probe configurations. In general, detailed comparisons of the laboratory ICP results agree very well with the three metal sensor *in situ* and bench *ex situ* data. Table 5 contains the contingency analysis summarizing the four site demonstrations.

Table 5. Contingency Analysis Results Summary of Benchtop Laboratory Data Obtained by the Three Sensors for the Four Site Demonstrations.

	<b>XRF</b>	<b>FO-LIBS</b>	<b>DL-LIBS</b>
True Positive	116/127	124/127	125/127
True Negative	38/41	39/41	38/41
False Positive	3	2	3
False Negative	11	3	2
<b>Accuracy</b>	<b>91.7%</b>	<b>97.0%</b>	<b>97.0%</b>

## **6. Cost Assessment**

### **6.1 Cost Performance**

Factors affecting the cost of the metal sensor/CPT operations include labor, material, travel, permitting, utility location, location surveying, work plan and report preparation, and equipment mobilization. Additional cost may be incurred for coring if the media surface is too hard for penetration (cement). SCAPS CPT/METAL SENSOR or SCAPS Membrane Interface Probe (MIP) costs has been quoted as approximately \$6380 per 10-hour day plus per diem. It is expected that the operating costs for the SCAPS metal sensor systems will be comparable.

### **6.2 Cost Comparisons to Conventional and Other Technologies**

This demonstration has focused on comparing the effectiveness of three CPT-based metal sensor technologies to perform field screening at a heavy metal impacted hazardous waste site. Table 6 presents a direct comparison between the costs using a CPT/metal sensor technology versus the following: (1) conventional drilling, sampling, and laboratory analysis for field screening, and (2) direct push sampling and laboratory analysis.

For a site investigation with 10 holes to a depth 30 feet, the table shows the cost for SCAPS CPT/Metal Sensor is approximately 47% of the cost of conventional sampling with a sampling ratio of 30 to 1 in favor of CPT/Metal Sensor. On a per sample basis, Table 6 shows that on a cost-per-sample basis, SCAPS metals sensor technologies offer approximately a 98% cost savings compared with conventional soil borings and laboratory analyses and a 96% savings compared to direct push sampling methods. The cost savings realized from direct push sensing methods compared to conventional drill rigs and direct sampling are due to the following: (1) the speed with which direct push techniques access depth versus drilling methods, (2) the low amount of investigation derived waste produced by the direct push methods, and (3) the ability of direct push technique to acquire near continuous data. Further savings not documented in Table 6 may be realized using the SCAPS sensors because onsite real-time data acquisition allows the sampling strategy to be modified in the field to more accurately delineate the extent of contamination. In contrast, traditional sampling strategies depend on results from laboratory analyses that are usually not available for days or weeks after samples are collected, and often require return trips to the field when initial results indicate that further sampling is required to complete delineation of the contaminated zone. The greater vertical sampling rates provided by the SCAPS sensors compared to conventional sampling methods (every 2 inches compared to every 5 feet) minimizes the chances that significant zones of contamination are missed because

5-foot sampling intervals performed with soil boring do not provide the resolution necessary to resolve some contaminant layers. For the CPT/Metal Sensor technique, regulators may require a minimum number of confirmatory samples, which can be obtained using CPT sampling devices. This requirement will increase the SCAPS CPT/Metal Sensor cost as presented in the table, but only three or four samples would be required at less than \$1000 in additional cost.

**Table 6.** Cost Comparison of SCAPS Metal Sensors with Conventional Sampling and Direct Push Sampling.

<b>SCAPS Metal Sensor <i>in situ</i> Measurement<sup>1</sup></b>		<b>Conventional Drilling (Hollow Stem Auger, Split Spoon, and Offsite Analyses)<sup>1</sup></b>		<b>Direct Push and Offsite Analysis<sup>2</sup></b>	
10 pushes to 30 ft Metals and geotechnical data	Cost	10 Borings to 30 ft (60 soil samples for ICP analysis)	Cost	10 Borings to 30 ft (60 soil samples for ICP analysis)	Cost
Two 10-hr field days @ \$6,380/day	\$12,760	Drilling and sampling @ \$50/ft for 300 ft (approx three 10-hr days)	\$15,000	Drilling and sampling for 300 ft (approx two 10-hr days)	\$3000
One sample/ 2 inches for metals = 1800 total samples	Included in basic cost	ICP laboratory @ \$50 per sample x 60 samples	\$4800	ICP laboratory @ \$50 per sample x 60 samples	\$4800
One sample/inch for geotechnical data	Included in basic cost	Geotechnical laboratory analysis @ \$100/sample x 5 samples	\$500	Geotechnical laboratory analysis @ \$100/sample x 5 samples	\$500
Four waste drums @ \$40/drum	\$160	28 waste drums @ \$40/drum	\$1120	1 Waste drum @ \$40/drum	\$40
Decon water testing	\$1000	Decon water testing	\$1000	Decon water testing	\$1000
Waste soil testing	\$0	Waste soil testing	\$3000	Waste soil testing	\$0
Waste soil not produced	\$0	Waste soil disposal 20 drums @ \$100/drum	\$2000	Waste soil not produced	\$0
Decon water disposal for four drums @ \$100/drum	\$400	Decon water disposal	\$800	Decon water disposal for one drum @ \$100/drum	\$100
Four-man crew	Included in cost	Geologist @ \$75/hr x 36 hrs	\$2700	Geologist @ \$75/hr x 36 hrs	\$1400
		Technician @ \$40/hr x 40 hrs	\$1600		
<b>TOTAL</b>	<b>\$14,320</b>	<b>Total</b>	<b>\$30,520</b>	<b>Total</b>	<b>\$10,240</b>
Per sample cost for 1800 samples	\$7.95/sample	Per sample cost for 60 samples	\$509/sample	Per sample cost for 60 samples	\$181/sample

1– ESTCP Technology Demonstration Report, April 2001

2 – Personal Communication, TerraProbe, 10 May 1999



## 7. Regulatory Issues

### 7.1 Approach to Regulatory Compliance and Acceptance

As described earlier, the metal sensors evaluated as part of this effort represent one of a suite of sensor systems that have been developed or that are still under development for deployment with direct push systems. The LIF sensor for petroleum hydrocarbons was the first major chemical sensor system developed for this system. During the early stages of technology transfer of the LIF sensor, a common question raised by potential user was: “Is the technology approved by the regulators?” From this question grew the concept that if the LIF technology were “approved” by the regulatory community, then the users would embrace it. The quest for regulatory approval led to a successful multi-year effort (partially funded by ESTCP) to gain regulatory acceptance for the SCAPS LIF sensor technology based on assembling a comprehensive set of field measurements that directly compare the performance of the sensor system with traditional EPA methods for various contaminants under different hydrogeological conditions. The cornerstone of obtaining as broad an acceptance as possible is linking these technical efforts with multi-state and national certification/verification programs such as the US EPA Consortium for Site Characterization Technology “verification” program and “certification” by the California EPA Department of Toxic Substance Control’s Technology Certification Program (Cal Cert). For the case of the SCAPS nitrogen laser LIF sensor system, these opportunities were subsequently linked to the Western Governors Association, Demonstrating Onsite Innovative Technologies (WGA/DOIT) project. Interest by the WGA/DOIT project subsequently led to the establishment of a SCAPS-LIF Interstate Technology and Regulatory Cooperation (ITRC) workgroup, Technology Specific Task Group (TSTG) with the goal to achieve acceptance by each of the seven TSTG member-states (Utah, Nebraska, New Mexico, Louisiana, New Jersey, Idaho, California) and using Cal Cert as the protocol. For the SCAPS nitrogen laser LIF system these efforts resulted in the successful certification by the Cal Cert Program (CALIFORNIA ENVIRONMENTAL PROTECTION AGENCY DEPARTMENT OF TOXIC SUBSTANCES CONTROL, 1996), verification by the US EPA (BUJEWSKI and RUTHERFORD, 1997), 1997) and endorsement of the Cal Cert certification by the WGA (CONE PENETROMETER TASK GROUP REPORT, 1996).

Significant lessons were learned from the Tri-Service SCAPS Program in the process of obtaining regulatory acceptance of the SCAPS LIF sensor. Specifically, there appears to be no path to gain universal acceptance of new technology by the regulatory community. However, and probably more importantly, it was learned that obtaining regulatory acceptance does not

guarantee user acceptance. While regulatory acceptance is a desirable goal, the users can not be convinced that the new technology will enable them to do their jobs faster, better, and cheaper. Experience from the SCAPS LIF program suggests that the most effective way to build user acceptance is to build a user base one user at a time. Discussions with both government and commercial LIF service providers indicate that the key to growing the business is to provide a product that meets the customers needs at a competitive price (personal communications, Tim Shields, PWC San Diego, San Diego California; Racyp Yilmaz, Fugro Geoscience, Inc., Houston, Texas). Satisfied users generate repeat business and tell other prospective customers. Regulatory approval by itself may not generate user acceptance. In retrospect, experience seems to suggest that many perspective users that initially expressed reluctance to use SCAPS LIF because of “lack of regulatory acceptance” may have found other reasons not to use a new technology even if the regulatory community approved the technology.

Based on lessons learned from the SCAPS LIF sensor technology, it appears the most effective means to promote acceptance of a new field-screening technology is to aggressively market the technology and grow a user base for the technology. Experience suggests the need to convince individual users and regulators of the merits of the technology coupled with the fact that there is often high turnover in both communities requires a long-term and persistent marketing effort. In general, a motivated commercial vendor can rally more marketing savvy (knowledge and experience) for a product or service than a government technology developer. While the SCAPS LIF ESTCP project focused almost exclusively on gaining acceptance of the technology by regulators, the efforts of the SCAPS metal sensors ESTCP project were directed more toward generating a link with commercial partners that ultimately take the lead for marketing the technologies to users and regulators. This strategy has the advantage of offering a longer term solution to the difficult problem of nurturing a new technology through its infancy than the previous approach that focused almost exclusively on the single issue of regulatory acceptance at the expense of other factors required for successfully establishing a new technology in the marketplace.

During the SCAPS LIF ESTCP project, it also became apparent that, in general, regulators and users were often slow to accept new methods and technologies due to limited exposure, inadequate technical understanding, and lack of high quality validation data that support developers and/or vendor claims. Ultimately, acceptance requires exposure leading to understanding, as well as comprehensive data validation. With the goal to document the performance of these sensor systems under various conditions with “hard data,” a comprehensive effort was conducted to make available the results of this demonstration/validation program and related work. To inform regulators, government agencies, and commercial users, the SCAPS

metal sensing technologies have been presented in national and international environmental conferences and peer-reviewed, scientific journals. Tables 7 through 9 list the publications/presentations for each metals sensor. The SCAPS metals sensor technologies were also demonstrated at the annual SCAPS User’s meetings. The SCAPS operational teams are very interested in increasing their capabilities to detect heavy metal contaminants of DoD environmental concern.

Table 7. Summary of Publications for ERDC DL-LIBS Metals Sensor

Reference	Article <sup>a</sup>
Cortes, J., Cespedes, E.R., and Miles, B.H. “Development of Laser-Induced Breakdown Spectroscopy for Detection of Metal Contaminants in Soils.” Technical Report IRRP-96-4. U.S. Army Engineer Waterways Experiment Station, Vicksburg, MS, 1996.	3
Miles, B.H., Cortes, J., and Cespedes, E.R. “Laser-induced Breakdown Spectroscopy (LIBS) Detection of Heavy Metals Using a Cone Penetrometer: System Design and Field Investigation Results.” in Proceedings of <i>Field Analytical Methods for Hazardous Wastes and Toxic Chemicals</i> , 671-680 (Air and Waste Management Association, Las Vegas, Nevada, 1997)	2, 4
Alexander, D.R. and Poulain, D.E. “Quantitative Analysis of the Detection Limits for Heavy Metal-Contaminated Soils by Laser-Induced Breakdown Spectroscopy.” Miscellaneous Paper IRRP-97-2. University of Nebraska-Lincoln, prepared by the U.S. Army Engineer Waterways Experiment Station, Vicksburg, MS, 1997.	4
Alexander, D.R., Poulain, D.E., and Cespedes, E.R. “Detection Limits of Heavy Metals in Soils by Laser-Induced Breakdown Spectroscopy.” Trends in Optics and Photonics (TOPS), <i>Environmental Monitoring and Instrumentation</i> , Volume 8, 8-13, 1997.	1
Miles, B. and Cortes, J. “Subsurface Heavy-Metal Detection With the Use of a Laser-Induced Breakdown Spectroscopy (LIBS) Penetrometer System”. <i>Field Analytical Chemistry and Technology</i> , 2(2) 75-87, 1998.	1

a. 1 = peer reviewed article, 2 = proceedings paper, 3 = technical report, 4 = presentation

Table 8. Summary of Publications for NRL XRF Metals Sensor

Reference	Article <sup>a</sup>
Elam, W.T. and Gilfrich, J.V. "Design of an X-Ray Fluorescence Sensor for the Cone Penetrometer." <i>Advances in X-Ray Analysis</i> , 38, 699-704, 1995.	1
Elam, W.T., Adams, J., Hudson, K.R., McDonald, B.J., Eng, D., Robitaille, G. and Aggarwal, I. (1997). "Field Demonstration of the SCAPS XRF Metals Sensor," in <i>Proceedings of Field Analytical Methods for Hazardous Wastes and Toxic Chemicals</i> , 681-689 (Air and Waste Management Association, Las Vegas, Nevada, 1997).	2, 4
Elam, W.T. and Gilfrich, J. V. "Demonstration of an X-ray Fluorescence Sensor for the Cone Penetrometer." <i>Advances in X-Ray Analysis</i> , 39, 861-867 (1997).	1
Elam, W.T., Adams, J.W., Hudson, K.R., McDonald, B., and Gilfrich, J.V. "Use of the SCAPS XRF Metals Sensor to Detect Subsurface Lead Contamination." in <i>Proceedings of EnviroAnalysis 98</i> , 25-30 (Ottawa, Canada, 1998).	2, 4
Elam, W.T., Adams, J.W., Hudson, K.R., McDonald, B.J., Gilfrich, J.V., and Galambos, J. "In situ Environmental XRF." <i>Denver X-Ray Conference</i> (Colorado Springs, Colorado, 1998).	4
Elam, W.T., Adams, J.W., Hudson, K.R., McDonald, B., and Gilfrich, J.V. "Subsurface Measurement of Soil Heavy Metal Concentrations with the SCAPS X-Ray Fluorescence (XRF) Metals Sensor," <i>Field Analytical Chemistry and Technology</i> , 1(1), 75-87, 1998.	1
Elam, W.T. "Determination of Metals in Soil by XRF Spectrometry via Cone Penetrometry (SCAPS)." <i>Current Protocols in Field Analytical Chemistry</i> . John Wiley and Sons, Inc. New York, 3B.3.1- 3B.3.10, 1998.	1
McDonald, B.J., Unsell, C.W., Elam, W.T., Hudson, K.R., and Adams, J.W. "A Cone Penetrometer X-Ray Fluorescence Tool for the Analysis of Subsurface Heavy Metal Contamination." <i>Nuclear Instruments and Methods in Physics Research A</i> , 422, 805-808, 1999.	1
Elam, W.T., McDonald, B.J., and Unsell, C.W. "A Cone Penetrometer XRF Sensor for <i>in situ</i> Analysis of Heavy Metals in Soils," 219 <sup>th</sup> ACS National Meeting (American Chemical Society, San Francisco, California, 2000).	4
Elam, W.T., McDonald, B.J., and Unsell, C.W. "A Cone Penetrometer XRF Sensor for <i>In situ</i> Analysis of Heavy Metals in Soils," <i>Onsite Analysis 2000</i> ( Lake Las Vegas, Nevada, 2000).	4

a. 1 = peer reviewed article, 2 = proceedings paper, 3 = technical report, 4 = presentation

Table 9. Summary of Publications for SSC San Diego FO-LIBS Metals Sensor.

Reference	Article <sup>a</sup>
Therriault, G. A., Lieberman, S. H. & Knowles, D. S. "Laser-induced Breakdown Spectroscopy for Rapid Delineation of Metals in Soils," in <i>Proceedings of the Fourth International Symposium on Field Screening Methods for Hazardous Waste and Toxic Chemicals</i> 863-872 (Air & Waste Management Association, Las Vegas, Nevada, 1995).	2,4
Therriault, G. A. & Lieberman, S. H. "Remote <i>in situ</i> Detection of Heavy Metal Contamination Using a Fiber Optic Laser-Induced Breakdown Spectroscopy (FO-LIBS) System," in <i>Proceedings-Environmental Monitoring and Hazardous Waste Site Remediation, June 19-21, 1995, Munich, FRG</i> (eds. Vo-Dinh, T. & Nießner, R.) 75-83 (SPIE-The International Society for Optical Engineering, Bellingham, WA, 1995).	2,4
Therriault, G. A. & Lieberman, S. H. "Field Deployment of a LIBS Probe for Rapid Delineation of Metals in Soils," in <i>Proceedings-Advanced Technologies for Environmental Monitoring and Remediation, August 6-8, 1996, Denver, CO</i> (ed. Vo-Dinh, T.) 83-88 (SPIE-The International Society for Optical Engineering, Bellingham, WA, 1996)	2,4
Therriault, G. A. & Lieberman, S. H. "A Cone Penetrometer Probe for the <i>In situ</i> Detection of Metals in Soils," in <i>Fifth International Symposium on Field Analytical Methods for Hazardous Wastes and Toxic Chemicals</i> 690-701 (Air & Waste Management Association, Las Vegas, Nevada, 1997).	2,4
Therriault, G. A., Bodensteiner, S. & Lieberman, S. H. "A Real-Time Fiber-Optic LIBS Probe for the <i>in situ</i> delineation of Metals in Soils. <i>Field Analytical Chemistry and Technology</i> 2, 117-125 (1998).	1
Therriault, G. A., Mosier-Boss, P. A. & Lieberman, S. H. "Application of LIBS to <i>in situ</i> Assessment of Metal Contaminated Soils," in <i>Proceedings-Advanced Sensors and Monitors for Process Industries and the Environment, November 4-5, 1998, Boston, MA</i> (ed. de Groot, W. A.) 141-145 (SPIE-The International Society for Optical Engineering, Bellingham, WA, 1999).	2,4
Lieberman, S. H., Mosier-Boss, P. A. & Andrews, J. A. "A Direct Push Sensor Probe for Real-Time <i>in situ</i> Measurement of Metals in Soil Via Laser-Induced Breakdown Spectroscopy (LIBS)," in <i>LIBS 2000 (1st International Conference on Laser Induced Plasma Spectroscopy and Applications)</i> (Pisa, Italy, 2000).	4

a. 1 = peer reviewed article, 2 = proceedings paper, 3 = technical report, 4 = presentation



## **8. Technology Implementation**

### **8.1 DoD Need**

Heavy metal contamination has been identified at 940 military sites in soils and sludges. Typical military activities associated with heavy metal contamination includes plating operations, firing ranges, motor pool activities, metal finishing, incineration activities, cooling water treatment, and burning pits.

### **8.2 Transition**

Although there is no formal DoD-supported effort for transitioning metal sensor technology to Army- or Navy-operated SCAPS systems (currently three SCAPS systems are operated by the Army Corps of Engineers and two systems by the Naval Public Work Centers) efforts have been taken as part of the ESTCP-funded Demonstration/Validation effort to facilitate the transition of the SCAPS metal sensor technologies to the operational SCAPS users. Representatives from Army and Navy operational teams and users from the Department of Energy (DOE) system operated at the Savannah River Site in South Carolina attended the SCAPS users workshop in San Diego that was scheduled to coincide with the ESTCP visitor day at the NAS North Island demonstration site. DoD and DOE SCAPS users were briefed on the three technologies and a demonstration of the LIBS sensor was conducted. Discussions were held concerning mechanisms for transitioning the capability to the operational systems. Discussions were also held during the demonstrations with personnel from the Pacific Northwest National Laboratory concerning the transition of FO-LIBS technology to the DOE Hanford Site. There is also possible use of SCAPS metals sensors at Travis AFB and an EPA Superfund Site (Atlantic Wood Industries, Portsmouth, VA). Because there is no formal mechanism for technology transition, each technology transition is negotiated with and funded by individual DoD and DOE operational users. Each DoD system operational system is operated independently on a cost reimbursable basis and requires the support of installation restoration activities. There are recent precedents for the transition of technologies to the DOE SCAPS system: the Navy/SERDP developed GeoVIS soil-video imaging system was transitioned to the DOE SCAPS system in Fiscal Year (FY) 1999, the ERDC spectral gamma sensor in 1998, and the Tri-Service developed LIF petroleum sensor in 1994.

Lessons learned during the SCAPS LIF ESTCP project suggest that the most effective long-term strategy for transferring the metals sensor technology to the user is through the commercial sector. However, transition to the DoD and DOE SCAPS Teams is ongoing and represents a

viable interim pathway for transitioning technology. Government owned and operated systems help build acceptance for a new technology by expanding the user base.

Because of the ESTCP support Demonstration/Validation effort described in this report, transitions of the XRF and LIBS technologies are currently in progress. As a result of the international conference on laser-induced breakdown spectroscopy (LIBS2000), representatives of Mitsubishi Heavy Industries are currently negotiating a Cooperative Research and Development Agreement (CRDA) with SSC San Diego for the commercialization of the FO-LIBS sensor system. Amp-Tek, Inc. and Niton Corporation became interested in the XRF sensor through presentations at the Denver X-Ray Conference and the OnSite 2000 Conference in Las Vegas, NV. Finally, technology transfer of the SCAPS metal sensor technologies demonstrated in this ESTCP project are also being facilitated by offering licenses of government patents, the same approach used successfully by ERDC for technology transfer of the SCAPS LIF sensor technology. At the Camp Keller site, personnel of AMS, Inc., observed the XRF field demonstration.

## 9. Lessons Learned

As was learned during the validation process for the other SCAPS sensor technologies, a singular all-encompassing acceptance is not possible within the framework of regulations, jurisdictions, and organizations defining the regulatory community. Furthermore, obtaining regulatory acceptance does not always guarantee the transition of field technology. For field technology to transition, it has to be accepted by the users whose responsibility it is to delineate the contaminant plume and decide the best approach for remediation. Hence, it is important that the technology be transitioned to a viable commercial entity that understands the usefulness and cost-effectiveness of the technology. For the Demonstration/Validation of the LIBS and XRF heavy metals sensors, our approach was to generate a field performance database in which a side-by-side comparison of the three technologies was presented. It is expected that the database will provide commercial developers an understanding of the capabilities of the three technologies and will help site managers select a viable approach for field-screening sites for heavy metal contamination.

### 9.1 Technical Lessons

During the course of the field demonstrations, several lessons were learned that will greatly enhance SCAPS metals sensor technology performance.

**9.1.1 SCAPS FO-LIBS Metals Sensor.** The presence of soil moisture decreases the LIBS response because part of the laser excitation energy vaporizes the moisture in the soil. At HPS and Camp Keller, the effect of soil moisture on the LIBS response could be minimized by using higher laser pulse energies, by using preliminary laser pulses to vaporize the water before data acquisition, and by optimizing the timing of the detector gate with the broadband background. In the present instrumental configurations, these parameters are site-specific and require manual adjustment. However, modifications may be possible in the acquisition software to automate this process.

The magnitude of the LIBS response is affected not only by moisture content of the soil, but also by soil composition and grain size. Ideally, if identical quantities and composition of matter were ablated to form the micro plasma, the spectra would fall one atop the other. However, this is not observed and is attributed to differences in plasma volume. An effective correction for differences in plasma volume is to normalize the areas under the spectra to one. Another approach is to normalize the response of the system to a spectral line of a fixed plasma

component that varies with moisture content. This approach would likely involve the use of ion-implantation of a normalization component into the sapphire window. Preliminary data using a Zr-coated sapphire window are shown in Figure 25. The Zr doublet near 424 nm could be used to normalize the response of the system for variations in plasma volume.

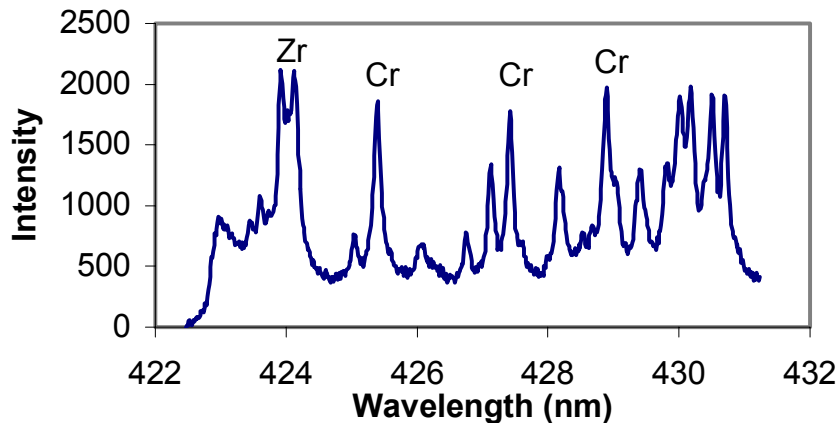


**Figure 25.** FO-LIBS Spectrum of NASNI Soil Obtained Using a Zr-Coated Sapphire Window

**9.1.2 SCAPS XRF Metals Sensor.** The primary lesson learned during the ESTCP field demonstrations was that a more reliable window configuration is needed for the XRF probe. The current window mounting system failed during the demonstration at Hunters Point Shipyard, causing water to enter the probe and preventing collection of data. A thin window (0.25-mm thick) was used to enhance the detection capability for chromium. The window mount did not hold the window material securely. The probe pushing against subsurface rock may have caused the window material or window mount to fail. A solution may be to use a window with thick edges and a thinner center to optimize the x-ray pass-through. This window would provide mounting strength while still providing optimal detection of chromium.

**9.1.3 SCAPS DL-LIBS Metals Sensor.** The primary lesson learned during the ESTCP demonstration was that variations in soil moisture can have a significant impact on the quantification of DL-LIBS *in situ* measurements. However, the variability on LIBS sensitivity that results from variations in soil moisture content can be minimized by using moist soil calibration curves instead of dry soil calibrations curves for the determination of the *in situ* concentrations. Site-specific soil moisture calibration curves improve the accuracy of DL-LIBS quantification. The integration of a reliable real-time moisture sensor with LIBS metals sensor technology will provide the means to correct the LIBS response for moisture variations in the soil.

The recessed window slot geometry of the DL-LIBS probe configuration was successfully demonstrated and was strong and reliable. However, the recessed window in saturated soil can become plugged with subsurface media. A modification in probe geometry is needed to correct the “plugging” problem and to increase the performance of the DL-LIBS probe in saturated soil.



## 10. References

- Bujewski, G. and B. Rutherford. 1997. "Innovative Technology Verification Report: The Site Characterization and Analysis Penetrometer System (SCAPS) Laser-Induced Fluorescence (LIF) Sensor and Support System," pp. 83. US Environmental Protection Agency, National Exposure Research Laboratory.
- California Environmental Protection Agency Department of Toxic Substances Control. 1996. "Final Hazardous Waste Technology Certification Program Report: Site Characterization and Analysis Penetrometer System with Laser-Induced Fluorometry (SCAPS-LIF) as an *in situ* Field Screening Technology for the Detection of PNA-Containing Petroleum Hydrocarbons," pp. 47.
- Cone Penetrometer Task Group Report. 1996. "Multi-State Evaluation of an Expedited Site Characterization Technology: Site Characterization and Analysis Penetrometer System Laser-Induced Fluorescence (SCAPS-LIF)," pp. 12. Western Governors' Association DOIT Initiative, Interstate Technology and Regulatory Cooperation Workgroup.
- Cortes, J., E. R. Cespedes, and B. H. Miles. 1996. "Development of Laser-Induced Breakdown Spectroscopy for Detection of Metal Contaminants in Soils." U.S. Army Engineer Waterways Experiment Station.
- Criss, J. W. 1976. "Particle Size and Composition Effects in X-Ray Fluorescence Analysis of Pollution Samples," *Analytical Chemistry*, vol. 48, pp. 179–186.
- EA Engineering Science and Technology. 1994. "Draft Remedial Investigation Report of Operable Unit LCAAP," Independence, MO.
- Fichet P., P. Mauchien, J. -F. Wagner, and C. Moulin. 2001. "Quantitative Elemental Determination in Water and Oil by Laser-Induced Breakdown Spectroscopy," *Analytica Chimica Acta*, vol. 429, no. 2, pp. 269–278.
- Fordham, O. 1997. "Draft EPA SW-848 Method 6200, Field Portable X-Ray Fluorescence Spectrometry for the Determination of Elemental Concentration in Soil and Sediment." EPA Office of Solid Waste.
- Lieberman, S. H. 1998. "Direct-Push, Fluorescence-Based Sensor Systems for *in situ* Measurement of Petroleum Hydrocarbons in Soils," *Field Analytical Chemistry and Technology*, vol. 2, no. 2, pp. 63–73.
- McDonald, B. J., J. J. Trautner, A. G. Seelos, and R. K. Glanzman. 1996. "Calibration of XRF and Laboratory Analyses of Soil." In *Uncertainty in the Geological Environment*, vol. 1 C. D. Shackelford, P. P. Nelson, and M. J. S. Roth, Eds., pp. 287–296, American Society of Civil Engineers.

- Miles, B. H., J. Cortes, and E. R. Cespedes. 1992. "Laser-Induced Breakdown Spectroscopy Final Report." Waterways Experiment Station.
- Therriault, G., P. A. Boss, and S. H. Lieberman. 1999. "White Paper: SCAPS Heavy Metal Sensors (ESTCP Project 199716)," pp. 15, Space and Naval Warfare System Center, San Diego, CA.
- Unsell, C. W. 1998. University of Toledo.

## **Appendix A: Points of Contact**

Dr. Stephen Lieberman  
SSC San Diego  
D361  
49575 Beluga Rd.  
San Diego, CA 92152-6325  
(619) 553-2778 FAX: (603) 909-8049

Dr. Pamela A. Boss  
SSC San Diego  
D363  
45650 Lassing Rd.  
San Diego, CA 92152-6171  
(619) 553-1603 FAX: (619) 553-1269

Dr. W. Tim Elam  
10551 158<sup>th</sup> Ave. NE  
Redmond, WA 98052-2659  
(425) 867-9002

Mr. Charles M. Dozier  
Naval Research Laboratory  
Code 6175  
4555 Overlook Ave.  
Washington, DC 20375-5345  
(202) 767-2154 FAX: (202) 767-4868

Mr. John H. Ballard  
U.S. Army Engineer Research and Development Center (ERDC)  
3909 Halls Ferry Rd.  
Vicksburg, MS 39180-6199  
(601) 634-2446 FAX (601) 634 2854

Mr. Javier Cortes  
U.S. Army Engineer Research and Development Center (ERDC)  
3909 Halls Ferry Rd.  
Vicksburg, MS 39180-6199  
(601) 634-2447 FAX: (601) 634-3518

## APPENDIX B: DATA ARCHIVING

### B1. Introduction

The validation process for the two LIBS and XRF sensors consists of deploying each probe at four predetermined sites. For each site, two sets of measurements are conducted. In the first set, *in situ* measurements are conducted at a number of holes. These measurements provide a general picture of the contaminant distribution at the site. In the second set of measurements, discrete samples gathered at each site are homogenized and analyzed by each sensor in the laboratory *ex situ*. Splits of these samples are sent to an analytical laboratory for analysis. The results from the analytical laboratory are compared to the results of the metal sensor *ex situ* laboratory analysis of the samples on a scatter plot. Field validation data (hardcopy plots, field notes, work plans, analytical laboratory results, and data reports) collected as part of this project are archived in the SSC San Diego SCAPS Project Office, San Diego. Requests for copies of the data or reports should be made to Dr. Stephen Lieberman at the address listed in Appendix A, Points of Contact.

The raw and processed data for *in situ* pushes and the *ex situ* laboratory samples and a description of data treatment for each sensor has been assembled and archived on CD-ROMs and included in this report. The appendix provides a general description of how each metal sensor manipulated their spectral data. *The data and description of the data manipulations for all three sensors demonstrated are provided to assist prospective users in choosing the sensor technology appropriate for their need. This information is also useful in assessing the capabilities and limitations of each technology, either in the quality of data obtained or in the manipulation of such data.*

### B2. FO-LIBS

The LIBS signal is generated by the application of a focused, high-power laser pulse to the sample to ablate material and form a microplasma. This microplasma contains both single and multiple ionized species that were present in solid form at the focus of the beam. The early evolution of the plasma is characterized by an initial broadband emission that decays with time as the plasma cools. After a delay on the order of 1 microsecond, the plasma has cooled to a temperature at which its spectrum is characterized by narrow atomic emission lines from the plasma constituents.

The LIBS response is subject to matrix effects. Soil type, porosity, and moisture content can affect the magnitude of the response. The primary matrix effects are due to variation in soil grain size, soil type, and soil moisture. These matrix effects affect the precision and accuracy of the LIBS measurements. The accuracy of the measurements is affected because the slope of the instrument calibration curves change for different soil grain sizes and moistures. The precision of the measurements is affected because, while the calibration curves are generated using site-specific soil samples with representative grain size distributions and moisture contents, there are variations in these two parameters within the site itself. These variations manifest themselves in the precision of the reported *in situ* results. How the LIBS data have been corrected for these effects has been an evolutionary process. The raw and processed data for each site have been archived on a CD-ROM as Microsoft® Excel (.xls) spreadsheets. The spreadsheets are self-explanatory. The spreadsheets and word document for each site contain information on the experimental parameters (i.e., delay times, number of laser shots, and other parameters) used to obtain the spectral data and describe how the data were manipulated to correct for matrix effects and how the LIBS response was converted into concentration. The following is a brief summary of how the FO-LIBS *ex situ* laboratory and *in situ* data were manipulated for each of the site demonstrations.

**B2.1 Preparation of Calibration Standards.** Uncontaminated soil obtained from the site was used to prepare standards. It was assumed that this soil is representative of the grain size distribution of the site and was used to generate a site-specific calibration curve. The soil was dried and standards were prepared by spiking 15-g aliquots of soil with known quantities of a solution containing 10,000 ppm of the metal contaminant of interest. For LCAAP and NASNI, an aqueous 10,000 ppm standard solution was used. After spiking, the LCAAP and NASNI calibration standards were heated to remove the water. Higher soil metal concentrations (>2000 ppm) require multiple spikings and heatings. Repeated spikings and heatings of the sample degraded the soil matrix. To avoid degradation of the soil matrix, the calibration standards for HPS were prepared using an ethanolic solution of 10,000 ppm Cr. Camp Keller calibration standards were prepared using a 50:50 ethanol:water solution of 10,000 ppm Pb. After spiking, the samples were allowed to air dry. After preparation, these standards were used to generate the site-specific calibration curve. In the spectral region between 403 and 412 nm, Pb has an emission line at 405.8 nm that is used for calibration purposes. In the spectral region between 423 and 432 nm, Cr has emission lines at 425.5, 427.5, and 428.9 nm. The 427.5 and 428.9 nm Cr lines were obscured by Ca, Mn, Fe, and Ti emission lines (materials present in the soil matrix). Therefore, only the 425.5-nm Cr line was used for calibration purposes.

**B2.2 Generation and Manipulation of Spectral Data for the Calibration Curve and *ex situ* Laboratory Data.** The calibration and *ex situ* laboratory samples are dry. Consequently, these samples do not require correction for moisture content. To compensate for variations in the soil matrix, the primary experimental parameters that can be adjusted are the laser pulse energy and the delay time of the detector gate. In the laboratory, these experimental parameters are optimized using soil from the site. The experimental parameters used for each site are summarized in the archived spreadsheets.

As was stated earlier, treatment of the spectral data have been as evolutionary process. Our first demonstration occurred at a Pb site in LCAAP. Figure B-1 shows spectra for a LCAAP *ex situ* laboratory sample obtained from Hole 1 at a depth of 0 to 6 inches bgs. We see that the intensity of the Pb peak varies considerably. This variability is attributed to variations in soil grain size, soil composition, and soil porosity. At this stage in the investigation, no reliable means of compensating for this variability had been devised. The ideal method for correcting for these effects, as well as moisture effects, would have been to use an internal standard for normalization purposes. It was suggested that the emissions due to iron present in the soil could be used for this purpose. However, to use this method the iron concentration within the soil has to remain constant. In practice, it was found that the iron concentration varied considerably as a function of depth. Alternatively, since the window is ablated during the LIBS experiment, the spectral data could be normalized to a component within the window itself. Sapphire is composed of Si and Al. Neither of these metals have emission lines that would be useful for normalization purposes. Furthermore, soil contains significant amounts of these metals. Whatever is used as an internal standard would have to be relatively rare in nature and exhibit emission lines in the visible range. The metal Zirconium, atomic number 40, meets both criteria and zirconium oxide ( $ZrO_2$ ) windows are commercially available. However, it was found that, due to the optical properties of  $ZrO_2$ , a micro plasma could not be formed and LIBS spectra could not be obtained. It was then suggested that the normalization component could be ion-implanted into the sapphire window. Although calculations looked promising, there were no funds available to pursue this area of research.

Since we had no reliable means of correcting for soil matrix effects at the time of the LCAAP demonstration, the background of the spectral data were normalized to zero at 405.38 nm. The Pb peak area was then integrated between 405.62 and 406.13 nm and the average Pb peak area for each calibration standard was calculated. The average Pb peak area for the calibration standards was plotted as a function of concentration and a site-specific calibration curve was

used to convert the peak areas of the *ex situ* laboratory samples into concentration. These procedures can be easily followed in the spreadsheets archived on the CD-ROMs.

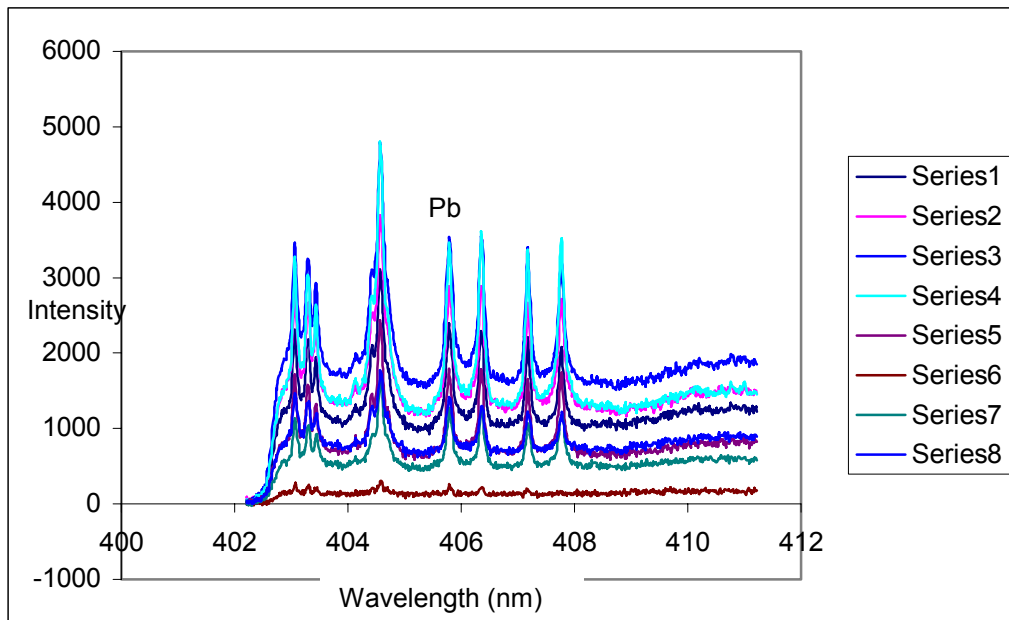


**Figure B-1.** FO-LIBS Spectra Obtained for a LCAAP Laboratory Sample Obtained from Hole 1 at a Depth of 0 to 6 bgs

The second demonstration took place at the IWTP at NASNI. The contaminant of concern was Cr. Figure B-2 shows spectra obtained for a laboratory sample from Hole 1 at a depth of 36 to 48 inches bgs. The top set of spectra was not normalized. There was significant variability in the intensity of the emission lines due to the metals. Ideally, if identical quantities and composition of matter were ablated to form the microplasma, the spectra would fall one atop the other. However, this was not observed and was attributed to differences in plasma volume. Within the soil, there may be voids and some materials may ionize more readily than others. To correct for differences in plasma volume, the areas under the spectral curves were normalized to one. The bottom set of spectra in Figure 2 shows the result of this normalization. The variability in the peak intensity was dramatically reduced. After normalization, the intensity of the Cr peak at 425.5 nm was measured (background corrected) and plotted as a function of concentration to create a site-specific calibration curve. This calibration curve was used to convert peak intensities of the *ex situ* laboratory samples into concentration. The data manipulations are provided in the spreadsheets. This approach of normalization gave very good agreement between the ICP laboratory results and FO-LIBS results, not only at NASNI, but also at HPS and Camp Keller.

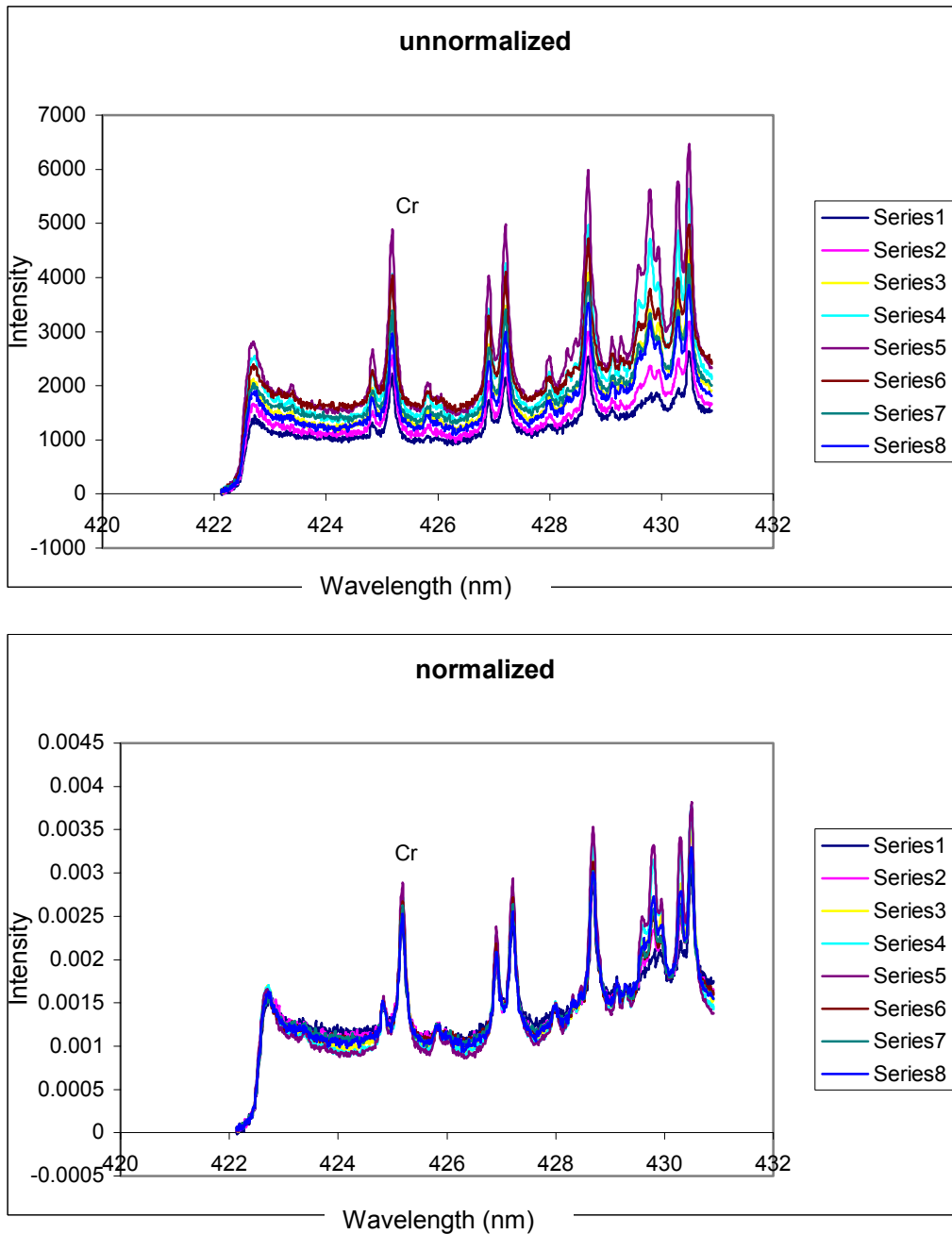


**Figure B-2.** Un-Normalized and Normalized LIBS Spectra of a NASNI Laboratory Sample Obtained from Hole 1 at a Depth of 36 to 48 bgs

**B2.3 Generation and Manipulation of Spectral Data for the *in situ* Push Data.** All LIBS data for the four demonstration sites were obtained using a modified form of the software originally developed to obtain LIF data. At LCAAP, NASNI, and HPS, the *in situ* push data were obtained using the 'profile' mode of the software. In 'profile' mode, the spectral data,

depth, and strain gauge data are automatically recorded for each push. During each push at these first three sites, the probe was stopped at 2-inch intervals to obtain spectral data. For each depth, only one spectrum was obtained. Once in 'profile' mode, experimental parameters such as delay time, number of warm-up shots, number of acquisition laser shots, and other parameters cannot be modified. At Camp Keller, to obtain spectral data, the experimental parameters had to be optimized for each depth during the push. Therefore, the *in situ* pushes at Camp Keller were obtained using the software in 'manual' mode (the same mode used to obtain data for the *ex situ* laboratory and calibration samples). In 'manual' mode, the strain gauge data and depth are not recorded automatically by the computer.

At LCAAP, the *in situ* spectral data were obtained using the same experimental parameters as the calibration standards. For each depth, one spectrum was obtained using 300 shots. The area of the Pb peak at 405.8 nm was measured in the same manner as described for the calibration and *ex situ* laboratory samples, and converted to concentration using the calibration curve. However, this concentration value was not corrected for moisture effects or to differences in plasma volume. Moisture content can dramatically affect the magnitude of the LIBS response (Figure B-3). The data shown in Figure B-3 were generated on Fisher sea sand, a worst case scenario due to its large pore sizes. From the LCAAP, *ex situ* laboratory samples, the average moisture content of the site was 12%. A 12% moisture content corresponds to a fourfold drop in signal intensity. To correct for moisture content, the apparent lead concentration was multiplied by a factor of 4. As described in the previous section, we had not yet devised a means of correcting the data for differences in plasma volume. To correct for plasma volume differences, the moisture corrected lead concentration was multiplied by a factor of 0.1, a very rough correction. All data manipulations can be followed in the spreadsheets for the site archived on the CD-ROM.

At NASNI, the *in situ* spectral data were obtained using the same experimental parameters as the calibration standards. For each depth, one spectrum was obtained using 300 shots. The areas under the spectral curves were normalized to one to correct for differences in plasma volume. The intensity of the Cr peak at 425.5 nm was measured and converted to concentration using the calibration curve. From the NASNI *ex situ* laboratory samples, the average moisture content of the site was 8%. An 8% moisture content corresponds to a threefold drop in signal intensity. To correct for moisture content, the apparent chromium concentration was multiplied by a factor of 3. The amount of sample ablated during the LIBS measurement was on the order of micrograms while the ICP analysis was conducted on 1-g samples. The *ex situ* samples were collected over 1-foot intervals and were homogenized. To plot the *in situ* results on a comparable spatial scale

as the ICP analysis, a running average of the LIBS data were plotted as a function of depth using the following linear filter:

$$\hat{y}_i = \sum_{n=-NL}^{NR} c_n y_{i+n} \quad \text{where } c_n = \frac{1}{NL + NR}.$$

In the above equations, NL and NR refer to the number of points to the left and right to average. Since the ICP analysis was conducted on homogenized samples collected over a 1-foot interval and the LIBS data were collected over 2-inch intervals, NL = NR = 3. All data manipulations are provided in the spreadsheets for the NASNI.

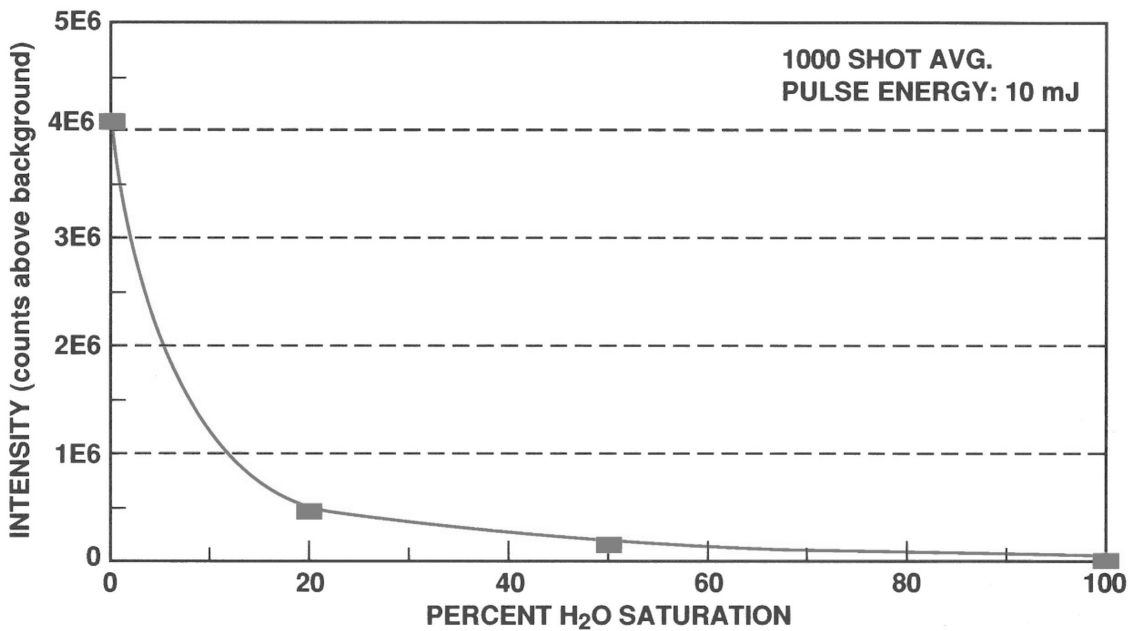


**Figure B-3.** Effect of Moisture Content on LIBS Signal. Data were obtained on Fisher Sea Sand and were considered to the worst case scenario. (Where 100% water saturation corresponds to 33% water by weight.)

At HPS, experimental parameters to obtain the *in situ* push data were optimized onsite to account for the presence of water. The spectral data were obtained using a higher laser power than that used for dry samples. In addition, 600 warm-up shots were used to drive off water before the acquisition laser shots. The areas under the spectral curves were normalized to 1 to correct for differences in plasma volume. The intensity of the Cr peak at 425.5 nm was measured and converted to concentration using the calibration curve. Because higher laser power was used to obtain spectral data in the saturated zone, it was deemed unnecessary to correct the concentration values for moisture, as was done for data obtained at the LCAAP and NASNI. Either due to

voids present in the subsurface media or to ablating gravel fill instead of contaminated soil, gaps were observed in the FO-LIBS *in situ* HPS data. Due to the gaps in HPS data, a running average of the LIBS data were not plotted as a function of depth, as was done for the NASNI *in situ* data. All data manipulations are provided in the HPS spreadsheets.

To obtain *in situ* data at Camp Keller, the delay and the number of acquisition laser shots and warm-up shots were varied. This variation required running the instrument software in manual mode. Spectral data were obtained at 4-inch intervals. The areas under the spectral curves were normalized to 1 to correct for differences in plasma volume. The intensity of the Pb peak at 405.8 nm was measured and converted to concentration using the calibration curve. Because the site had been under drought conditions for several months and the water table was 33 ft bgs, it was deemed unnecessary to correct the concentration value for moisture. Because the data were obtained at 4-inch intervals, a running average of the LIBS data were not plotted as a function of depth, as was done for the NASNI *in situ* data. All data manipulations are provided in the Camp Keller spreadsheets.

The data obtained at the four demonstration sites are archived on CD-ROMs. The following tables summarize the data archived in folder 'FO-LIBS data' on the CD-ROMs.

**Table B-1.** Summary of Archived FO-LIBS LCAAP Raw and Processed Data (Folder ‘LCAAP’ in Folder ‘FO-LIBS Data’).

<b>LCAAP data manipulation.doc</b>	Microsoft® Word document that summarizes LCAAP FO-LIBS data manipulation
<b>LCAAP FO-LIBS calibration.xls</b>	Microsoft Excel® spreadsheet of LCAAP FO-LIBS calibration. Contains raw & processed data and calibration curve.
folder ‘Laboratory Data’	<ol style="list-style-type: none"> <li>1. Folder ‘Raw &amp; Processed Data’: contains <b>hole1.xls, hole2.xls, hole3.xls, hole4.xls, hole5.xls, and hole6.xls</b> spreadsheets</li> <li>2. <b>LCAAP laboratory results.xls</b> spreadsheet contingency data and plot</li> </ol>
folder ‘ <i>In situ</i> Data’	<ol style="list-style-type: none"> <li>1. Folder ‘Raw &amp; Processed Data’: contains <b>push2soil6.xls, push3soil4.xls, push4soil1.xls, push6soil3.xls, push7soil2.xls, and push8soil5.xls</b> spreadsheets</li> <li>2. <b>Summary of <i>in situ</i> data.xls</b> spreadsheet of push data (Pb concentration as a function of depth)</li> </ol>

**Table B-2.** Summary of Archived FO-LIBS NASNI Raw and Processed Data (Folder ‘NASNI’ in Folder ‘FO-LIBS Data’).

<b>NASNI data manipulation.doc</b>	Microsoft® Word document that summarizes NASNI FO-LIBS data manipulation
<b>NASNI FO-LIBS calibration.xls</b>	Microsoft® Excel spreadsheet of NASNI FO-LIBS calibration. Contains raw & processed data and calibration curve.
Folder ‘Laboratory Samples’	<ol style="list-style-type: none"> <li>1. Folder ‘<i>ex situ</i> nasni data’: contains <b>hole1normal.xls, hole2normal.xls, hole3 normal.xls, hole4 normal.xls, hole5normal.xls, and hole6normal.xls</b> spreadsheets</li> <li>2. <b>NI scatter plot normal.xls</b> spreadsheet containing contingency data and plot</li> </ol>
folder ‘ <i>In situ</i> Data’	<ol style="list-style-type: none"> <li>1. Folder ‘Raw &amp; Processed Data’: contains <b>push1.xls, push2.xls, push3.xls, push4.xls, push5.xls, and push6.xls</b> spreadsheets</li> <li>2. <b>summary of <i>in situ</i> data.xls</b> spreadsheet of push data (Cr concentration as a function of depth)</li> </ol>

**Table B-3.** Summary of Archived FO-LIBS HPS Raw and Processed Data (Folder ‘HPS’ in Folder ‘FO-LIBS Data’).

<b>HPS data manipulation.doc</b>	Microsoft® Word document that summarizes HPS FO-LIBS data manipulation
<b>HPS FO-LIBS calibration.xls</b>	Microsoft® Excel spreadsheet of HPS FO-LIBS calibration. Contains raw & processed data and calibration curve.
Folder ‘Laboratory Data’	<ol style="list-style-type: none"> <li>1 Folder ‘Raw &amp; Processed Data’: contains <b>hole1push2normal.xls, hole2push10normal.xls, hole3push3normal.xls, hole4push8normal.xls, hole5push6normal.xls, and hole6push9normal.xls</b> spreadsheets</li> <li>2 <b>HPS laboratory results.xls</b> spreadsheet containing contingency data and plot</li> </ol>
Folder ‘ <i>In situ</i> Data’	<ol style="list-style-type: none"> <li>1 Folder ‘Raw &amp; Processed Data’: contains <b>push2soil6.xls, push3soil4.xls, push4soil1.xls, push6soil3.xls, push7soil2.xls, and push8soil5.xls</b> spreadsheets</li> <li>2 <b>summary of <i>in situ</i> data.xls</b> spreadsheet of push data (Cr concentration as a function of depth)</li> </ol>

**Table B-4.** Summary of Archived FO-LIBS Camp Keller Raw and Processed Data (Folder ‘Camp Keller’ in Folder ‘FO-LIBS Data’).

<b>Camp Keller data manipulation.doc</b>	Microsoft® Word document that summarizes HPS FO-LIBS data manipulation
<b>camp keller calibration.xls</b>	Microsoft® Excel spreadsheet of HPS FO-LIBS calibration. Contains raw & processed data and calibration curve.
Folder ‘Laboratory Data’	<ol style="list-style-type: none"> <li>1 Folder ‘Raw &amp; Processed Data’: contains <b>hole1push13.xls, hole2push12.xls, hole3push8.xls, hole4push9.xls, hole5push10.xls, and hole6push11.xls</b> spreadsheets</li> <li>2 <b>contingency plot.xls</b> spreadsheet containing contingency data and plot</li> </ol>
Folder ‘ <i>In situ</i> Data’	<ol style="list-style-type: none"> <li>1 Folder ‘Raw &amp; Processed Data’: contains <b>push10hole5.xls, push11hole6.xls, push12hole2.xls, push13hole1.xls, push8hole3.xls, and push9hole4.xls</b> spreadsheets</li> <li>2 <b>summary of <i>in situ</i> data.xls</b> spreadsheet of push data (Cr concentration as a function of depth)</li> </ol>

### **B3. XRF**

The data and acquisition parameters and the calibration samples for all four sites are summarized in the file 'XRF Data.doc', which is found in the folder 'xrf data' on the CD ROMs.

**B3.1 Spectral Data.** X-Ray Fluorescence (XRF) spectra are collected using Energy Dispersive X-Ray Fluorescence (EDXRF). In this method, the detector produces a single pulse for each x-ray emitted by heavy metal atoms in the soil. The height of each pulse is proportional to the energy of the x-ray. The spectrum is collected in a multichannel analyzer (MCA), which typically has 1024 channels. Each channel has an assigned pulse height (and, thus, energy range). The MCA determines the corresponding channel for each x-ray pulse and increments that channel by one count. The XRF spectrum is thus the number of counts in each channel, which gives the number of x-rays detected as a function of x-ray energy. The energy range of each channel (typically, 20 eV) is much less than the energy resolution of the detector (typically, 250 eV), so that the MCA output is a complete representation of the x-ray spectrum.

The energy range corresponding to the MCA channels are established by calibration. This relationship is very stable and is usually established only once for each detector and is checked periodically. EPA Method 6200 (FORDHAM, 1997) recommends that this be checked daily, which is the frequency adhered to in this study. A linear relationship is used between channel and energy and is established using two known x-ray emission peaks. Peaks typically used were the iron K alpha (Fe Ka, 6.40 keV) and the Pb L alpha (Pb La, 10.55 keV) from the National Institutes of Standards and Technology (NIST) Standard Reference Material (SRM) 2710, the manganese K alpha (Mn Ka, 5.90 keV) from an Fe-55 radioactive source in the laboratory, and the molybdenum K alpha (Mo Ka, 17.44 keV) from a pure Mo foil. This calibration generally drifted less than 0.05 keV and was not corrected, since this is less than the detector resolution.

The raw data are in files with an extension ".asp". The file can be opened in Microsoft<sup>®</sup> Notepad. The file consists of a column of numbers from lines 1 to 1025. These are followed by 14 lines of descriptors. The data present in the file can be used to generate the original raw spectrum. To illustrate, we will use file 'Lc1s4la.asp', which is a data file obtained for LCAAP. Line 1 indicates the number of channels, which is 1024. The following 1024 numbers (lines 2 through 1025) correspond to the intensity, or number of x-rays detected, in each channel. The first line of descriptors indicates that there is a two-point calibration to convert channel number into energy. The next five lines of descriptors indicate that, for channel number 332.740, the energy is 6.4 keV, while for channel number 899.080 the energy is 17.440 keV. The non-integer calibration channels are the actual centroids of the peaks corresponding to the emission lines

used for calibration. This calibration procedure gives energy calibration precision better than one channel, which is possible since the peak position can be calculated more accurately than one channel. To get the energy for any channel, a linear interpolation based in the two calibration points must be conducted. Figure B-4 shows the resultant spectrum. The last line of descriptor in the file 'Lc1s4la.asp' identifies the sample used to generate the XRF spectrum.

**B3.2 Calibration.** The main calibration necessary for XRF spectra is to establish the relation between the number of x-rays detected for a particular element and the weight concentration of that element in the soil measured. To establish this relationship, the number of x-rays from the element of interest must be isolated from the spectrum, identifying the peak corresponding to the particular element, subtracting any background, which may be present from the instrument, and integrating the counts in the peak. Since the energy calibration is stable, a fixed region for the element peak can be chosen from one of the calibration spectra that contains a strong peak of the chosen element. This region is chosen to encompass the entire peak but avoid any nearby peaks from other elements. The energy resolution is adequate for all elemental peaks except for a few interferences that were not encountered in this study. The principal background in this instrument is scattered continuum radiation from the x-ray tube, which can be treated as a linear function of energy over the short energy ranges of the element characteristic peaks. This background is determined by taking the number of counts at each end of the defined region, using a three-point average. The slope and intercept are used to interpolate the background value at each point under the peak and it is subtracted from the data. For peaks with more than 100 total counts (after background subtraction), the actual centroid location is calculated and used as the center location of the peak. The centroid is the first moment divided by the integral, over the entire region. For peaks with less than 100 total counts, this calculation is unstable and the center of the region is used as the centroid of the peak. Next, the full width at half maximum (FWHM) of the peak is calculated and the integration range taken as 1.2 times the FWHM. This procedure optimizes the signal to noise of the peak integral. Since the FWHM depends on the second moment of the peak, which is unstable for weak peaks, the integration range is restricted to within the defined region regardless of the FWHM calculation.

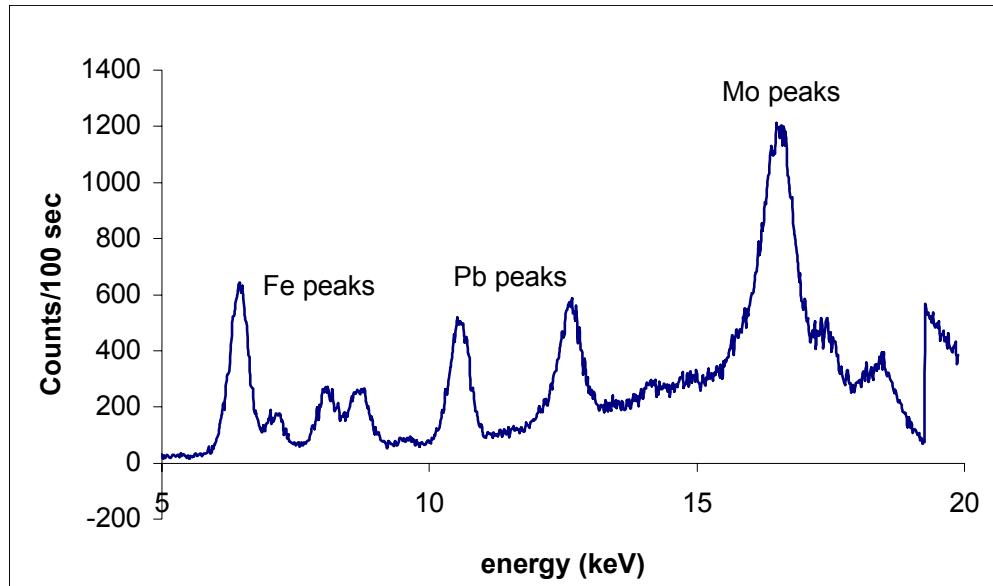


**Figure B-4.** XRF Spectrum Generated using data summarized in file Lc1s41a.asp. The Mo peaks are from the excitation source.

Once the numbers of x-rays detected from a chosen element are quantified, the relationship between number of x-rays and element concentration depends on the probe geometry and the matrix. Soils consist mostly of low atomic number elements with atomic number less than 20. The difference in atomic number between the soil matrix and the metal contaminants makes soil an ideal matrix for detection of heavy elements, with atomic number greater than about 20, since their characteristic x-rays have higher energies and are not heavily absorbed by the lighter elements in soils. If insignificant amounts of heavy metals are present (less than about 3% by weight), the relation between the number of x-rays detected and the concentration is linear. Hence, only the slope need be determined, assuming the background subtraction is adequate. If any residual background remains, the slope and intercept must be used. The slope varies only slightly with soil composition. Since this sensor is intended for field screening, with accuracies of 20 to 50% rather than the analytical laboratory requirement of 1%, variation with soil type can be generally ignored. The calibration used standard reference materials or spiked standards verified by *ex situ* laboratory analysis. Soils similar to the site under investigation were used to prepare spiked standards; actual soil from the site was used when possible. Peak integral intensities from these standards, calculated as described above, were used to obtain a linear fit to the known element concentrations. This calibration will be probe-specific, and must be performed whenever the configuration of the probe is changed, such as replacing the x-ray tube. For this reason, the probes were originally given a numerical designation. As more x-ray tubes were used, the probe designation was changed to an alphabetical designation that was associated

with the x-ray tube in the probe. If heavy metals are present in large quantities, greater than a few percent, they must be taken into account in the calibration. These are usually detected in the XRF spectrum and their concentration can be inferred. The heavy metal encountered in this study was the analyte of interest itself, which was sometimes present in concentrations above 10%. To compensate for this, a hyperbolic relationship between x-ray counts and concentration was used, which is valid at any analyte concentration. This calibration procedure required establishing the relationship at high and low concentrations. At high concentrations, the relationship was established by measuring pure metal oxides. At low concentrations, the relationship was adjusted to match the linear calibration curve established from the SRMs or site-specific standards.

The hyperbolic equation for the relationship between x-ray net counts and concentration (Tertian and Claisse, 1997) is

$$\text{ppm} = 1.0\text{e}6 * K * \text{RXI} / ( 1 + \text{RXI} * ( K - 1 ) ),$$

where ppm = element concentration in parts per million by weight, K is a calibration constant, and RXI is the number of x-ray counts divided by the counts for a pure element. Note that this equation references the peak counts to the counts from a pure element, which compensates for geometrical and other multiplicative effects and makes the equation more numerically stable. Hence, the hyperbolic constant, K, will be similar for all probe configurations. Since metals typically occur in oxide form in soils, the pure element counts used to compute the RXI for a given calibration were obtained by extrapolating the oxide counts using the fundamental parameters code NRLXRF (Criss, Birks, and Gilfrich, 1978). This connection makes the calibration more accurate for the concentration range for metal contamination in soils.

To illustrate the analysis process for a typical spectrum, the following calibration example is provided. The spectrum for this example will be the data taken at Lake City Army Ammunition Plant (LCAAP), at push location 8, 5 feet in depth. The spectrum was collected on 22 June 1998 with XRF Probe number 1, which was configured with a Mo anode x-ray tube and was operated at 30 kV and 20 microamps. The probe had a 1/2-inch-diameter boron carbide window, which was 0.040-inch thick. The MCA data file for this spectrum is LC1W8BN.ASP, which denotes Lake City, probe configuration 1, NRL (Washington) push location 8, and a two-letter sequence designation. The first line in the file provides the number of channels. The following lines contain the number of counts per each channel. At the end of the file is the auxiliary data for interpreting the spectrum in keyword format. The energy calibration is first. Note that there are two calibration points for a linear calibration at 6.4 keV (Fe Ka) and 17.44 keV (Mo Ka). The

date and time of data collection are given, along with the data collection live time and MCA dead time (not used in the analysis). The last line contains a user-entered comment, and is used to enter the site, push location, and depth (or standard sample if this is a calibration or check sample). Note that the comment for this file contains lcaap, the site designation, Hole 8 for the push location, and 5 feet in depth. This raw data file is produced directly by the commercial MCA software. The first steps in the process are to calculate the energy per channel and to calculate the net intensity for the element peak under investigation. These steps are performed by two FORTRAN programs, which process raw data files in batches and write a single file with the net intensities for a set of raw data files. The peak intensity file for LCAAP is named "LCAAP XRF Peak Data.txt". At the top of the file is information on the peak regions, followed by several columns of peak intensity and other data. The region definitions are read from a Region of Interest (ROI) file, which is reproduced in the peak file. The start, and end energies of each region are given, the default peak center and FWHM, and the column header for the results. A flag is included before the column name and the background under a peak can be written also. The regions defined in these data are the Pb La peak and background between 10.00 and 11.10 keV, the Pb L beta peak between 12.1 and 13.1 keV, and the Mo Ka peak (which is a Compton scattered peak from the x-ray tube). The columns of spectral data follow the ROI information. Both the net counts in each peak and the background counts for each peak are reported in the file. The last columns contain the filename of the original spectrum file to enable tracing the data to its origins and the depth extracted from the user comment. The data file LC1W8BN appears in the 74th line of the peaks file, and the column "Pb La" shows 6294.62 counts in the Pb La peak for lead. Only this peak was used to analyze the lead content in the data since the Pb Lb peak has a significantly larger background. The peaks file is imported into the spreadsheet "LCAAP XRF Analysis.xls", where only the Pb La counts and depth columns, plus the filenames, are retained. The "Pb La" column was converted to ppm Pb using the quantitative calibration equation above, with the parameters at the top of the spreadsheet. This ppm Pb data, together with the depth column, provides ppm Pb versus depth data for each push location, as well as the check samples (included at the end of the peaks file). The calibration was obtained on the second spreadsheet in the file, where the calibration data are included.

The parameters used in the quantitative calibration for each of the sites and sample sets are below. For the LC1W8BN spectrum, the RXI is the "Pb La" counts divided by the pure element counts, or  $6294.62 / 71749 = 0.088$ . The K constant is 0.072199, which gives 6842 ppm Pb in the hyperbolic calibration equation. These numbers are given for Probe 2 push data at the LCAAP site in the tables below and in the calibration parameters in each of the spreadsheets from the LCAAP site. Note that separate calibrations are used for the push and soil samples for

the NASNI and HPS sites since the configuration of the probe changes slightly between the field work and the *ex situ* laboratory spectra for soil samples.

The data obtained at the four demonstration sites are archived on a CD-ROM in the folder ‘XRF’. The raw data are in files with an extension of “.asp” and are archived on the CD-ROM in folders labeled ‘SITE raw data’. The following table summarizes the peak files and the data analysis spreadsheets for each site that are archived on a CD-ROM.

**Table B-5.** Summary of Files Archived in Folder ‘xrf data’ on the CD-ROM

Site Folder	Raw Data Folders	Peak Files	Analysis Spreadsheet
LCAAP	LCAAP raw data	LCAAP XRF Peak Data.txt	LCAAP XRF analysis.xls
NASNI	NASNI raw data	NASNI XRF Peak Data.txt	NASNI XRF analysis.xls
HPS	HPS raw data	HPS XRF Peak Data.txt	HPS XRF analysis.xls
Camp Keller	Camp Keller raw data	KAFB XRF Peak Data.txt	KAFB XRF analysis.xls

### **B3.3 XRF References**

Oliver Fordham. 1997. "Draft EPA SW-846 Method 6200, Field Portable X-ray Fluorescence Spectrometry for the Determination of Elemental Concentrations in Soil and Sediment," EPA Office of Solid Waste.

R. Tertian and F. Claisse. 1982. "Principles of Quantitative X-ray Fluorescence Analysis," ISBN 0-85501-709-0, Heyden, London, UK.

J. W. Criss, L. S. Birks, and J. V. Gilfrich. 1978. "Versatile X-ray Analysis Program Combining Fundamental Parameters and Empirical Coefficients," *Analytical Chemistry*, vol. 50, pp. 33–37 (1978)

### **B4. DL-LIBS**

Like the FO-LIBS system, the DL-LIBS response is also subject to matrix effects. Consequently, the earlier discussion on matrix effects and how they affect the LIBS response is applicable here. The raw and processed DL-LIBS data are archived on a CD-ROM. The following is a summary of how the DL-LIBS *ex situ* laboratory and *in situ* data were manipulated to account for matrix effects.

#### **B4.1 Preparation of Calibration Standards**

For LCAAP, HPS, and Camp Keller, standards were prepared by weighing an appropriate amount of lead nitrate or potassium dichromate into a beaker and dissolving the salt in water. An appropriate amount of soil from the site was added to the beaker to create a slurry. The beaker containing the slurry was placed inside an oven and dried. An aliquot of the prepared calibration standard was analyzed by ICP to determine the metal concentration. These samples were used to generate a calibration curve for the *in situ* and *ex situ* laboratory analyses. At Camp Keller, the same dry sample calibration curve was used for the *in situ* demonstration data and the *ex situ* laboratory sample analyses. For HPS, 8% by moisture content was added to the calibration samples for the generation of the *in situ* calibration curve. The 8% moisture calibration curve was used to compensate for the effects of moisture on the LIBS signal and was used to convert peak intensity of the heavy metal into concentration for the *in situ* demonstration data.

Before the demonstration at North Island, samples in and around the paint waste sludge basin were collected. These samples were analyzed for chromium content by ICP. The samples were

used to generate the calibration curves and to analyze *ex situ* laboratory samples. These same samples, after the addition of 8 % moisture content by weight, were also used to generate an *in situ* calibration curve that was used to analyze *in situ* demonstration data in real time.

## B4.2 Data Manipulation

The raw and processed DL-LIBS data for the four demonstration sites are archived on a CD-ROM. Tables B-6 to B-9 summarize the files archived. Examples of data manipulation for each site are provided in Microsoft<sup>®</sup> Excel spreadsheets. A summary of data manipulations is described below.

The CCD array of the detector contains 1024 pixels in the x-direction and 256 pixels in the y-direction. In the x-direction, only 703 pixels are intensified (pixel numbers 160 through 862). Analyses of the spectral data are limited to the intensified pixels. For each sample, 50 to 250 spectra are obtained. As with the FO-LIBS data, the DL-LIBS data are normalized to correct for differences in the plasma volume. The normalization procedure differed for each site.

**B4.2.1 LCAAP.** Spectra were obtained from 399.16 to 412.26 nm. The Pb peak occurred at 405.8 nm. For each sample (*in situ* and *ex situ*),  $x$  number of spectra were obtained. For each spectrum,  $i$ , the intensity of the Pb peak was determined and the pixel intensities of the spectrum were summed. The normalized intensity of the Pb peak for each spectrum,  $I_i^{Pb}$ , is given by

$$I_i^{Pb} = \frac{1000I_i}{\sum_{p=160}^{862} I_p},$$

where  $p$  is the pixel number,  $I_p$  is the intensity of pixel  $p$ , and  $I_i$  is the intensity of the Pb peak. The average, normalized Pb peak,  $\bar{I}_{Pb}$ , is calculated by

$$\bar{I}_{Pb} = \frac{1}{x} \sum_{i=1}^x I_i^{Pb},$$

where  $x$  is the number of spectra obtained for the sample.

In the *ex situ* laboratory samples, a large amount of strontium was present that greatly affected the data manipulations. To correct for the presence of strontium, only the pixel intensities from

pixel numbers 160 to 560 were summed in the normalization procedure. The *in situ* demonstration data for LCAAP was smoothed by averaging five concentrations and five depths.

**Table B-6.** Summary of Archived DL-LIBS LCAAP Data (Folder ‘LCAAP’ in Folder ‘DL-LIBS data’)

<p>folder: ‘<i>Ex situ</i> Calibration’</p>	<ol style="list-style-type: none"> <li>1. folder ‘LIBS data’: contains raw data as .txt files. Can be opened in Excel</li> <li>2. <b>read me first.doc</b>: word document summarizing contents in the folder ‘ex-situ calibration’</li> <li>3. <b>notes.doc</b> : word document on data collection and/or manipulation</li> <li>4. <b>example of calculations soil250.xls</b>: excel spreadsheet showing how data were manipulated</li> <li>5. <b>calibration curve.xls</b>: excel spreadsheet summarizing LIBS response versus analytical laboratory concentration</li> <li>6. <b>calibration fitting.txt</b>: .txt document summarizing the fitting parameters for the LIBS response as a function of calibration</li> <li>7. <b>calibration plot.ppt</b>: plot of the calibration curve used to analyze <i>ex situ</i> laboratory data</li> </ol>
<p>folder: ‘<i>Ex situ</i> Laboratory Samples’</p>	<ol style="list-style-type: none"> <li>1. folder ‘LIBS data’: contains raw data as .txt files. Can be opened in Excel</li> <li>2. <b>read me first.doc</b>: word document summarizing contents in the folder ‘<i>ex situ</i> laboratory samples’</li> <li>3. <b>example of calculations s6h2-31-41.xls</b>: excel spreadsheet showing how data were manipulated</li> <li>4. <b>ex-situ data results.xls</b>: excel spreadsheet summarizing LIBS results versus the analytical laboratory ICP results</li> </ol>
<p>folder: ‘<i>In situ</i> Calibration’</p>	<ol style="list-style-type: none"> <li>1. folder ‘LIBS data’: contains raw data as .txt files. Can be opened in Excel</li> <li>2. <b>read me first.doc</b>: word document summarizing contents in the folder ‘<i>in situ</i> calibration’</li> <li>3. <b>notes.doc</b> : word document on data collection and/or manipulation</li> <li>4. <b>example of calculations.xls</b>: excel spreadsheet showing how data were manipulated</li> <li>5. <b>calibration curve.xls</b>: excel spreadsheet summarizing LIBS response versus analytical laboratory concentration</li> <li>6. <b>calibration fitting.txt</b>: .txt document summarizing the fitting parameters for the LIBS response as a function of calibration</li> <li>7. <b>calibration plot.ppt</b>: plot of the calibration curve used to analyze <i>in situ</i> push data</li> </ol>
<p>folder: ‘<i>In situ</i> Push Data’</p>	<ol style="list-style-type: none"> <li>1. folder ‘LIBS data’: contains raw data as .txt files. Can be opened in Excel</li> <li>2. <b>read me first.doc</b>: word document summarizing contents in the folder ‘<i>in situ</i> push data’</li> <li>3. <b>example of calculations v2t2.xls</b>: excel spreadsheet showing how data generated during a push was manipulated</li> <li>4. <b>in situ results.xls</b>: excel spreadsheet summarizing Pb concentration determined by LIBS as a function of depth</li> </ol>

**B4.2.2 NASNI.** The *in situ* data were normalized as follows. For each spectrum, the areas of the Cr peaks at 425.4 and 427.5 nm were measured and the pixel intensities of the spectrum were summed. The normalized Cr peak area for each spectrum,  $A_i^{Cr}$ , is given by the following expression, where  $A_{425.4}$  and  $A_{427.5}$  are the Cr peak areas,  $p$  is the pixel number, and  $I_p$  is the intensity of pixel  $p$ :

$$A_i^{Cr} = \frac{1000(A_{425.4} + A_{427.5})_i}{\sum_{p=160}^{862} I_p}.$$

The average for  $x$  number of spectra for each sample, normalized Cr peak area,  $\bar{A}_{Cr}$ , was calculated by

$$\bar{A}_{Cr} = \frac{1}{x} \sum_{i=1}^x A_i^{Cr}.$$

The *in situ* demonstration data for NASNI was smoothed by averaging five concentrations and five depths.

The *ex situ* data were normalized using a different procedure. For each spectrum, the intensities for the Cr peaks at 425.4, 427.5, and 428.9 nm were measured. Likewise, the intensities for Fe peaks at 425.1, 426.0, and 427.2 nm were measured. For each spectrum,  $i$ , the normalized Cr response,  $I_i^{Cr}$ , was calculated by dividing the sum of the Cr peak intensities by the sum of the reference Fe peak intensities:

$$I_i^{Cr} = \frac{(I_{425.4} + I_{427.5} + I_{428.9})_i}{(I_{425.1} + I_{426.0} + I_{427.2})_i}.$$

As before, for  $x$  number of spectra for each sample, the average, normalized Cr peak intensities,  $\bar{I}_{Cr}$ , was then calculated by

$$\bar{I}_{Cr} = \frac{1}{x} \sum_{i=1}^x I_i^{Cr}.$$

**Table B-7.** Summary of Archived DL-LIBS NASNI Data (Folder ‘NASNI’ in Folder ‘DL-LIBS data’)

<p>folder: ‘<i>Ex situ</i> Calibration’</p>	<ol style="list-style-type: none"> <li>1. folder ‘LIBS data’: contains raw data as .txt files. Can be opened in Excel</li> <li>2. <b>read me first.doc</b>: word document summarizing contents in the folder ‘<i>ex situ</i> calibration’</li> <li>3. <b>example of calculations pd-h6-1-6.xls</b>: excel spreadsheet showing how data were manipulated</li> <li>4. <b>calibration curve.xls</b>: excel spreadsheet summarizing LIBS response versus analytical laboratory concentration</li> <li>5. <b>calibration fitting.txt</b>: .txt document summarizing the fitting parameters for the LIBS response as a function of calibration</li> <li>6. <b>calibration plot.ppt</b>: plot of the calibration curve used to analyze <i>ex situ</i> laboratory data</li> </ol>
<p>folder: ‘<i>Ex situ</i> Laboratory Samples’</p>	<ol style="list-style-type: none"> <li>1. folder ‘LIBS data’: contains raw data as .txt files. Can be opened in Excel</li> <li>2. <b>read me first.doc</b>: word document summarizing contents in the folder ‘<i>ex situ</i> laboratory samples’</li> <li>3. <b>example of calculations h1-36-48.xls</b>: excel spreadsheet showing how data were manipulated</li> <li>5. <b>ex-situ data results.xls</b>: excel spreadsheet summarizing LIBS results versus the analytical laboratory ICP results</li> </ol>
<p>folder: ‘<i>In situ</i> Calibration’</p>	<ol style="list-style-type: none"> <li>1. folder ‘LIBS data’: contains raw data as .txt files. Can be opened in Excel</li> <li>2. <b>read me first.doc</b>: word document summarizing contents in the folder ‘<i>in situ</i> calibration’</li> <li>3. <b>notes.doc</b> : word document on data collection and/or manipulation</li> <li>4. <b>example of calculations h3-1-6.xls</b>: excel spreadsheet showing how data were manipulated</li> <li>5. <b>calibration curve.xls</b>: excel spreadsheet summarizing LIBS response versus analytical laboratory concentration</li> <li>6. <b>calibration fitting.txt</b>: .txt document summarizing the fitting parameters for the LIBS response as a function of calibration</li> <li>7. <b>calibration plot.ppt</b>: plot of the calibration curve used to analyze <i>in situ</i> push data</li> </ol>
<p>folder: ‘<i>In situ</i> Push Data’</p>	<ol style="list-style-type: none"> <li>1. folder ‘LIBS data’: contains raw data as .txt files. Can be opened in Excel</li> <li>2. <b>read me first.doc</b>: word document summarizing contents in the folder ‘<i>in situ</i> push data’</li> <li>3. <b>example of calculations sd2.xls</b>: excel spreadsheet showing how data generated during a push was manipulated</li> <li>4. <b><i>in situ</i> results.xls</b>: excel spreadsheet summarizing Cr concentration determined by LIBS as a function of depth</li> </ol>

**B4.2.3 HPS.** The *in situ* data were normalized as follows. For each spectrum,  $i$ , the intensity of the Cr peak at 425.4 nm was measured and the intensity of the Fe peak at 427.2 nm was measured. The normalized Cr response for each spectrum,  $I_i^{Cr}$ , was calculated by dividing the intensity of the Cr peak by the intensity of the reference Fe peak area:

$$I_i^{Cr} = \frac{(I_{425.4})_i}{(I_{427.2})_i}.$$

For  $x$  number of spectra for each sample, the average, normalized Cr peak area,  $\bar{I}_{Cr}$ , was then calculated by

$$\bar{I}_{Cr} = \frac{1}{x} \sum_{i=1}^x I_i^{Cr}.$$

The *in situ* push data for HPS was smoothed by averaging five concentrations and five depths.

The *ex situ* laboratory data were normalized using a different procedure. For each spectrum,  $i$ , the intensity of the Cr peak at 425.4 nm was determined and the pixel intensities of the spectrum were summed. The normalized intensity of the Cr peak for each spectrum,  $I_i^{Cr}$ , is given by

$$I_i^{Cr} = \frac{1000 I_i}{\sum_{p=160}^{862} I_p},$$

where  $p$  is the pixel number,  $I_p$  is the intensity of pixel  $p$ , and  $I_i$  is the intensity of the Cr peak at 425.4 nm. The average, normalized Cr peak,  $\bar{I}_{Cr}$ , is then calculated by

$$\bar{I}_{Cr} = \frac{1}{x} \sum_{i=1}^x I_i^{Cr},$$

where  $x$  is the number of spectra obtained for the sample.

**Table B-8.** Summary of Archived DL-LIBS HPS Data (Folder ‘HPS’ in Folder ‘DL-LIBS data’)

<p>folder: ‘<i>Ex situ</i> Calibration’</p>	<ol style="list-style-type: none"> <li>1. folder ‘LIBS data’: contains raw data as .txt files. Can be opened in Excel</li> <li>2. <b>read me first.doc</b>: word document summarizing contents in the folder ‘<i>ex situ</i> calibration’</li> <li>3. <b>notes.doc</b> : word document on data collection and/or manipulation</li> <li>4. <b>example of calculations k.xls</b>: excel spreadsheet showing how data were manipulated</li> <li>5. <b>calibration curve.xls</b>: excel spreadsheet summarizing LIBS response versus analytical laboratory concentration</li> <li>6. <b>calibration fitting.txt</b>: .txt document summarizing the fitting parameters for the LIBS response as a function of calibration</li> <li>7. <b>calibration plot.ppt</b>: plot of the calibration curve used to analyze <i>ex situ</i> laboratory data</li> </ol>
<p>folder: ‘<i>Ex situ</i> Laboratory Samples’</p>	<ol style="list-style-type: none"> <li>1. folder ‘LIBS data’: contains raw data as .txt files. Can be opened in Excel</li> <li>2. <b>read me first.doc</b>: word document summarizing contents in the folder ‘<i>ex situ</i> laboratory samples’</li> <li>3. <b>example of calculations h3-48-66.xls</b>: excel spreadsheet showing how data were manipulated</li> <li>4. <b>ex-situ data results.xls</b>: excel spreadsheet summarizing LIBS results versus the analytical laboratory ICP results</li> </ol>
<p>folder: ‘<i>In situ</i> Calibration’</p>	<ol style="list-style-type: none"> <li>1. folder ‘LIBS data’: contains raw data as .txt files. Can be opened in Excel</li> <li>2. <b>read me first.doc</b>: word document summarizing contents in the folder ‘<i>in situ</i> calibration’</li> <li>3. <b>notes.doc</b> : word document on data collection and/or manipulation</li> <li>4. <b>example of calculations pd-h2-12-18.xls</b>: excel spreadsheet showing how data were manipulated</li> <li>5. <b>calibration curve.xls</b>: excel spreadsheet summarizing LIBS response versus analytical laboratory concentration</li> <li>6. <b>calibration fitting.txt</b>: .txt document summarizing the fitting parameters for the LIBS response as a function of calibration</li> <li>7. <b>calibration plot.ppt</b>: plot of the calibration curve used to analyze <i>in situ</i> push data</li> </ol>
<p>folder: ‘<i>In situ</i> Push Data’</p>	<ol style="list-style-type: none"> <li>1. folder ‘LIBS data’: contains raw data as .txt files. Can be opened in Excel</li> <li>2. <b>read me first.doc</b>: word document summarizing contents in the folder ‘<i>in situ</i> laboratory samples’</li> <li>3. <b>example of calculations s4.xls</b>: excel spreadsheet showing how data generated during a push was manipulated</li> <li>4. <b>in situ results.xls</b>: excel spreadsheet summarizing Cr concentration determined by LIBS as a function of depth</li> </ol>

**B4.2.4 Camp Keller.** The *in situ* and *ex situ* data were manipulated in the same fashion. For each sample,  $x$  number of spectra were obtained. For each spectrum,  $i$ , the intensity of the Pb peak was determined and the pixel intensities of the spectrum were summed up. The normalized intensity of the Pb peak for each spectrum,  $I_i^{Pb}$ , is given by

$$I_i^{Pb} = \frac{1000I_i}{\sum_{p=160}^{862} I_p},$$

where  $p$  is the pixel number,  $I_p$  is the intensity of pixel  $p$ , and  $I_i$  is the intensity of the Pb peak. The average, normalized Pb peak,  $\bar{I}_{Pb}$ , is then calculated by

$$\bar{I}_{Pb} = \frac{1}{x} \sum_{i=1}^x I_i^{Pb},$$

where  $x$  is the number of spectra obtained for the sample.

The *in situ* push demonstration data for Camp Keller was smoothed by averaging five concentrations and five depths.

**Table B-9.** Summary of Archived DL-LIBS Camp Keller Data (Folder ‘Camp Keller’ in Folder ‘DL-LIBS data’)

<p>folder: ‘<i>Ex situ</i> Calibration’</p>	<ol style="list-style-type: none"> <li>1. folder ‘LIBS data’: contains raw data as .txt files. Can be opened in Excel</li> <li>2. <b>read me first.doc</b>: word document summarizing contents in the folder ‘<i>ex situ</i> calibration’</li> <li>3. <b>notes.doc</b> : word document on data collection and/or manipulation</li> <li>4. <b>example of calculations c1300.xls</b>: excel spreadsheet showing how data were manipulated</li> <li>5. <b>calibration curve.xls</b>: excel spreadsheet summarizing LIBS response versus analytical laboratory concentration</li> <li>6. <b>calibration fitting.txt</b>: .txt document summarizing the fitting parameters for the LIBS response as a function of calibration</li> <li>7. <b>calibration plot.ppt</b>: plot of the calibration curve used to analyze <i>ex situ</i> laboratory data</li> </ol>
<p>folder: ‘<i>Ex situ</i> Laboratory Samples’</p>	<ol style="list-style-type: none"> <li>1. folder ‘LIBS data’: contains raw data as .txt files. Can be opened in Excel</li> <li>2. <b>read me first.doc</b>: word document summarizing contents in the folder ‘<i>ex situ</i> laboratory samples’</li> <li>3. <b>example of calculations h6-12-24.xls</b>: excel spreadsheet showing how data were manipulated</li> <li>4. <b>ex-situ data results.xls</b>: excel spreadsheet summarizing LIBS results versus the analytical laboratory ICP results</li> </ol>
<p>folder: ‘<i>In situ</i> Calibration’</p>	<ol style="list-style-type: none"> <li>1. folder ‘LIBS data’: contains raw data as .txt files. Can be opened in Excel</li> <li>2. <b>read me first.doc</b>: word document summarizing contents in the folder ‘<i>in situ</i> calibration’</li> <li>3. <b>notes.doc</b> : word document on data manipulation</li> <li>4. <b>example of calculations c1300.xls</b>: excel spreadsheet showing how data were manipulated</li> <li>5. <b>calibration curve.xls</b>: excel spreadsheet summarizing LIBS response versus analytical laboratory concentration</li> <li>6. <b>calibration fitting.txt</b>: .txt document summarizing the fitting parameters for the LIBS response as a function of calibration</li> <li>7. <b>calibration plot.ppt</b>: plot of the calibration curve used to analyze <i>in situ</i> push data</li> </ol>
<p>folder: ‘<i>In situ</i> Push Data’</p>	<ol style="list-style-type: none"> <li>1. folder ‘LIBS data’: contains raw data as .txt files. Can be opened in Excel</li> <li>2. <b>read me first.doc</b>: word document summarizing contents in the folder ‘<i>in situ</i> push data’</li> <li>3. <b>example of calculations w12t8.xls</b>: excel spreadsheet showing how data generated during a push was manipulated</li> <li>4. <b>in situ results.xls</b>: excel spreadsheet summarizing Pb concentration determined by LIBS as a function of depth</li> </ol>

**B5. Other Archived Data**

Provided on the on the CD-ROM are plots of the push data, contingency plots, and homogeneity data as well as a table summarizing the screening accuracy of each sensor. The data are presented in the folder ‘Summary of Data’. Table B-10 summarizes the data presented in this folder.

**Table B-10.** Summary of Data Archived in Folder ‘Summary of Data’

FOLDER	CONTENTS
LCAAP	<ol style="list-style-type: none"> <li>1. <b>contingency plots.doc</b>: FO-LIBS, DL-LIBS, and XRF contingency plots; homogeneity plot, summary of field screening accuracy of the three sensors</li> <li>2. <b>Fig 3 xrf in situ.doc</b> : xrf push data</li> <li>3. <b>Fig 4 DL in situ.doc</b> : dl-libs push data</li> <li>4. <b>Fig 5 FO in situ.doc</b> : fo-libs push data</li> </ol>
NASNI	<ol style="list-style-type: none"> <li>1. <b>contingency plots.doc</b>: FO-LIBS, DL-LIBS, and XRF contingency plots; homogeneity plot, summary of field screening accuracy of the three sensors</li> <li>2. <b>dllibspushes.doc</b> : dl-libs push data</li> <li>3. <b>folibspushes.doc</b> : fo-libs push data</li> <li>4. <b>xrf pushes.doc</b> : xrf push data</li> </ol>
HPS	<ol style="list-style-type: none"> <li>1. <b>contingency plots.doc</b>: FO-LIBS, DL-LIBS, and XRF contingency plots; homogeneity plot, summary of field screening accuracy of the three sensors</li> <li>2. <b>dllibs pushes.doc</b> : dl-libs push data</li> <li>3. <b>folibs pushes.doc</b> : fo-libs push data</li> <li>4. <b>xrf pushes.doc</b> : xrf push data</li> </ol>
Camp Keller	<ol style="list-style-type: none"> <li>1. <b>contingency plots.doc</b>: FO-LIBS, DL-LIBS, and XRF contingency plots; homogeneity plot, summary of field screening accuracy of the three sensors</li> <li>2. <b>DL-LIBS.doc</b> : dl-libs push data</li> <li>3. <b>FO-LIBS.doc</b> : fo-libs push data</li> <li>4. <b>XRF.doc</b> : xrf push data</li> </ol>

## INITIAL DISTRIBUTION

Defense Technical Information Center  
Fort Belvoir, VA 22060-6218 (4)

SSC San Diego Liaison Office  
C/O PEO-SCS  
Arlington, VA 22202-4804

Center for Naval Analyses  
Alexandria, VA 22302-0268

Office of Naval Research  
ATTN: NARDIC (Code 362)  
Arlington, VA 22217-5660

Government-Industry Data Exchange  
Program Operations Center  
Corona, CA 91718-8000

Environmental Security Technology  
Certification Program Support Office  
Herndon, VA 20170 (3)

Dr. W. Tim Elam  
Redmond, WA 98052-2659

Naval Research Laboratory  
Washington, DC 20375-5345

U.S. Army Engineer Research and  
Development Center (ERDC)  
Vicksburg, MS 39180-6199

Approved for public release; distribution is unlimited.